CASE STUDIES IN APPLIED GEOLOGY IN THE SOUTHEASTERN UNITED STATES

Sponsored by the Southeastern Section of the
Geological Society of America, Atlanta, Georgia
April 6, 1989

Edited by
Denny N. Bearce
and
Michael J. Neilson

GEORGIA DEPARTMENT OF NATURAL RESOURCES
ENVIRONMENTAL PROTECTION DIVISION
GEORGIA GEOLOGIC SURVEY

BULLETIN 122

The papers presented herewith have not undergone review procedures of the Georgia Geologic Survey's Quality Assurance Plan. They do not necessarily reflect the technical opinions of the Georgia Geologic Survey.

CASE STUDIES IN APPLIED GEOLOGY IN THE SOUTHEASTERN UNITED STATES

Sponsored by the Southeastern Section of the
Geological Society of America, Atlanta, Georgia
April 6, 1989

Edited by
Denny N. Bearce
and
Michael J. Neilson

Department of Geology
University of Alabama at Birmingham

Georgia Department of Natural Resources
Lonice C. Barrett, Commisssioner

Environmental Protection Division
Harold F. Reheis, Assistant Director

Georgia Geologic Survey
William H. McLemore, State Geologist

Atlanta
1990

BULLETIN 122

PREFACE

This volume includes three of the ten papers presented in the symposium "Applied Geology" and three papers presented in other symposia and technical sessions held at the Geological Society of America Southeastern Section Annual Meeting in Atlanta, 1989.

The idea of a symposium on Applied Geology developed from the editors' knowledge of geologic and property development circumstances contributing to slope failure that resulted in partial destruction and total evacuation of an apartment complex in Birmingham. The disregard of geologically-hazardous conditions in this instance was appalling, and we were determined to bring the incident to the attention of the Society members. The symposium served this purpose and included papers on a variety of other geotechnical problems and investigations. We intended it to initiate a sustained effort to bring topics of this most critical professional area to the attention of geologists attending a meeting that has traditionally been more academically oriented. We hope that it was a start toward encouraging a stronger participation in the Annual Meetings by geologists in the geotechnical industry and toward a stronger commitment on the part of Society members to work for more adequate public awareness of geologic processes and conditions that must be considered in land planning and resource utilization.

During the planning stage of the symposium, the Georgia Geological Survey expressed an interest in publishing the results, and we proposed assembling the papers in a symposium volume to the contributors. We regret that time constraints prevented many of the contributors from submitting manuscripts for the volume. We are also grateful that contributors of geotechnical papers in other sessions agreed to submit manuscripts in order that we might have sufficient papers for a volume.

We are grateful for the support of Earl A. Shapiro, Georgia Geological Survey, in encouraging us to assemble this volume and in obtaining approval for publication of the volume by the Georgia Geological Survey.

Denny N. Bearce
Michael J. Neilson
Department of Geology
University of Alabama at Birmingham
Birmingham, AL 35294

TABLE OF CONTENTS

BUILDING DAMAGE INCURRED DURING EXCAVATION ON DIP SLOPE OF RED MOUNTAIN, BIRMINGHAM, ALABAMA

Denny N. Bearce
Department of Geology, University of Alabama at Birmingham
Birmingham, AL 35294

ABSTRACT

Red Mountain, in Birmingham, Alabama, on the western edge of the Appalachian Valley and Ridge province, is a northeast-trending ridge composed mainly of the Silurian Red Mountain Formation and Ordovician Chickamauga Limestone. The southeast slope of Red Mountain is a dip slope capped by Red Mountain Formation dipping 20-30°. These strata are saprolitic, locally to depths of several meters, and highly jointed.

In Fall, 1987, excavation commenced on the dip slope of Red Mountain below an apartment complex to prepare an extensive highway-level terrace for a shopping mall. Excavation eventually resulted in a highwall sloping downward from the apartment property at 50° over a distance of about 27 meters to the mall terrace. A stratigraphic thickness of about 11 meters of saprolitic siltstone, dipping at 25°, was left unbuttressed. At this time initial movement of joint blocks occurred. The major slippage zone was a soft, plastic claystone bed that was exposed at the base of the newly excavated slope. At least 41,000 cubic meters of rock was involved. Initial movement of about 3-4 meters caused partial collapse of two buildings. Movement continued for two months with total displacement of about 12-15 meters.

Blasting was suggested as a triggering agent. However, initial movement occurred several hours after blasting. Rainfall had been light in weeks preceding the slide. Exposure of the claystone alone was probably sufficient to initiate sliding.

An initial attempt to stabilize the slope where the block slide occurred with steel reinforcing rods failed. Several months after the first block slide an additional 1.5 meter thickness of strata broke loose over a slightly larger area at the same site as the first block slide. The zone of slippage was another bed of soft plastic claystone. Presently at least 150 tiebacks are being installed on the slope to anchor the remaining strata through cables to the underlying Chickamauga Limestone.

In May, 1988, excavation at another location on the highwall reactivated a colluvial deposit, and slumping commenced on the apartment property, damaging a third building. A berm was constructed across the toe of the colluvial deposit, but movement continued. Fissures opened on the apartment property, eventually rendering the access road unsafe. The apartment complex was vacated at that time.

INTRODUCTION

The city of Birmingham, Alabama, lies at the western edge of the Appalachian Valley and Ridge province (fold and thrust belt) (fig. 1). Birmingham is underlain by sedimentary rocks of shallow marine and fluvial origin ranging in age from Cambrian to Pennsylvanian (Kidd and Shannon, 1977). These rocks were thrust faulted and folded during the Alleghanian orogeny (Pennsylvanian- Permian) (fig. 1). Subsequent erosion has resulted in "valley and ridge" topography; valleys are underlain by

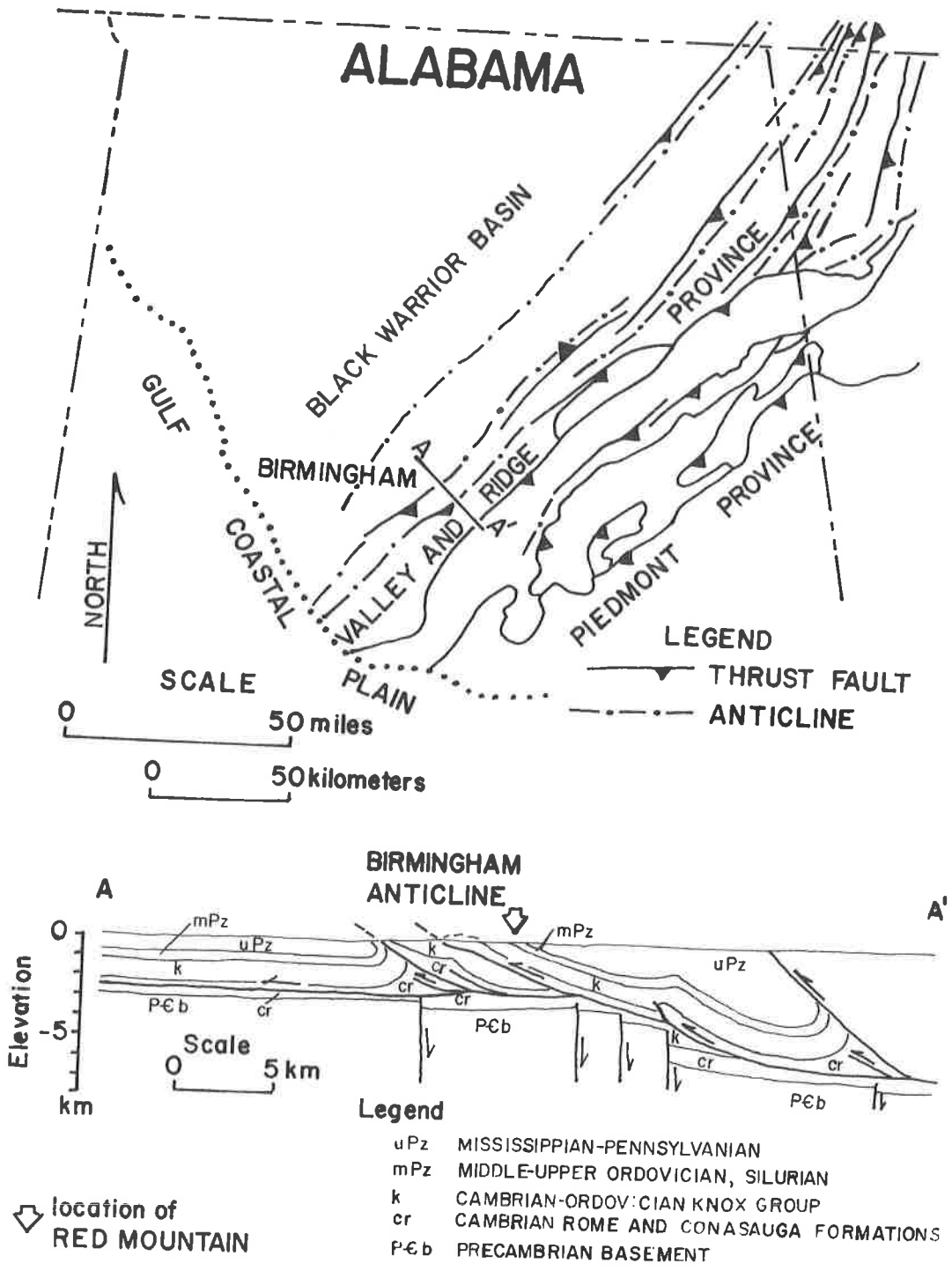

Figure 1 - Generalized geologic map of northern Alabama. Cross-section A-A': gross geologic structure of the Birmingham anticline, showing location and geologic setting of Red Mountain, a cuesta of gently dipping strata on the southeast limb. Modified from Thomas and Bearce, 1986.

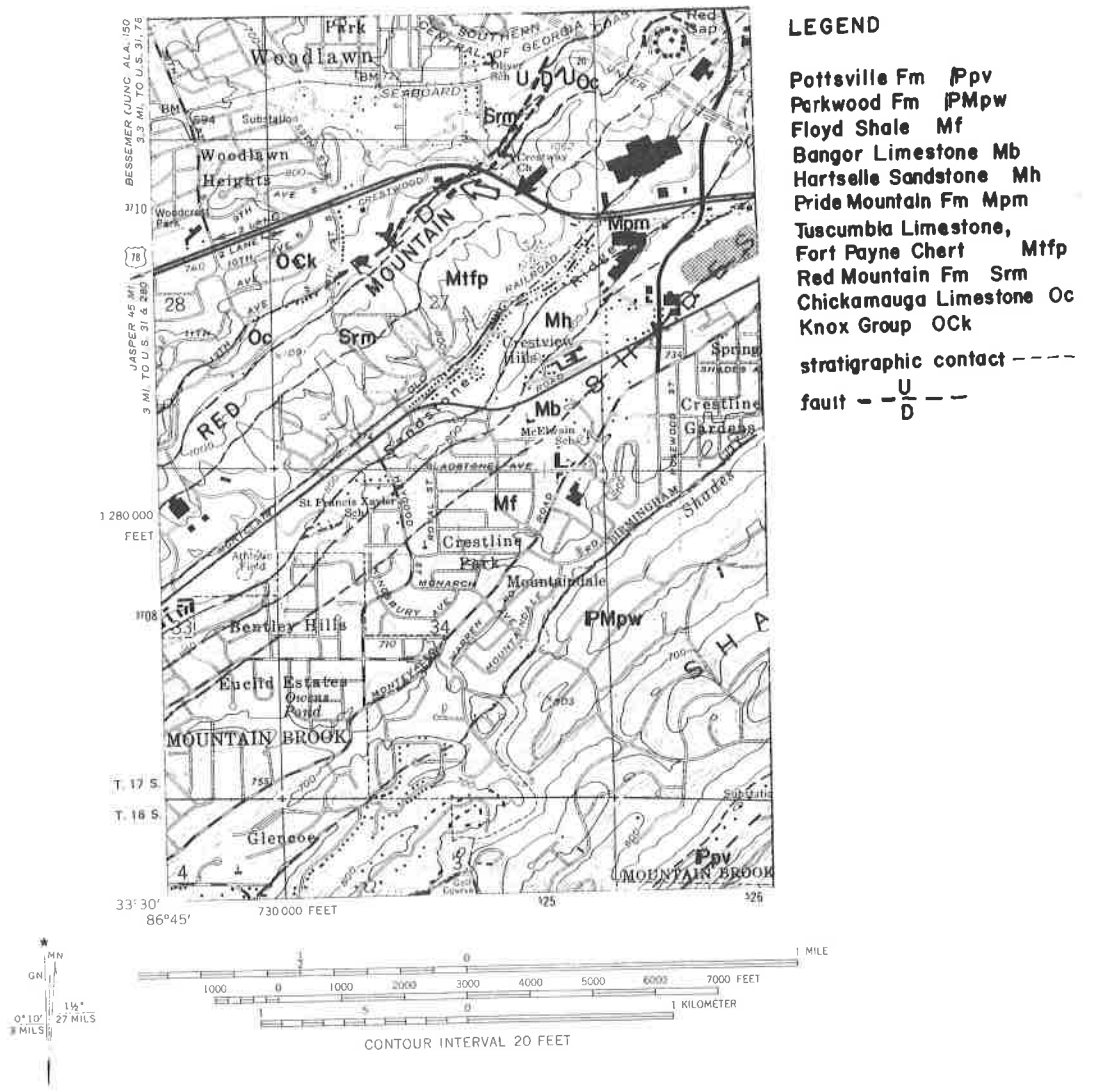

Figure 2 - Geology and urban setting of Red Mountain in the vicinity of Mountaintop Apartments (open arrow) and Festival Centre (black arrow) properties. Modified from Kidd and Shannon, 1977.

carbonate rocks or shale, and ridges are supported by resistant beds of sandstone and chert. Stresses from folding, faulting, and subsequent uplift have resulted in joint sets of various orientations in all rock types.

Red Mountain is a cuesta formed in southeast dipping strata and separating the carbonate valley in which the downtown part of Birmingham lies from other parts of the metropolitan area to the southeast. Red Mountain reaches a maximum altitude of about 330 meters (1100 feet) (Butts, 1910). Elevations in adjoining valleys are between 150 and 180 meters (500 to 600 feet). The crest of Red Mountain is formed of beds of hematite- and calcite-cemented sandstone of the Silurian Red Mountain Formation, which ranges in total thickness from less than 60 meters (200 feet) to more than 180 meters (600 feet) (Butts, 1926). Certain intervals of these sandstone beds were mined for iron ore from the mid 1800's to the early 1970's, initially by strip mining and finally by subsurface mining. The abandoned mine shafts lie at depths of a few 10's of meters beneath the southeast slope of Red Mountain. Both the southeast and northwest slopes of the mountain locally contain deposits of talus 10's of meters thick, much of which is undoubtedly mine tailings.

Since the founding of the city of Birmingham in 1871, Red Mountain has been a focal point of industrial activity, initially mining, and in the last three decades commercial and residential

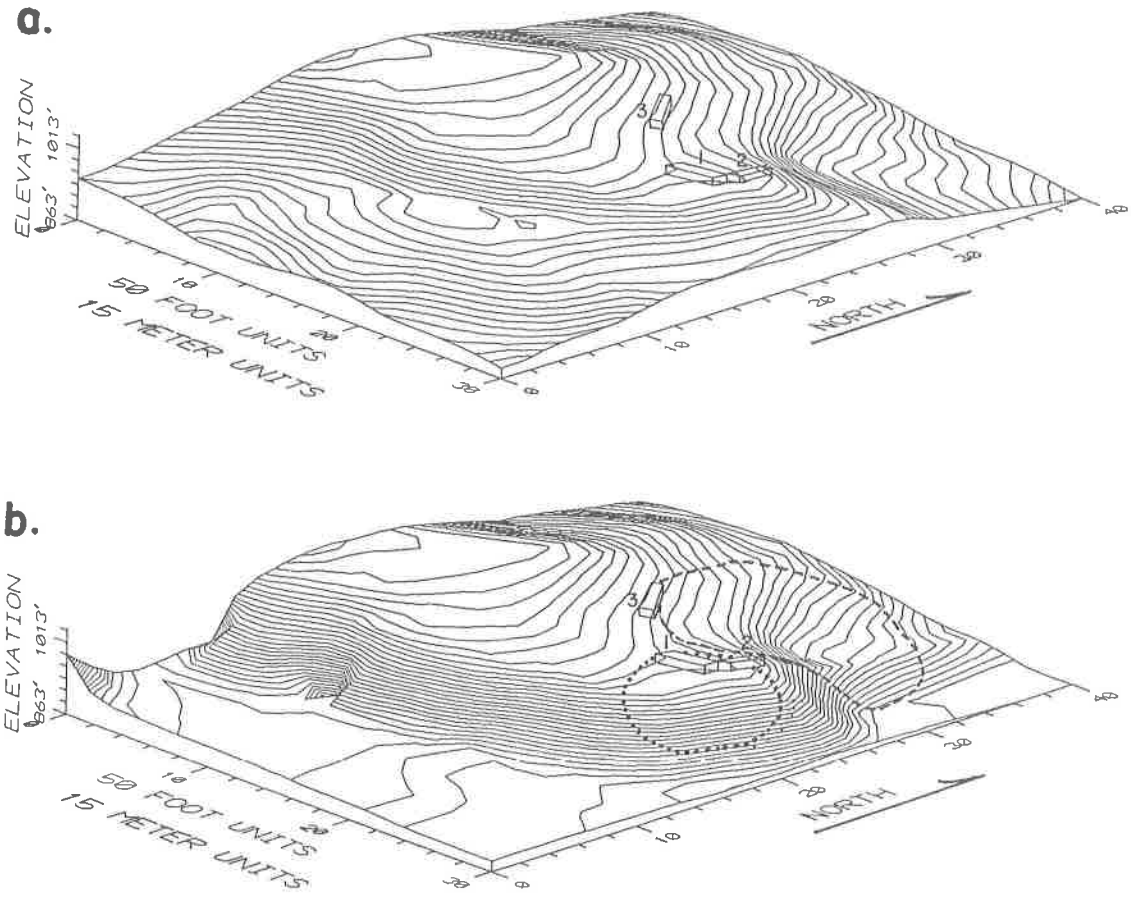

Figure 3 - Three-dimensional models showing relief of Red Mountain: a. prior to excavation for Festival Centre, and b. after excavation to final grade. Damaged apartments, numbered 1, 2, and 3 on Figure 4, are shown for reference, as well as locations and approximate dimensions of block slides (dots) and colluvial slump (broken line). Contour interval 5 feet.

development. Developers have encountered geologic hazards stemming from cuts made into talus deposits and dip slopes of jointed strata rendered more unstable by deep chemical weathering. After numerous publicized occurrences of slope failures, the city of Birmingham engaged a local geological engineering firm to make a feasibility study of slopes on Red Mountain (Vandevelde and others, 1982) Several locations were pinpointed in this study as geologically hazardous. The slopes within and bordering the property of the Mountaintop Apartments (Figs. 2 and 3a) were cited in the study as an example of unstable slope conditions. The study notwithstanding, a tract of sloping land adjoining the property of Mountaintop Apartments was proposed for development of a large shopping mall to be named the Eastwood Festival Centre (fig. 3b). The project was approved by the city. Plans called for excavation of rock to a maximum depth of about 21 meters (70 feet) to develop shop and parking area at about the same elevation as Crestwood Boulevard (U.S. Highway 78E), which crosses Red Mountain northeast of the Mountaintop Apartments (figs. 2 and 4). During planning stages three engineering firms were consulted concerning the geology of the project site. These firms pointed out the danger of excavating a dip slope. One of the firms advised tying back the strata on the dip slope prior to excavation. This was not done. Excavation commenced during Fall, 1987, and proceeded through Winter, 1988, cutting into the dip slope below the Mountaintop Apartments,

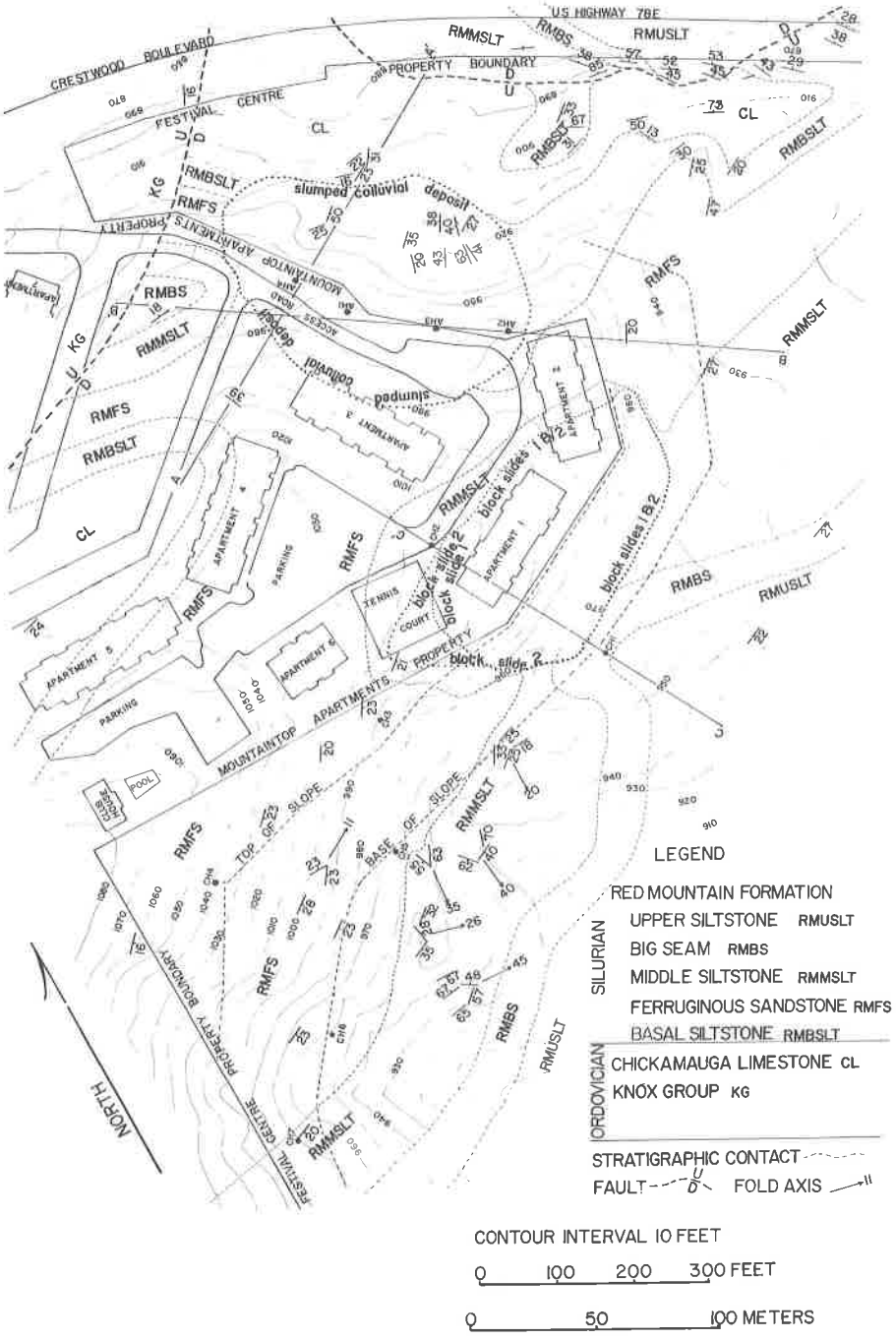

Figure 4 - Geologic map of adjoining parts of Mountaintop and Festival Centre properties. Contours reflect original topography prior to excavation. Locations of core holes denoted by CH, auger holes by AH. Cross-section lines refer to Figure 5.

terminating in a slope of about 50°, the upper edge of which was located a few meters east of two of the Mountaintop Apartment buildings (fig. 3b).

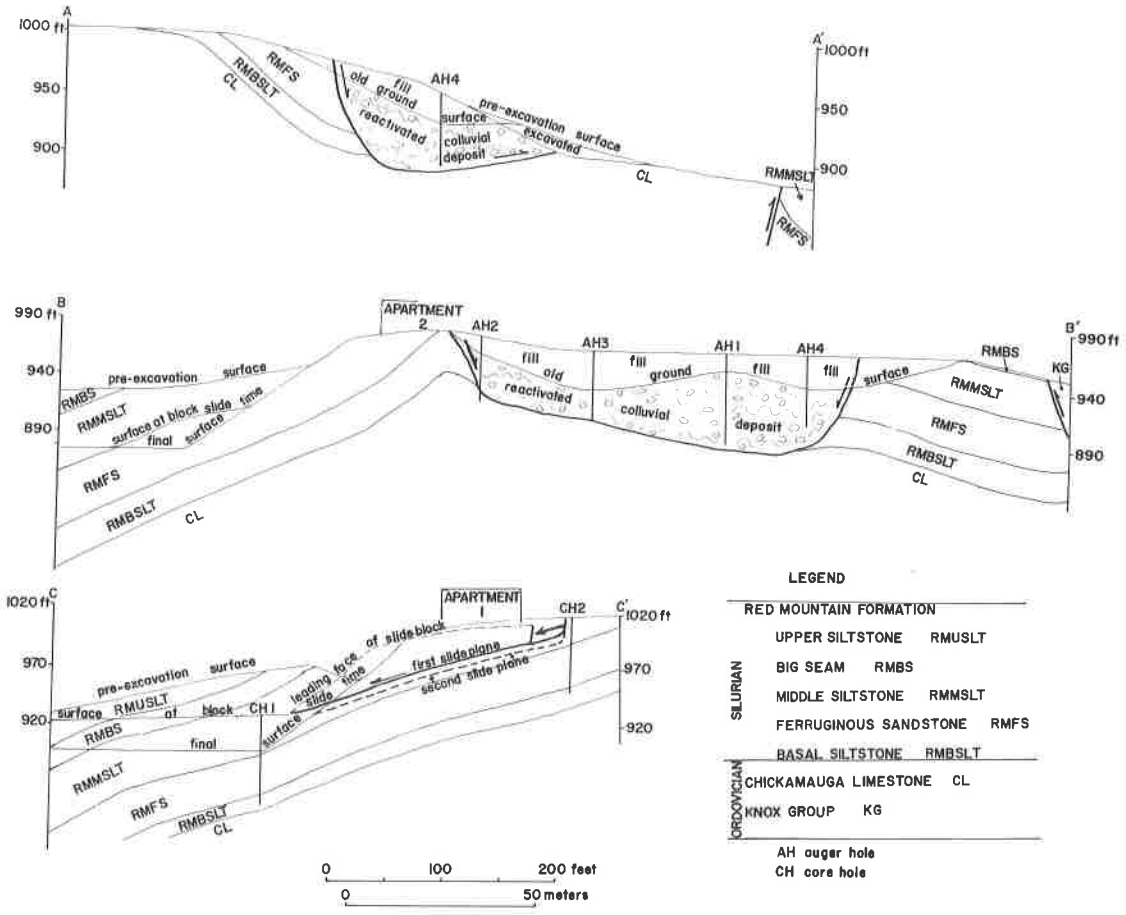

Figure 5 - Structural cross-sections through slope failure locations. Section lines shown on Figure 4.

BLOCK SLIDE

On the evening of March 15, 1988, a block slide occurred on the slope bordering the northwest side of the Festival Centre property. Approximately 41,000 cubic meters of rock was involved, and initial movement was 3 to 4 meters (fig. 6). Blocks of deeply weathered, fine-grained sandstone and siltstone separated along joints and slid independently on a single slide plane (fig. 5, cross-section C-C'). The two apartment buildings overlooking the excavation (fig. 4, apartments 1 and 2) lay entirely or partly on the sliding mass and were severely damaged. Movement and attendant damage were sudden, and residents exited hastily. Fortunately, only one injury was sustained: a broken ankle during a leap from a balcony. Slower movement continued during the following few weeks, aggregating 12 to 15 meters. Apartments 1 and 2 sustained progressive damage during continued slippage and were razed a few weeks after the initial movement.

Following the slide, the contractors were enjoined from further blasting until they could demonstrate that no more slides would occur. The contractors retained a geological engineering firm to stabilize the slopes bordering the excavation. That firm in turn engaged my services for the purpose of preparing a geologic map and structural cross-sections of the Mountaintop Apartments property and the Festival Centre property. Prior to commencement of the excavation the contractors had consulted engineering firms. A series of auger holes had been drilled and logged. However, no maps or cross-sections showing the detailed geology of the properties existed.

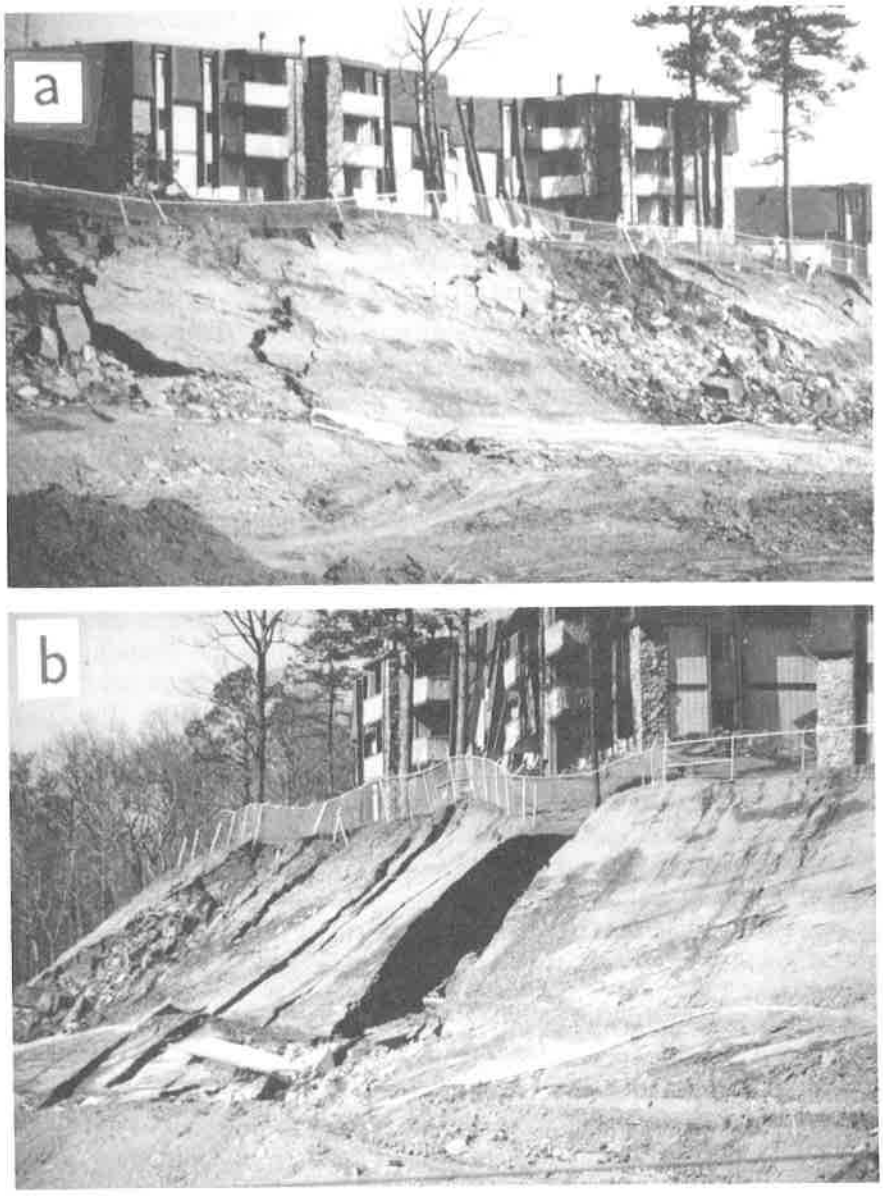

Figure 6 - Extent of movement of block slide approximately 12 hours after initiation of movement: a. view from southwest, and b. view from northeast. Photographs by M. J. Neilson.

GEOLOGY OF MOUNTAINTOP-FESTIVAL CENTRE PROPERTIES

Stratigraphy

The properties are on strata of the Silurian Red Mountain Formation and the Middle to Late Ordovician Chickamauga Limestone. These formations were deformed during the late Paleozoic Alleghanian

orogeny, sustaining folding and thrust-faulting (fig. 1, cross-section A-A'), both of which are manifested in exposures on the property.

Figure 7 shows the stratigraphy of the lower part of the Red Mountain Formation, informally subdivided, at the Festival Centre site. The upper part of the formation is concealed beneath fill used to build up the southeastern part of the Festival Centre terrace. This subdivision of the Red Mountain Formation shows the intervals that are lithologically distinctive and sufficiently persistent to be traced across the properties. Only the upper part of the Chickamauga Limestone is exposed or penetrated in boreholes on the properties. The lower part of the siltstone interval above the Big Seam is locally and poorly exposed on the properties. Thicknesses of the basal siltstone, ferruginous sandstone, and middle siltstone intervals were derived from cores and from field measurements.

The Red Mountain Formation is a clastic sequence that reflects for the most part marine nearshore to intertidal sedimentation in a deltaic setting (Chowns, 1972). It consists mainly of fine-grained sandstone and siltstone interbedded in platy to thin beds. These rocks are feldspathic and carbonate-cemented, and they weather soft and clayey. Ripple cross- laminations, mud cracks, and bioturbation are characteristic. Sandstone beds are at least as abundant as siltstone. The basal, middle, and upper siltstone intervals (fig. 7) are comprised of this lithology and are distinguishable from one another only in that they are separated by contrasting lithologies.

The Big Seam is a member of the Red Mountain Formation (Butts, 1926). The Big Seam and ferruginous sandstone interval reflect beach-barrier island sedimentation and tidal delta sedimentation respectively (Chowns, 1972). The Big Seam is coarse-grained, deep maroon, and has a high specific gravity due to a hematite content of approximately 30%. Hematite coats quartz grains and fossil fragments and forms oolites, resulting in sand grains with a glossy, submetallic luster. The Big Seam contains an interval of ferruginous limestone cobbles in its lower part. These cobbles are discoidal and may have formed from soft lime mud lenses in an intertidal zone through processes of desiccation and gentle wave abrasion (Bearce, 1973), or from the breakup of thin, poorly lithified coquina beds exhumed during beach erosion in a surf zone (M. Johnson, oral communication, 1989). At the properties the cobble zone is limited to a single layer of cobbles. The Big Seam is internally massively bedded with discontinuous partings and local cross-bedding. The ferruginous sandstone is lower in hematite content than the Big Seam and is generally reddish brown to maroon-grey in color. It is mostly fine-grained, with beds internally massive to laminated and cross-bedded and ranging in thickness from 2 centimeters to 1 meter. Lenticular intervals of siltstone ranging in thickness from centimeters to 1.5 meters are spaced stratigraphically from centimeters to a few meters apart. The ferruginous sandstone overlies an interval of interbedded siltstone and thin bedded, fine- to very fine-grained sandstone. Flow rolls up to 1 meter in diameter are ubiquitous at the base and in the lower part of the ferruginous sandstone. The underlying siltstone has flowed upward, forming flame tongues in the lower part of the ferruginous sandstone.

The sandstones of the Red Mountain Formation are cemented with calcite and contain up to 30% calcite locally. Where deeply weathered they are friable and weak.

The informally designated siltstone intervals in the Red Mountain Formation (fig. 7) are actually at least 50% sandstone. They are called siltstones to indicate that they are distinctly different lithologically from the Big Seam and the ferruginous sandstone. Sandstone beds are at most a few centimeters thick, light grey to bluish grey, calcite-cemented, fine- to very fine- grained and silty. They may be parallel- or cross-laminated or massive internally. They are typically burrowed and may be coarsely homogenized with siltstone interbeds by bioturbation. Siltstones are medium grey where fresh, sandy, laminated to massive internally, calcareous, and bioturbated in part. The basal siltstone is in part finely laminated, with partings delineated by black manganese oxide. Locally the basal siltstone is ferruginous and maroon in color.

The siltstone intervals weather to light grey brown, yellow brown, and red. Both sandstone and siltstone weather fissile and have a shaley appearance. Leaching of carbonate cement renders the rock friable or crumbly and in some cases very plastic. There are weathered silty claystone partings and beds from less than 1 centimeter to about 30 centimeters thick in all of the siltstone intervals (fig. 8). Both block slides occurred on such claystone beds (fig. 9).

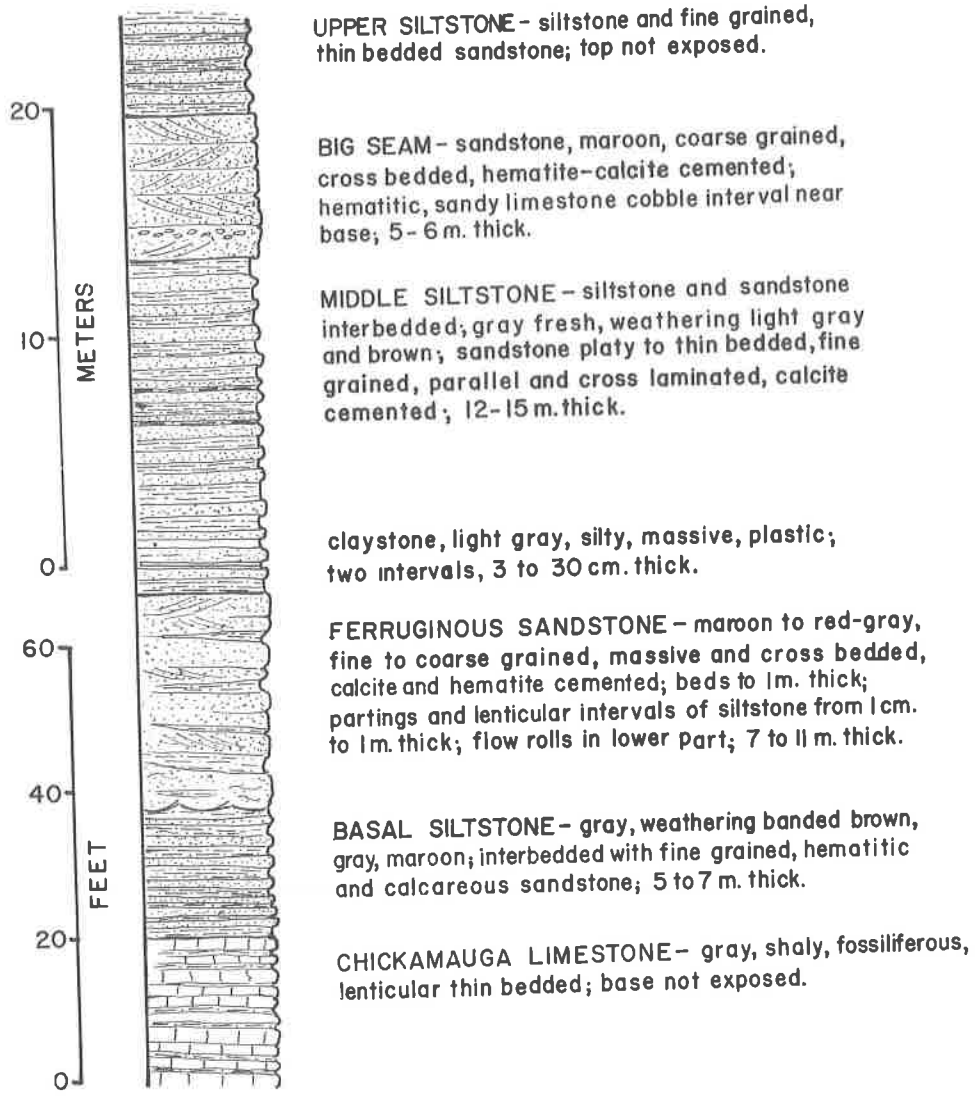

Figure 7 - Stratigraphic column of portions of Silurian Red Mountain Formation and Ordovician Chickamauga Limestone exposed on Festival Centre property.

The Ordovician Chickamauga Limestone unconformably underlies the Red Mountain Formation (fig. 7). It is mainly medium grey, thin-bedded silty, clayey, micritic to sparry, fossiliferous limestone. The Chickamauga limestone weathers to grey brown, shaley, silty clay residuum that looks much like the weathered shales of the Red Mountain Formation; however, the residuum lacks sand. Only the uppermost 6 to 8 meters of the Chickamauga is exposed on the properties.

Structure

Strata dip gently to the southeast (fig. 4 and fig. 5, cross-section C-C') over much of the Festival Centre property. Folds of wave length smaller than the extent of the property are present locally on the property. The middle siltstone interval, exposed before paving on the graded terrace immediately southwest of the Mountaintop Apartments block slide, contains numerous small plunging and non-plunging folds. Bearings and plunges of some of these folds are shown on Figure 4. The underlying ferruginous sandstone contains one or two small folds in this area, but the folds seem to

Figure 8 - Claystone interval in middle siltstone on which first block slide occurred. Hammer is 33 centimeters (13 inches) long. Bounding lithologies are thin beds of fine-grained sandstone with siltstone partings.

be mostly restricted to the middle siltstone interval. Some small folds can be seen in cross-section in the excavation wall along the west boundary of the property, and they commonly have thrust-faulted short limbs. As regional dip is to the southeast in the southwest part of the property, the small folds (wavelength 5 - 6 meters, amplitude 3 meters) commonly plunge east, south, or southeast. Some folds change from plunging to non-plunging in a distance of 7 to 10 meters. If regional dip were to be removed they would be seen as short, doubly plunging, noncylindrical, upright to moderately inclined, closed folds. Concentration of the folds in the middle siltstone interval, and their apparent abrupt diminishment northeastward (only a few very small, open folds are present in the area of the block slide) suggest that they are related to thrust-faulting that may follow a decollement parallel to bedding near the base of the middle siltstone interval. The folds may reflect a dying out of slip on the decollement. A three-point solution to regional dip on Chickamauga Limestone in the subsurface beneath the area of concentrated folds indicates a strike of N.40°E. and a dip of 20° to the southeast, similar to attitudes in the area of the block slide where folds are small and rare.

A large anticline is present on the northeast edge of the Festival Centre property adjacent to Crestwood Boulevard (fig. 4). Chickamauga Limestone is exposed in the hinge zone of this anticline, which plunges 13-17° S.72°E. The anticline is thrust-faulted on its northeast limb with stratigraphic throw of as much as 40-50 meters (fig. 5, cross-section A-A'). The anticline is truncated to the northwest by a high angle fault that juxtaposes Cambrian-Ordovician Knox Dolomite on the

Figure 9 - Thin claystone on which second slide took place. Note slickensides. View looking updip. Hammer is 33 centimeters (13 inches) long. Iron reinforcing rod (upper right corner) bent over during movement.

northwest against Chickamauga Limestone in an exposure on Crestwood Boulevard immediately west of the Festival Centre property.

A second anticline, evident from core hole and auger hole depths to the Chickamauga (fig. 5, cross-section B-B'), has a poorly constrained trend, possibly plunging very gently S.25°W. Surface exposures on the Mountaintop Apartments property (fig. 4) suggest other large folds. Limited exposure makes their interpretation very tenuous.

GEOLOGIC ASPECTS OF BLOCK SLIDE

The block slide that occurred in March, 1988 involved the middle siltstone interval (fig. 4 and fig. 5, cross-section C- C'). This interval comprises the uppermost strata on a small promontory on the dip slope (fig. 3b). The failure plane of this slide was a 30 centimeter thick bed of massive, plastic, silty claystone (fig. 8) located approximately 6 meters above the base of the middle siltstone interval. The claystone is 1-1.5 meters below ground surface at the top of the slope in the breakaway zone and lay beneath a maximum thickness of about 12 meters of strata on the dip slope (fig. 5, cross-section C-C'). Subvertical, northwest- and northeast-trending joints (fig. 10) facilitated breakaway and accommodated slippage past laterally-adjacent strata. The strata involved were deeply weathered and clay-rich throughout, due in part to the kaolinization of feldspar in fine-grained sandstone beds. Figure 5, cross-section C-C', indicates that the topography prior to excavation was such that a considerable thickness of the siltstone was unbuttressed on the dip slope. Such a situation would lead one to anticipate an eventual slide at this site, excavation or not. Yet, two of the apartment buildings were located on this site and remained there 20 years failure-free. The coefficient of friction on the unbuttressed bedding planes was evidently sufficiently high to forestall sliding on beds dipping at about 25°. No claystone beds comparable to that of the zone of slippage were evident in the pre-excavation unbuttressed section. It was not until excavation proceeded to the point of exposing the claystone bed that failure occurred. When it finally occurred it was within a few hours of the time of exposure of the claystone. It may be noted that the weather during the preceding winter had been unusually dry. Three days prior to the failure slightly more than 1 centimeter of rain fell.

Figure 10 - Shifted joint blocks of deeply weathered, fine-grained sandstone and siltstone on east side of damaged apartment (numbered 2 in Figure 4) two days after initial movement. View looking southeast across Festival Centre terrace under construction. Photograph by M. J. Neilson.

Slope Stabilization Efforts

Immediately after the block slide the Mountaintop Apartments owners filed suit to enjoin further excavation until it could be demonstrated that no more slides would occur. A local engineering firm was retained by the contractors to develop a slope stabilization plan. The engineering firm's initial plan to stabilize the slope where the slide occurred so that excavation could be resumed involved pinning the remaining middle siltstone strata to the underlying ferruginous sandstone by 2.5 centimeter thick steel reinforcing rods set in a grid pattern with 10 meter spacing. The plan was accepted, the slope was pinned, and excavation resumed, continuing through the Summer and Fall of 1988, to the final surface shown in Figure 5, cross-section C-C'. By late Fall it became evident that slippage had recommenced, and in December, 1988, an additional 1.5 meter thickness of strata broke loose in separate joint blocks, bending the reinforcing rods and sliding off the tips of the rods (fig. 9). Movement occurred on a single slide plane; a silty claystone bed about 5 centimeters thick. The breakaway zone of the second block slide was a few meters upslope from the first breakaway zone. Half of the Mountaintop Apartments tennis court was torn away, and the access road to the main parking lot of the apartment complex appeared to be in jeopardy. At this time the Mountaintop Apartments were vacated. The apartment owners once again sought and were granted an injunction against further excavation. Although the excavation was down to grade, there remained some blasting and trenching to be done at the base of the slope where the slide occurred for building foundations. This could not be accomplished until the injunction was lifted.

A second plan to stabilize the slope involved the emplacement of a series of tiebacks in rows across the entire slope parallel to the trend of the slope (fig. 11). Tieback installation involved drilling into the slope on an 18^{o} plunge opposite to dip direction for approximately 40 meters into strata as deep as the upper part of the Chickamauga Formation. Several cables were inserted in each drill hole and locked into the penetrated strata, stretched, cemented, and locked into a concrete buttress at the cut face on the slope. At this time over 150 tiebacks have been installed at a cost of $20-30,000 per tieback. The injunction remains in effect, and a review of the case is pending.

Figure 11 - Tiebacks installed at cut face in lower part of middle siltstone. Slippage plane for second block slide extends upslope from top of cut face. Cement blocks are approximately 2 feet x 5 feet x 7 feet. View looking southwest.

COLLUVIAL SLIDE

In May, 1988, excavation was proceeding into the hillside at the northeast end of the Mountaintop Apartments property adjacent to Highway 78E (fig. 4). Accelerated creep became manifested in a series of small thrust-like shears at the base of the slope and in the opening of fissures on the Mountaintop Apartments property. The fissures on the Mountaintop Apartments property were arranged in an arc that passed across the access road and beneath the down-hill side of an apartment building (fig. 4, apartment 3). Fissure opening and down-hill subsidence shortly resulted in damage sufficient to necessitate evacuation of the building. Examination of the excavated slope revealed an apparent chaotic structure. Bedding horizons could be traced only a short distance across the slope, possibly in part because of intense chemical weathering and disintegration of beds. Where bedding attitudes could be measured they were quite variable, and some small folds were present. Individual beds appeared to terminate against massive, silty and sandy clay matrix. Limited exposure of coarse-grained, thick sandstone beds revealed disruption and offset of the beds within the matrix. Much of the slope material is massive, silty, sandy clay, and is unstratified. What little of the stratigraphy can be interpreted suggests that it is out of continuity with the stratigraphy elsewhere on the property. Chickamauga Limestone is exposed at the base of the slope and probably extends a meter or two up slope. A discontinuous interval of ferruginous sandstone about 1 meter thick is present only a meter or so above the Chickamauga Limestone. The small shears at the base of the slope form an undulatory, but apparently single, continuous plane of slippage dipping gently into the slope. The slip planes are clay-coated and slickensided. They do not appear to follow bedding.

Prior to commencement of excavation for the Festival Centre, four auger holes were drilled along the access road on the northeast side of the Mountaintop Apartments. Position of the holes and interpretation of driller's logs are shown on Figure 4 and Figure 5, cross-sections A-A' and B-B'. The holes all penetrate 7 to 14 meters of fill at the top. Descriptions below the fill are ambiguous, but common characteristics are intense weathering to hole bottoms and the presence of sandy clay intervals containing sandstone fragments below the old fill-buried surface. These common features, combined with the chaotic nature of disrupted beds exposed on the cut face, suggest an ancient

Figure 12 - View southeast down slippage plane of second block slide toward completed shops across Festival Centre terrace in January, 1989. Two buildings are planned for location at the base of this slope but are enjoined at this time.

colluvial deposit accumulated in a hollow on the flank of a water gap or wind gap (the present-day saddle in Red Mountain through which Highway 78E passes). A talus deposit would be sufficiently permeable to become intensely weathered to depths of 20 to 30 meters, the depths of the auger holes. Cross-sections A- A' and B-B', Figure 5, are interpretive of the slump zone. Cross-section A-A' indicates that removal of only a 3 meter thickness of material at the base of the slope was sufficient to initiate slumping. The colluvial deposit probably rests on Chickamauga Limestone that is well-exposed on the excavated terrace at the base of the slope. Two of the auger holes bottom in limestone or massive, non-sandy clay, a typical carbonate residuum of the Chickamauga. This is the only correlatable horizon in any of the holes.

An earthen berm was constructed across the base of the slope at the toe of the slump to weight it down. However, fissures on the Mountaintop Apartments property above the cut continued to widen and lengthen, and down-hill subsidence across individual fissures increased to as much as 20 centimeters over the following several months. The access road to the apartments sustained extensive damage over a distance of about 75 meters, and is unsafe for use.

EPILOGUE

At this time several places of business, including various shops, a large drug store, and a theatre complex are open for business in the Festival Centre (fig. 12). Buildings planned for the base of the block slide slope are not yet under construction, and hearings on the state of stability of the slope are pending. The cost of stabilization attempts alone is running in the low millions, and several multi-million dollar lawsuits are pending.

CONCLUSIONS

Excavation for a shopping mall on property located downslope from an apartment complex on Red Mountain, Birmingham, Alabama, resulted in multiple slope failures and substantial damage to the apartment property, necessitating evacuation of the entire apartment complex. Slope stabilization

has proved exceedingly expensive. The shopping mall site location and excavation procedure both demonstrate a lack of understanding of geologically hazardous conditions, as well as a predisposition to ignore cautions and advice tendered by geologic consultants. The factors involved in the slope failures in this case include:

1. Excavation of strata on a dip slope, leaving strata unbuttressed.
2. Polygonal jointing of strata, permitting independent movement of joint blocks a few meters long.
3. Intensive weathering, resulting in stratigraphic intervals of soft claystone of low friction coefficient.
4. Deeply weathered colluvial deposits underlying both apartment and mall property.

REFERENCES

Bearce, D. N., 1973, Origin of conglomerates in Silurian Red Mountain Formation of central Alabama; their paleogeographic and tectonic significance: American Association of Petroleum Geologists Bulletin, vol. 57, p. 688-701.

Butts, C., 1910, Birmingham Folio, United States Geological Survey Geologic Atlas, Folio 175.

Butts, C., 1926, The Paleozoic rocks, in Adams, G. I., Butts, C., Stephenson, L. W., and Cooke, W., Geology of Alabama: Geological Survey of Alabama Special Report 14, p. 40-240.

Chowns, T. M., 1972, Molasse sedimentation in the Silurian rocks of northwest Georgia: in Chowns, T. M., ed., Sedimentary environments in the Paleozoic rocks of northwest Georgia: Georgia Geological Society Guidebook 11, p. 13-23.

Kidd, J. T., and Shannon, S.W., 1977, Preliminary areal geologic maps of the Valley and Ridge Province, Jefferson County, Alabama: Geological Survey of Alabama Atlas Series 10.

Thomas, W. A., and Bearce, D. N., 1986, Birmingham anticlinorium in the Appalachian fold-thrust belt, basement fault system, synsedimentary structure, and thrust ramp: in Neathery, T. L., ed., Southeastern Section Geological Society of America Centennial Field Guide, v. 6, p. 191-200.

Vandevelde, G. I., Gooding, P. H., Boudra, L. H., and Sowers, G. F., 1982, Report of Red Mountain landslide susceptibility study, Birmingham, Alabama: LETCO Job No. B-3113.

CORE FRACTURE ANALYSIS APPLIED TO GROUND WATER FLOW SYSTEMS: CHICKAMAUGA GROUP, OAK RIDGE, TENNESSEE

Enid Bittner and RaNaye B.Dreier
Alabama Department of Environmental Management, Montgomery, AL, 36130 and Environmental Sciences Division, Oak Ridge National Laboratory*, Oak Ridge, TN 37831-6317

ABSTRACT

The Chickamauga Group (CH) located in Bethel Valley on the DOE Oak Ridge Reservation is comprised of limestones and interbedded shales. Five core holes (CH 1-5), oriented across strike, provide a cross section of the CH and were mapped for fracture density, orientation and cross-cutting relationships as well as lithologic variations. Correlation of structural and lithologic features with downhole geophysical logs and hydraulic conductivity values shows a relationship between lithology, fracture density and increased permeability in an otherwise low-permeability environment.

Structures identified as influential in enhancing hydraulic conductivity include contractional bedding plane and tectonic stylolites and extensional fractures. Three sets of extensional fractures are indicated by cross-cutting relationships and various degrees of veining.

Hydraulic conductivity values (K) for the five wells indicate two ground water flow systems in the valley. A shallow system (up to 150 feet deep) shows a range in K from 10E-4 centimeters per second to 10E-6 centimeters per second. Shallow horizons show more open fractures than are observed at depth, and these fractures appear to control the enhanced K in the shallow system. A subhorizontal interface that is not defined by pre-existing structures or a stratigraphic horizon separates the two flow systems. The deeper system ranges in K values from 10E-9 centimeters per second to 10E-5 centimeters per second. The higher K values at depth correspond to increased fracture density at lithologic contacts, zones of tectonic stylolitization and partially veined extension fractures.

INTRODUCTION

A conceptual model of ground water flow systems is difficult to produce in a complex stratigraphic and structural terrane. Local and regional variations in hydraulic conductivity values are commonly a function of heterogeneities in the geologic media and the dominant processes that lead to variable conductivities vary between sites. In the Valley and Ridge province of the Appalachian fold belt in eastern Tennessee the ground water flow is not homogeneous but is influenced by fracture networks and stratigraphic layering.

The objective of this study is to correlate hydrologic properties with detailed geologic fabrics and to investigate the influence of a complex geologic setting on ground water systems. Our purpose

* Research sponsored by the Office of Energy Research, U. S. Department of Energy, under contract No. DE-AC05-84OR21400 with Martin Marietta Energy Systems, Inc.

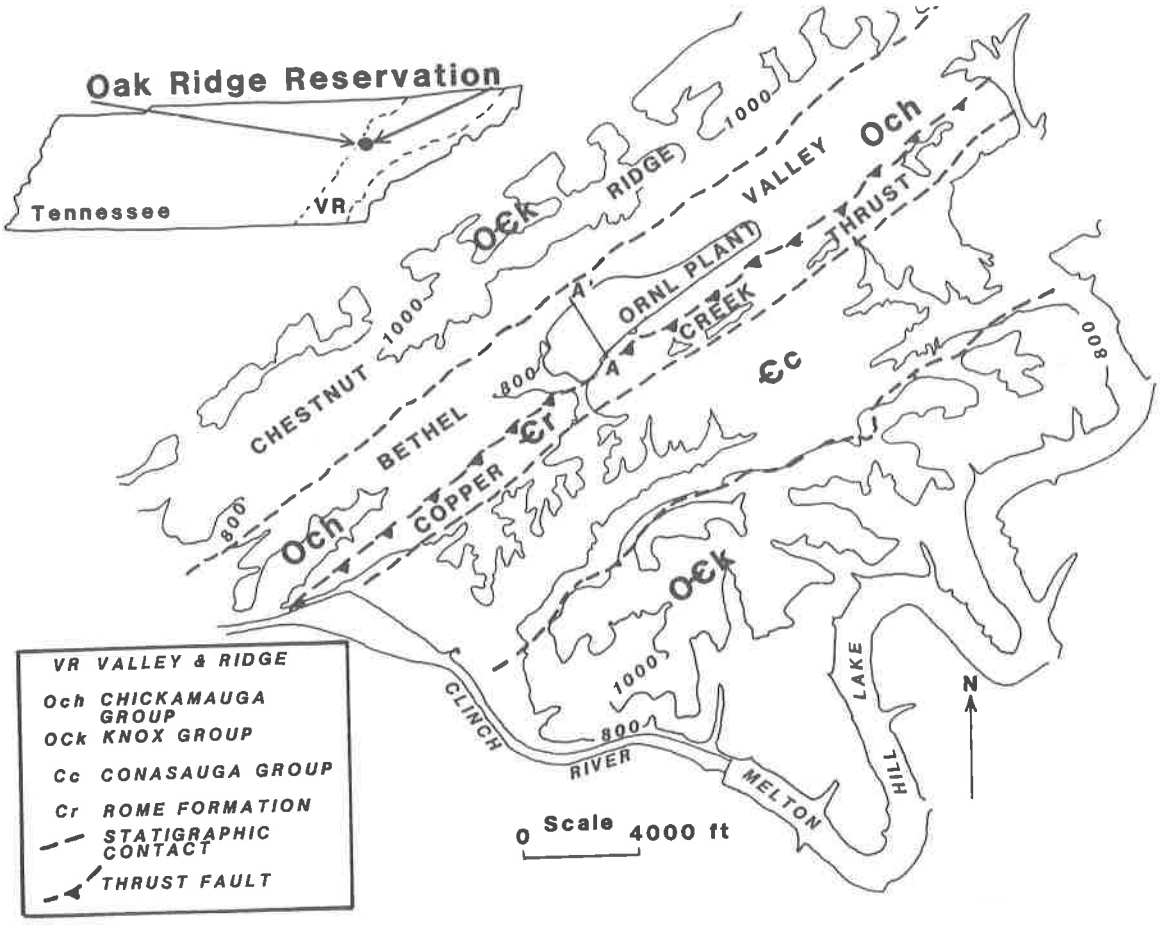

Figure 1 - Location map and regional geologic map of the Oak Ridge National laboratory and plant. The trend of core holes CH 1 through CH 5 and the line cross-section is designated by the line A - A' that is oriented across strike of the ORNL plant. Geologic map taken from Lee and Ketelle, 1988.

is to illustrate the use of structural and lithologic variations, coupled with hydrologic properties, to construct a conceptual flow model in a complex terrane.

The study area is located on the Department of Energy (DOE) Oak Ridge Reservation (ORR) in eastern Tennessee (fig. 1). The area consists of Cambrian and Ordovician rocks that have been stacked and transported to the northwest along thrust faults that ramp up from a basement detachment. This study focuses on the Middle Ordovician Chickamauga Group that lies within the White Oak Mountain thrust sheet, below the Copper Creek thrust fault in Bethel Valley (fig. 1).

Stockdale (1951) identified specific units within the Chickamauga Group on the ORR and assigned an informal alphabetic classification to the units, A through H. The eight formations are subdivided into facies c through t (fig. 2). Units Aa, Ab, Ad, Ae, Af, C, D, E, and G are massive, nodular, ribbon, and mottled limestones with interlayered, thin terrigenous clastic facies and chert beds. Units Ac and d, B, and F are comprised of calcareous maroon shales with interlayered gray siltstone and gray stylolitic limestone.

Lozier and Pearson (1987a) proposed an overall flow pattern for the Chickamauga Group in Bethel Valley to be downward from the recharge areas of Chestnut Ridge and the exposed Copper Creek thrust and upward in Bethel Valley (fig. 1). The water table in Bethel Valley roughly follows the topography and ranges in depth from 1 foot to as much as 35 feet near a ground-water divide (Webster, 1976). Recharge is confined to the White Oak Creek drainage basin and occurs primarily

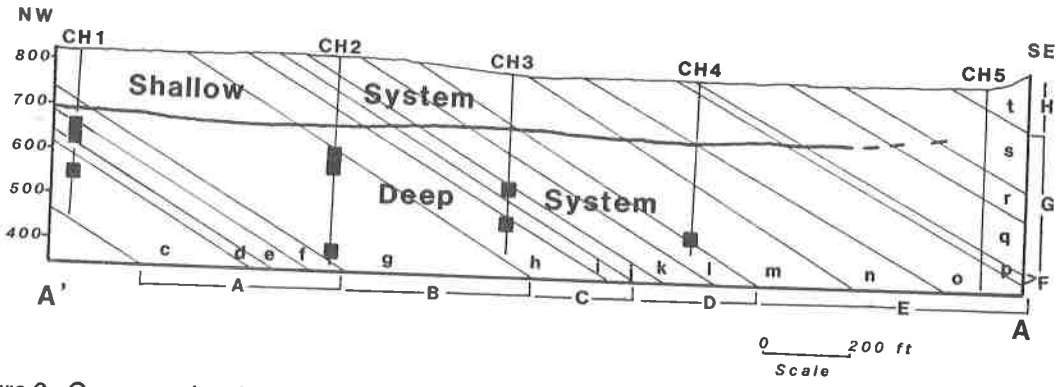

Figure 2 - Cross section A - A' of the Chickamauga Group from northwest to southeast across Bethel Valley. The cross- section shows depth of core holes CH 1 through CH 5 and the subhorizontal interface that divides the shallow system from the deep system. The shallow system represents hydraulic conductivities measured down each core hole of 10E-6 centimeters per second or greater. The deep system represents hydraulic conductivities ranging from 10E-5 centimeters per second to 10E-9 centimeters per second. Black squares located along core hole lines in the deep system represent high conductivities ranging from 1.7E-6 centimeters per second to 2.3E-5 centimeters per second (refer to table 1). The cross section also shows major units A through H and the unit facies subdivision (c through t). Figure modified from Lee and Ketelle, 1988.

by infiltration through the soil mantle and seasonally from the creek when the water table recedes below creek level (Webster, 1976).

The influence that the Chickamauga Group stratigraphy and structure has on ground water movement and storage was addressed by Webster (1976), and Dreier and others (1988). Webster noted that limestones of the Chickamauga Group are one of the major water-bearing units in the White Oak Creek Basin and therefore not desirable for the burial of waste. Dreier and others (1988) suggested that Bethel Valley as well as other parts of the ORR have two ground water flow systems, and that local variations in hydraulic conductivity within the flow systems are controlled by geologic structures and stratigraphy.

METHODS

Five core holes (CH 1 through CH 5) sample the Chickamauga Group in Bethel Valley in the plant area of Oak Ridge National Laboratory. The core holes are aligned across strike (fig. 1, trend of core holes A-A') and range from 370 feet to 470 feet in depth (fig. 2). Lithologic investigations of the core and geophysical logs acquired from the core holes enhanced Stockdale's classification of the Chickamauga Group (Lee and Ketelle, 1988). In addition, straddle packer tests were run in the boreholes to determine hydraulic conductivities and potentiometric head levels (Lozier and Pearson, 1987a and b).

As part of this study, a detailed core analysis of structural features and stratigraphic variabilities was conducted. Structural features such as fracture type, orientation, relative movement, spacing between like fractures, density, width, length, secondary mineralization, and cross-cutting relationships were documented for every 10 foot interval. Stratigraphic variabilities such as color changes, bioturbation and the visual percentage of limestone to shale per 10 foot interval were documented.

The down-hole hydraulic conductivity (K) and static head (H) values were determined by straddle-packer tests at selected 35 foot intervals. Thirty-eight packer tests were completed for core holes CH 1 through CH 5 by Golder and Associates. The packer assembly consisted of 2 sliding-end pneumatic packers, a downhole pneumatically activated shut-in valve and three downhole vibrating wire pressure transducers (for a complete description see Lozier and Pearson, 1987a). Packer placement was determined by geophysical logs and a cursory mapping of the core by Golder

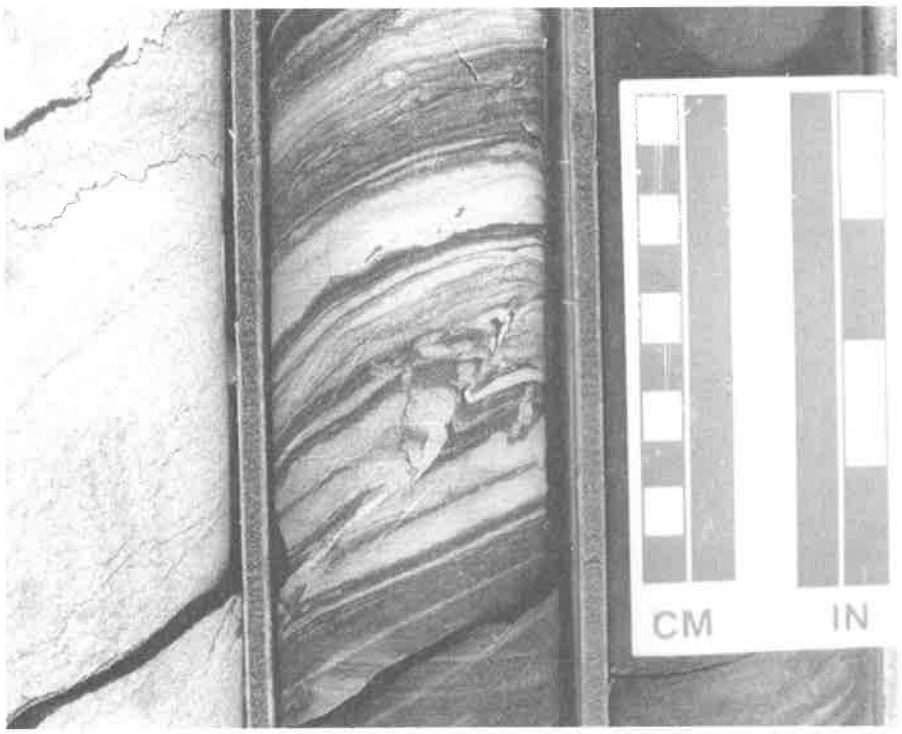

Figure 3 - Photograph of a high angle reverse fault showing drag of the bedding.

Figure 4 - Photograph of tectonic and bedding plane stylolites.

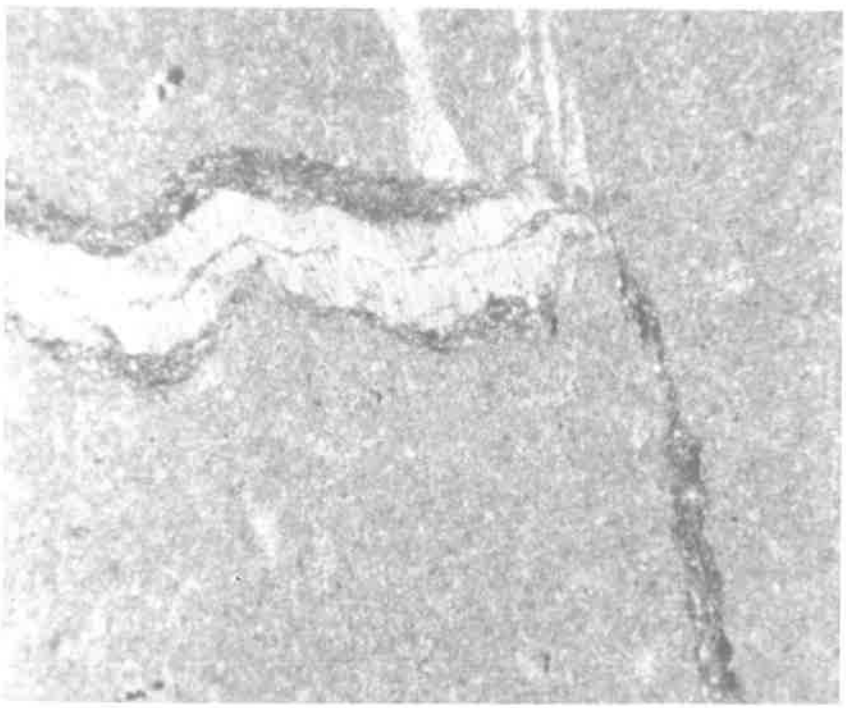

Figure 5 - Photomicrograph of a stylolite that has undergone extension and later filling of calcite. The growth of the calcite fibers from the stylolite walls towards the center of the fracture is clearly illustrated. Field of view is 3 mm x 2 mm.

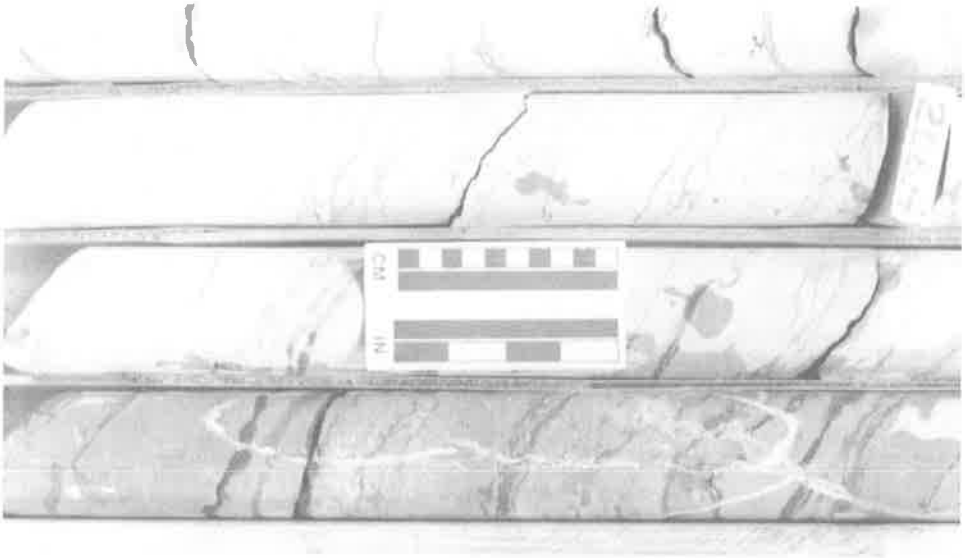

Figure 6 - Photograph of cross-cutting carbonate vein filled fractures.

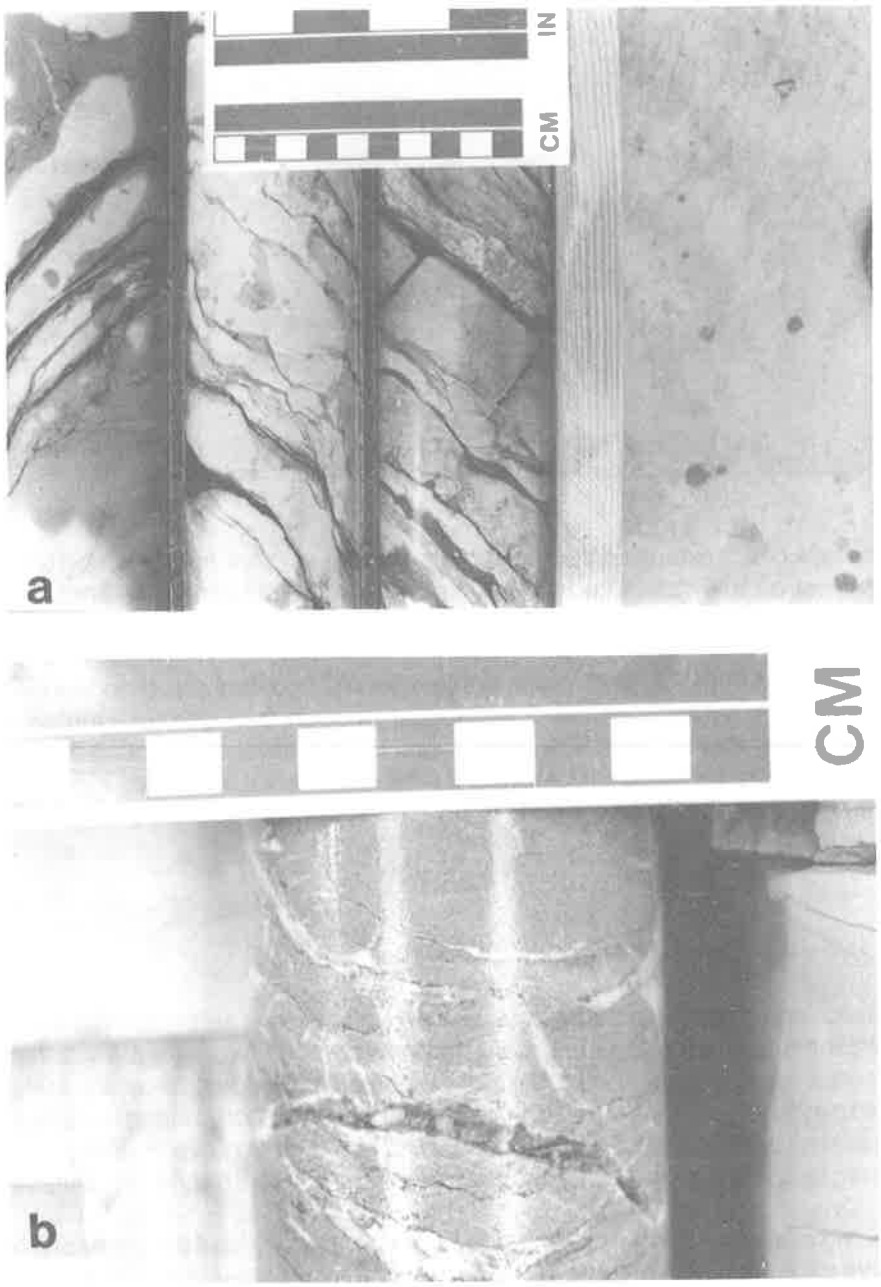

Figure 7 - Photographs of vugs formed (a) from the dissolution of carbonate veins along fractures and (b) formed from the incomplete filling of an extension fracture.

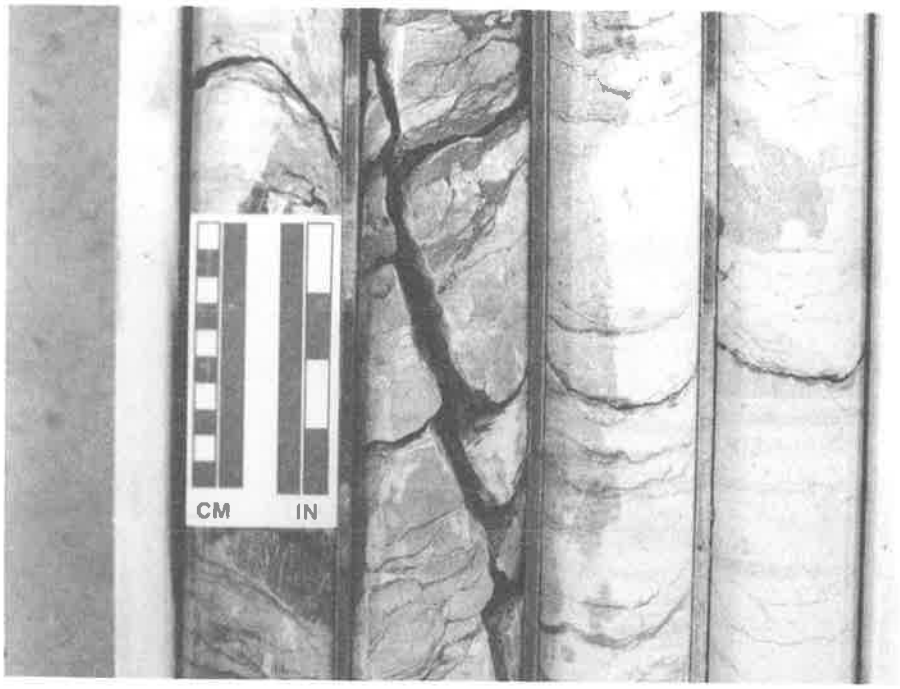

Figure 8 - Example of the extension fractures that cross-cut all other fractures and have a coating of carbonate crystals on the walls. The fractures are oriented parallel to strike and perpendicular to bedding.

Associates (Lozier and Pearson, 1987a). Natural gamma ray, spontaneous potential (SP), single point resistance, long-short normal resistivity, epithermal neutron and gamma-gamma compensated density logs were available for each hole. Both K and H were determined using the Horner Method. A variable head analysis was used to determine K when the interval recovered too rapidly to allow for sufficient data collection (Lozier and Pearson, 1987a and b).

RESULTS

Structure

Both extensional and compressional mesoscale and microscale deformational features are seen within the Chickamauga Group. Compressional features consist of a conjugate set of steeply dipping and subhorizontal faults and bedding plane slip surfaces. The bedding plane slip surfaces generally develop in thin clay/shale partings within the limestone. Slip is also noted along bedding plane partings of the maroon shales, although less frequently. Faults at a high angle to bedding show reverse slip and locally drag bedding (fig. 3). At shallow levels (less than 150 feet depth) the planes are commonly iron-stained.

Bedding plane and tectonic stylolites are pervasive throughout the limestone lithologies and exhibit variable cross-cutting relationships with respect to each other (fig. 4). Bedding plane-parallel stylolites are commonly reactivated and show shear strain. Some tectonic stylolites cut across bedding plane stylolites whereas other examples truncate at, or are offset by, bedding plane stylolites. Reactivation of the bedding plane stylolites has also caused dilation along some cross-cutting tectonic stylolites. Secondary mineralization subsequently filled the dilated stylolites (fig. 5).

Extensional features consist of strike-perpendicular, strike-parallel and oblique extension fractures. Early stages of deformation formed discontinuous fractures that are completely filled with calcite and cross-cut each other (fig. 6). Vugs and cavities are a result of dissolution (fig. 7a) or

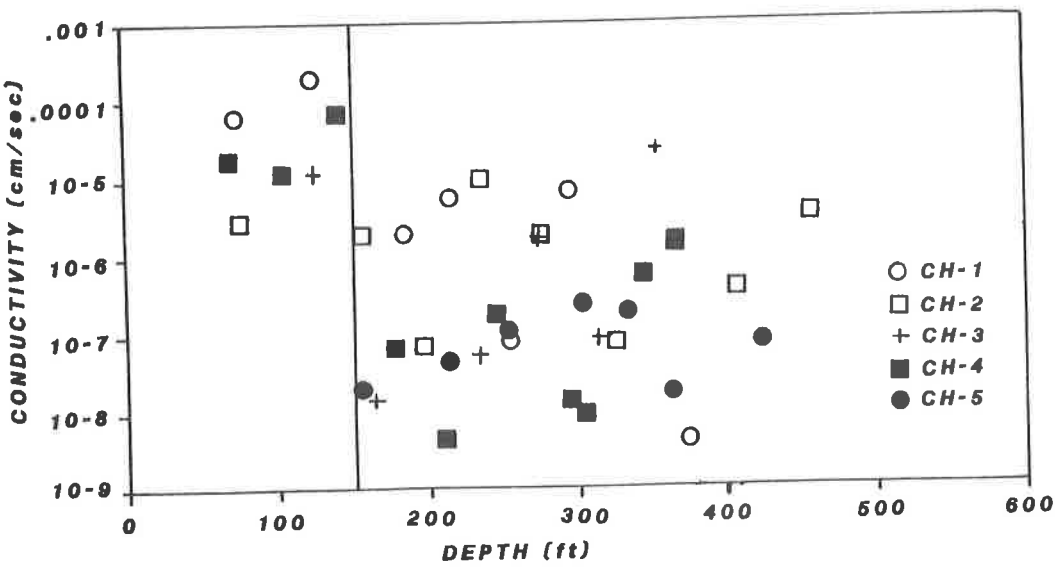

Figure 9 - Cross-plot of the hydraulic conductivity versus depth at 35 foot intervals down core holes CH 1 through CH 5. The vertical line at 150 foot marks the interface between the high conductivities of the shallow system and the variable conductivities of the deep system.

incompletely filled fractures (fig. 7b) and are locally oil stained. The veins and shear surfaces are cut by high angle extension joints that parallel strike and are perpendicular to bedding (fig. 8). The high angle joints have a rough surface coating of calcite, local (secondary) pyrite, and are discolored by iron staining down to a depth of 100 to 150 feet.

Zones of combined fracture types occur along the core and are referred to as broken zones. These zones are a combination of bedding plane shear and high angle extension joints and locally include low angle fractures. The zones vary from 6 inches to 2.5 feet thick and show no relationship to either depth or lithology. The fractures and fragments of rock are locally filled and cemented with mud and clay (in most cases infiltrated drilling mud), but are mostly uncemented.

HYDROLOGY

Hydraulic conductivity values (K) for boreholes CH 1 through CH 5 indicate both a shallow and a deep ground water flow system in the valley (fig. 9). The shallow flow system extends to depths of approximately 150 feet and has K values that range from 10E-4 centimeters per second to 10E-6 centimeters per second. The flow systems are separated by a subhorizontal interface. Hydraulic conductivity values for the deeper system range from very low (10E-9 centimeters per second) to very high (10E-5 centimeters per second). Average K-values for the Chickamauga Group are considered to fall within the range 10E-7 to 10E-6 (see fig. 9).

The transition depth between the two flow systems was initially determined by visual inspection. However, in order to support this qualitative classification, a segmented curved fit test was conducted on the K vs depth data (fig. 9) to independently identify the transition depth. In the model, two zero-slope lines are joined by a sloping line. The conductivity intercepts of the zero-slope lines and the length and slope of the join segment are then allowed to vary in order to make a best fit to the data. The transition zone between flow systems is determined by the depth range of the sloping line. Results of this test are identical to the visual inspection. The join between the two plateaus (zero- slope lines) occurs between 141.8 and 151.9 feet, both of which are between two neighboring data points at depths of 141.6 and 154.6 feet. Hence the transition depth is approximately 147.5 feet. In addition the conductivity values assigned to each plateau, which are representative of the different flow systems, are significantly different from each other. The shallow system plateau conductivity is 1.8E-5 centimeters per second with a 95% confidence level between 9.9E-5 centimeters per second

Table 1 - Conductivity values for the deep system. Deep system grouped by average, high, and low K-values. Shale percent and the number of stylolites per 35 foot interval are listed. Lithology abbreviations are i = interlayered, sh = shale, ls = limestone, silt = siltstone, mot = mottled.

COREHOLE	UNIT	DEPTH (feet)	K (cm/s)	LITHOLOGY	% SHALE	STYLOLITES
AVERAGE K						
1	Ac/Ad	220-255	8.2E-8	ish-ls	45	6
2	Ch	161-197	7.2E-8	mot	45	45
2	B	291-327	7.7E-8	sh	90	31
2	B	372-408	3.9E-7	sh-silt	80	0
3	Dk	200-235	5.3E-8	mot-ls	30	83
3	C/Dj	280-315	8.3E-8	mot-ls	50	55
4	E2	140-175	6.8E-8	sh	80	5
4	E2/E1	210-245	1.7E-7	mot	25	3
4	E1	310-345	5.6E-7	mot-ls	40	62
4	E1/D	332-368	1.4E-6	ish-ls,mot	40	69
5	G2	179-214	4.3E-8	ls		310
5	Gq/Gr	219-255	1.1E-7	mot-ls	25	350
5	Gq	269-305	2.4E-7	ish-ls	15	283
5	Gq	299-334	1.9E-7	mot-ls	15	363
5	E3	389-424	7.7E-8	ish-ls	10	325
LOW K						
1	A2	340-375	4.1E-9	mot-sh	95	0
3	D1	129-164	1.4E-8	ils-sh		181
4	En	176-212	4.6E-9	sh-mot	> 55	0
4	Em	261-296	1.3E-8	mot-sh	> 50	2
4	Em	270-306	8.6E-9	mot	> 45	2
5	Gs	119-155	2.0E-8	ils-sh	40	176
5	Gq	329-364	1.7E-8	ils-sh	50	330
HIGH K						
1	Ae	180-215	5.6E-6	ls	0	20
1	A2	260-295	6.9E-6	silt-sh	22	0
1	Ae/Af	150-185	1.9E-6	ls	0	32
2	Ch	121-157	1.9E-6	ls	0	26
2	B/Ch	210-237	1.0E-5	ls	0	76
2	B	241-277	1.8E-6	ls-sh	45	0
2	B	421-457	3.1E-6	silt-sh		0
3	Bj/Dk	239-275	1.7E-6	ls	5	218
3	Ch/Ci	319-355	2.3E-5	ls	0	11

and 3.2E-6 centimeters per second, whereas the deep system plateau conductivity is 2.2E-7 centimeters per second with a 95% confidence level between 4.9E-7 centimeters per second and 9.7E-8 centimeters per second.

Deep System

Average K-values for the deep flow system range from 4.3E-8 centimeters per second to 1.4E-6 centimeters per second (table 1). The values are primarily from units Eo/En (CH 4) and Gq/Gr (CH

Table 2 - Conductivity values for the shallow system. Shallow system K-values and units related to fracture density (that includes both extensional and compressional sets) and down-dip equivalent variables (starred rows). Two intervals in CH 4 do not have down-dip equivalent intervals available for comparison. Fractures measured as the number of fractures per unit depth interval.

CORE HOLE	UNIT	DEPTH (feet)	K (cm/s)	FRACTURES
1	B	40-75	2.2E-5	95
*2		375-410	3.9E-7	87
1	B	90-125	2.0E-4	75
*2		421-457	3.1E-6	100
2	Dj	40-75	2.7E-6	98
*3		240-275	1.7E-6	48
3	Em/D	l90-125	1.2E-5	112
*4		332-368	1.4E-6	150
4	E3	36-71	1.8E-5	176
*5		390-425	7.7E-8	117
4		71-107	1.2E-5	140
4		107-142	7.0E-5	103

5) as well as from units B, Ch (CH 2), Dk/Dj (CH 3) and Ac/Ad (CH 1) (see fig. 2 for unit subdivision locations). Lithologic characteristics for these units range from massive shales with interbedded fine-medium grained limestone beds (unit B and Ac/Ad) to nodular olive gray limestone with shaley interbeds and partings that may include thick (0.10 to 0.25 inch) undulose stylolites (units Gq, Gr, Eo, En). The amount of shale in the intervals ranges from 15% to 80%.

In the deep system, the correlation of structural and lithologic features with downhole geophysical logs and hydraulic conductivity values shows a relationship between lithology, dissolution features, and increased permeability. A decrease in shale content and a relative increase in stylolite development can be roughly correlated with an increase in K (table 1). For example, the interval from 140 - 175 feet in core hole CH 4 has a shale content of approximately 80% and a K of 6.8E-8 centimeters per second. In the same borehole the K values increase to 5.6E-7 centimeters per second for the interval from 315-350 feet, which has an average shale content of 40%. Stylolite density also increases within these intervals from 5/interval at 140 feet to 62/interval at 315 feet.

Minimum K-values in the deeper system range from 4.1E-9 centimeters per second to 2.0E-8 centimeters per second. These low values are representative of shale rich facies (shale content ranging from 40% to 95%) of Ac (CH 1), Dl (CH 3), En/Em (CH 4) and Gs/Gq (CH 5) (table 1). The rocks consist of mottled limestones with dark shale layers (Ac, En, Em), gray nodular stylolitic limestones with thick black shale layers (Dl), and limestone layers interbedded with massive shale (Gs, Gq). Stylolite density in the low K intervals is generally low except for units Dl, Gs and Gq in which the density is moderate to high but consists of thick irregular undulose stylolites or closely spaced wispy laminae. The minimum K-value (4.1E-9 centimeters per second) is in a shale-rich mottled limestone that contains approximately 90% shale for half of the interval and has no stylolites.

The maximum K-values for the deep system range from 1.7E-6 centimeters per second to 5.6E-5 centimeters per second and are determined from units Ae/Af (CH 1), Ch, B (CH 2) and Dj/Dk, Ch/Ci (CH 3). With the exception of unit B in CH 2, the lithologies consist of massive nodular and laminated limestones with 5% to 22% shale content and a generally high percentage of stylolite development. Dissolution vugs developed in carbonate veins are also characteristic of these limestones. High values of conductivity are considered to be a function of the low shale content in addition

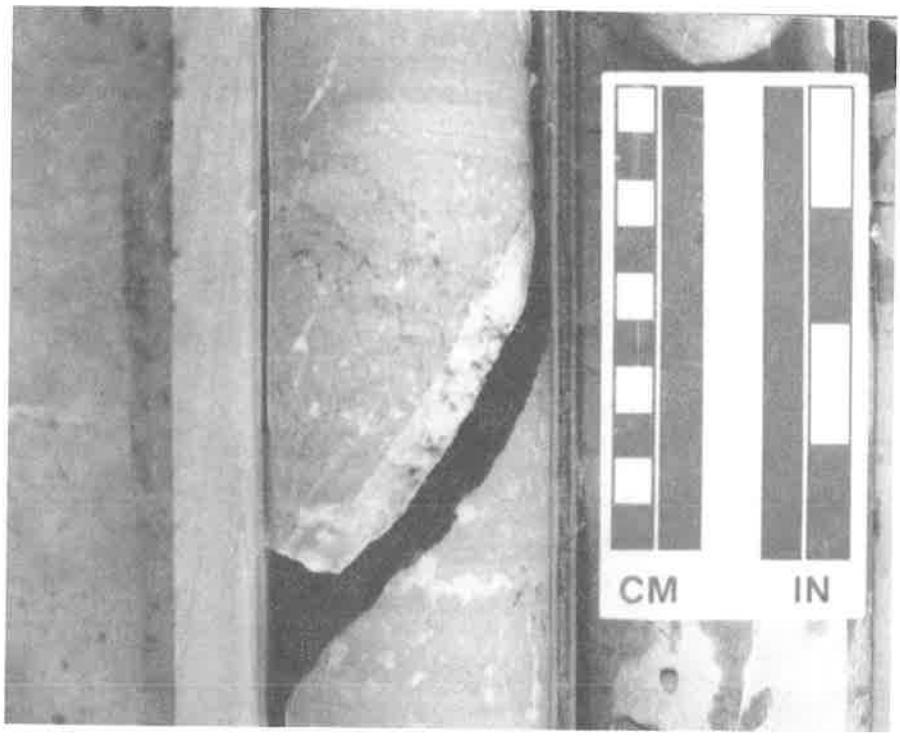

Figure 10 - Photograph of a recracked fracture after vein filling in the shallow system.

to a high stylolite density. For example, unit Ae (CH 1, 180-215 feet) and unit B/Ch (CH 2, 201-237 feet), both of which are stylolitic limestones with no shale, show K's of 5.6E-6 centimeters per second and 1.0E-5 centimeters per second, respectively (table 1). High permeability in unit B and A2 is a function of thick (5 feet to 10 feet thick) interbedded relatively pure calcilutite and stylolitic limestone layers within the maroon shales.

Shallow System

In the shallow system (less than 150 feet deep) the high conductivities are influenced not only by shale and stylolite density but also by the presence of open fractures. K-values measured from CH 1 - CH 4 range from 2.0E-4 centimeters per second to 2.7E-6 centimeters per second; CH 5 was not sampled at shallow levels (table 2). The packed-off intervals are correlative to stratigraphic horizons that showed either average or high conductivities at depth (table 2). The lithologies are primarily a stylolitic limestone such as Dj (Ch 2), Em/Dl (CH 3), and E3 (Ch4), but also include massive shales of unit B (CH 1), which are interlayered with a calcilutite and limestone.

In addition to features observed in the units at depth, the shallow system shows a higher density of open fractures, separated stylolites, recracked veins and iron staining on fracture and bedding plane surfaces. The importance of open fractures or the amount of dilation of a fracture is shown in unit B (CH 1, 40 - 75 feet) and unit Em/Dl (CH 3, 90 - 125 feet). Unit B, a massive maroon shale with a K value of 2.2E-5 centimeters per second, contains three broken zones in which there is a high degree of dilation. Bedding plane fractures, extension fractures and low angle shear fractures all contribute to the broken zones and show total separation of the fracture walls as well as iron staining on the fracture surfaces. The correlative unit at depth (CH 3, 375 - 410 feet) has approximately the same to slightly lower overall fracture density and a lower K value of 3.9E-7 centimeters per second. The fractures are not closely spaced or interconnected as is common in broken zones and less than 25% of the fractures show total separation. There is no iron staining on the fracture surfaces.

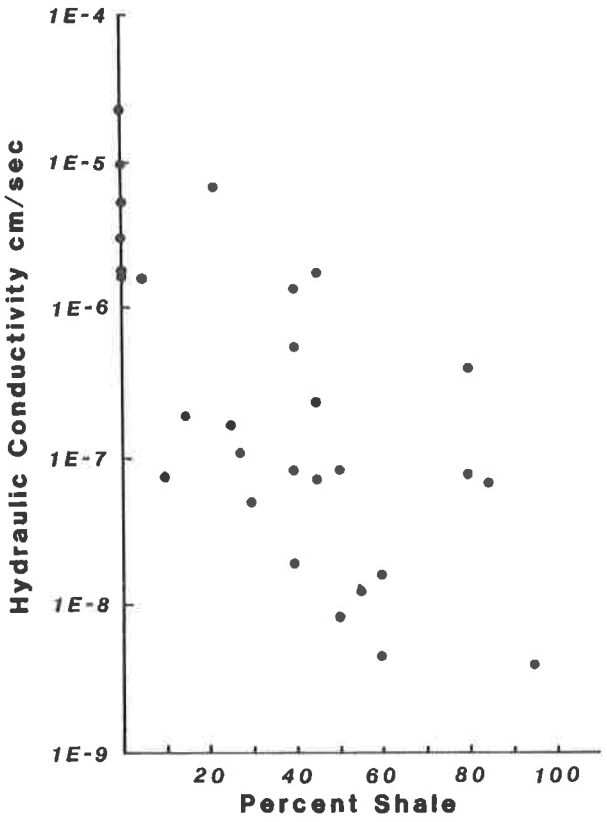

Figure 11 - Cross-plot of the deep system hydraulic conductivities versus the percent shale at 10 ft intervals. The plot shows an inverse relationship of conductivity versus shale percentage.

Em/Dl, a mottled to stylolitic limestone with a K value of 1.2E-5 centimeters per second, contains bedding plane, extension and low-angle shear fractures that show total separation of the fracture walls. The fractures occur both as broken zones and as bedding plane fracture zones. Irregular breaks also occur along bedding plane and tectonic stylolites. The correlative unit at depth (CH 4, 335- 370 feet) has a high density of fractures, however, few fractures show complete separation or significant dilation and the K value is 1.4E-6 centimeters per second or an order of magnitude smaller.

Units Dj and E3 have a higher density of fractures at shallow levels than the correlative intervals at depth. Dj (CH 2, 40 - 75 feet, K = 2.7E-6 centimeters per second) has approximately twice as many fractures as its down-dip equivalent in CH 3 (240 - 275 feet, K = 1.7E-6 centimeters per second: table 2). Contributing to the higher density is a broken zone (42.5 - 47.2 feet) made up of bedding plane and extension fractures. The fractures are iron-stained and recracking of previously formed fractures is evident at 70 feet where a vein has been broken away from the fracture wall and the new fracture surface subsequently iron stained (fig. 10). In unit E3 (CH 4, 35 - 70 feet, K = 1.8E-5 centimeters per second) the rock contains approximately a third more fractures than at deeper levels (CH 5, 390 - 425 feet, K = 7.7E-8 centimeters per second: see table 2). The shallower interval contains broken zones consisting of bedding plane, extension and shear fractures that cross-cut each other and show total separation or dilation. Stylolites are separated and give the appearance of irregular breaks that have a film of carbonate coating the surface of insoluble residue.

DISCUSSION

Deep System

Potential channels for fluid flow in carbonate rock include bedding planes, stylolites and fractures. Tectonic deformation or subsequent unloading can result in the formation of fractures. In addition, separated or open stylolite seams may later be partially filled with cement or act as an open conduit of flow (Bathurst and Land, 1986). A network of interconnected "opened" stylolites, vein openings and bedding planes will create a channelized flow path for fluids and a directional permeability in an otherwise low permeability and low porosity rock (Nelson, 1985; Rye and Bradbury, 1988).

Conductivities at depth in Bethel Valley are a function of both structure (eg., stylolite density) and lithology (ie., shale content). Conductivity is considered to be enhanced by the presence of both bedding plane and tectonic stylolites. The interconnectivity of cross-cutting stylolites and the coatings of insoluble residue provide pathways and a secondary permeability for fluid migration that has caused dissolution in veins.

The inverse relationship between shale percentage and conductivity for all the intervals within the deep system is shown in Figure 11. Bathurst and Land (1986) have noted that ten percent or greater clay content in a carbonate can inhibit stylolite formation. Therefore in the rocks with low and average conductivities the shale may serve the dual purpose of (1) a net reduction in permeability and (2) inhibiting the formation of stylolites. Without the stylolites the rock is essentially sealed and has few pathways along which fluids can flow.

Shallow System

Conductivities at shallow levels are a function of lithology and a higher density of fractures as well as recracking and dilation of previously formed fractures and stylolites. Conductivities that range from average to high at depth remain high for up-dip equivalent units in the shallow system and exceed the K-values for the deeper system. The increased K-values can be partly attributed to the same factors that affected the lower system (ie., stylolite density and shale content). Furthermore, the increased K- values in the shallow system reflect the correlation between fracture density and the degree of fracture and stylolite dilation.

The presence of dilated stylolites, recracked veined fractures and broken zones suggests a tensional stress that has reactivated previously formed features that were stable at depth. The subhorizontal interface that divides the deep system from the shallow system may represent the interface along which uplift and subhorizontal stretching occur during unloading (Suppe, 1985; Price, 1968).

Iron stains, found at a maximum depth of 150 feet in CH 1 and from 50 feet to 100 feet in CH 2 and CH 3, occur below the water table, which ranges from 1 - 35 feet below land surface. The presence of fresh pyrite (FeS_2) at depths below 150 feet (CH 1) or 80 feet (CH 4) indicates an insitu source for iron that may be carried in the ground water and precipitated upon mixing with oxidized water at shallow depths (less than 150 feet). Iron stain below the water table indicates mixing of reduced, iron saturated water (possibly from the deep system) in an oxidizing flow environment. The zone of mixing is marked by the shallow system interface and is a result of higher conductivities enhanced by a greater permeability from dilated fractures and stylolites.

SUMMARY

1. There are two ground water systems in Bethel Valley Chickamauga Group, a shallow and a deep system.
2. The interface between the shallow and deep system is not a function of stratigraphy or previously existing structures, but marks the depth of unloading structures and mixing between oxidized and reduced waters.

3. High conductivities in the deep system are a function of low shale content and stylolite formation in the pure limestones and are independent of fracture density or type.
4. High conductivities in the shallow system are a function of low shale content and fracture density in the form of recracked veins and stylolites.

ACKNOWLEDGEMENTS

Research sponsored as a Faculty Research Grant by the Office of Energy Research, U. S. Department of Energy, under contract No. DE-AC05-84OR21400 with Martin Marietta Energy Systems, Inc. We are grateful to Joel Melville for helpful comments and discussions and John J. Beauchamp for helping with the statistical analysis.

REFERENCES

Bathurst, R.G.C., and Land, L.S., 1986, Carbonate depositional environments modern and ancient Part 5: Diagenesis I: Colorado School of Mines Quarterly, vol. 81, no. 4, p. 1-25.

Dreier, R.B., Lutz, C.T., Toran, L.E., and Bittner, E., 1988, Fracture and hydraulic conductivity investigation in a complex low permeability geologic environment: [abstract] Ground water, vol. 26, no. 6, p. 789.

Lee, R.R., and Ketelle, R.H., 1988, Subsurface geology of the Chickamauga Group at Oak Ridge National Laboratory: Oak Ridge National Laboratory, ORNL/TM-10749.

Lozier, W.B., and Pearson, R., 1987a, Installation of packers and hydraulic testing of core holes CH 1 through CH 5 ORNL plant area: Oak Ridge National Laboratory, ORNL/sub/86-32136/3/vol. 1.

_____,1987b, Installation of packers and hydraulic testing of core holes Ch 1 through Ch 5 ORNL plant area: Oak Ridge National Laboratory, ORNL/sub/86-32136/3/vol. 2.

Nelson, R.A., 1985, Geologic analysis of naturally fractured reservoirs: Contributions in Petroleum Geology and Engineering, vol. 1.

Price, N.J., 1968, Fault and joint development in brittle and semibrittle rock: Pergamon Press.

Rye, D.M., and Bradbury, H.J., 1988, Fluid flow in the crust: an example from a Pyrenean thrust ramp: American Journal of Science, vol. 288, no. 3, p. 197-235.

Suppe, John, 1985, Principles of Structural Geology: Prentice Hall, Inc.

Stockdale, P.B., 1951, Geologic conditions at the Oak Ridge National Laboratory (X-10) are relevant to the disposal of radioactive waste: ORO-58, Department of Energy, Oak Ridge, Tennessee.

Webster, D.A., 1976, A review of hydrologic and geologic conditions related to the radioactive solid-waste burial grounds at Oak Ridge National Laboratory, Tennessee: United States Geological Survey Open-file report 76- 727.

OCCURRENCE AND SOURCE OF NATURAL RADIOACTIVITY IN GROUND WATER FROM THE UPPER FLORIDAN AQUIFER IN THE APALACHICOLA EMBAYMENT-GULF TROUGH AREA, GEORGIA

Lee L. Gorday and Madeleine F. Kellam
Georgia Geologic Survey
19 Martin Luther King Jr., Dr., S.W.
Atlanta, GA 30334

ABSTRACT

The Upper Floridan aquifer in southwestern and south-central Georgia locally yields ground water containing elevated levels of natural radioactivity. Gross-alpha activity levels in excess of 100 picocuries per liter, most contributed by Radium-226, have been reported. The radioactivity is associated with the presence of the Apalachicola Embayment and Gulf Trough, the buried remains of a paleomarine channel system on the Atlantic/Gulf Coastal Plain.

The presence of radioactivity in ground water from the Upper Floridan aquifer is controlled by the depositional history of the embayment-trough. Phosphatic pellets in Miocene sediments overlying and confining the aquifer contain Piedmont-derived Uranium-238 in their crystal structure and in uraniferous inclusions. Oxidizing waters entering the confining layer mobilize Uranium-238, which is soluble under oxidizing conditions. The uranium-enriched waters enter the aquifer and carry the uranium in solution until reducing conditions are encountered. The embayment-trough provides reducing conditions in two ways: 1) by the decay of organic matter trapped in sinkholes within the top of the Oligocene limestones and in the deepest portions of the channel; and 2) by long ground water residence time resulting from sluggish flow through the dense, thickly confined limestones that compose the aquifer in the embayment-trough.

Thus, uranium-enriched ground water entering the aquifer encounters reducing conditions, and uranium-bearing minerals are deposited on the aquifer matrix. The uranium then decays to Radium-226, which enters the ground water.

INTRODUCTION

The Floridan aquifer system is the most widely used aquifer in the Coastal Plain of Georgia. It is composed of a thick sequence of permeable limestones, ranging in age from Paleocene to early Miocene. Throughout most of its extent in Georgia, the aquifer is confined above by clastic and carbonate rocks, mostly Miocene in age.

The hydrogeology of the Upper Floridan aquifer in southwestern and south-central Georgia is dominated by the presence of a subsurface geologic feature known as the Apalachicola Embayment and by its narrow, northeastward extension, the Gulf Trough (fig. 1). Within the Gulf Trough and Apalachicola Embayment, both the quality and quantity of water available from the Floridan aquifer system are reduced. Of particular interest is the presence of elevated levels of natural radioactivity in ground water, most contributed by Radium-226. The presence of the radioactivity has necessitated the replacement of several public supply wells.

The purpose of this paper is to define the hydrogeologic controls on the origin and distribution of natural radioactivity in the Gulf Trough/Apalachicola Embayment area. A complex interaction of trough-embayment morphology and facies changes reduces the permeability of limestones of the Floridan system in the study area. The reduced permeability, in turn, produces conditions favorable for the precipitation of uranium-bearing minerals on the aquifer matrix. Decay of these uraniferous minerals releases radium into ground water.

EXTENT AND ORIGIN OF THE GULF TROUGH-APALACHICOLA EMBAYMENT

The Gulf Trough-Apalachicola Embayment extends, in Georgia, from the extreme southwest corner of the State northeastward to central Bulloch County (fig. 1). The feature is sinuous and trough-shaped, widest at the southwest and narrowing northeastward. The Gulf Trough-Apalachicola Embayment channel system was produced by a marine current, the Suwannee Current, which was active in the study area from the middle Eocene through the early Oligocene (Huddlestun and others, in press). This current flowed northeastward from the Gulf of Mexico to the Atlantic, inhibiting sedimentation in the Apalachicola Embayment and Gulf Trough during the late Eocene (fig. 2a). Rising sea level during the late Oligocene and Miocene caused the cessation of the current. Filling of the trough-embayment occurred during the Oligocene and early Miocene (fig. 2b).

The Suwannee Current controlled sedimentation in the Gulf Trough and Apalachicola Embayment from late Eocene through early Miocene. As a result, the Floridan aquifer system in the trough-embayment changes character. Thick sequences of dense, relatively impermeable, deep-water limestones replace the more permeable limestones which are present outside the trough-embayment. Overlying the aquifer system in the trough-embayment are thick clastic deposits of Miocene age, also relatively impermeable. These factors combine to reduce the permeability of the aquifer in large portions of the trough-embayment area.

RADIOACTIVITY OF GROUND WATER IN THE GULF TROUGH-APALACHICOLA EMBAYMENT

Elevated levels of radioactive elements are closely associated with the Gulf Trough-Apalachicola Embayment (fig. 3). Several public supply wells have yielded water that exceeds drinking water standards for natural radioactivity and have been plugged or reconstructed as a result (Kellam and Gorday, in press). In other cases, water from affected and unaffected wells is combined in the municipal water system, and the mixed water then meets drinking water standards.

Radioactivity is a product of the unstable decay of a number of different naturally occurring radioactive isotopes. The Georgia Rules for Safe Drinking Water specify Maximum Contaminant Levels (MCLs) for several specific isotopes as well as for total particle activity. Within the study area, two parameters are known to exceed the MCLs: gross alpha activity and Radium-226. Radium-226 is a part of the Uranium-238 decay series. Radium-226 decays to form Radon-222 and a succession of short-lived daughter products. The activity levels of these isotopes vary. Some, like Uranium-238, have low alpha-particle activity, while others, such as Radium-226, are shorter-lived and have high activity levels. All municipal water systems are tested for gross alpha activity, for which the MCL is 15 picocuries per liter (pCi/l), excluding uranium. Water samples which exceed 5 pCi/l gross alpha activity are then tested for combined activity of Radium-226 and Radium-228 (MCL 5 pCi/l). Both Radium-226 and 228 are of concern from a health standpoint because they can be ingested and can accumulate in the bones; daughter products of these isotopes are particularly harmful (Gilkeson and others, 1983). Laboratory results, shown in Figure 4, indicate that Radium-226 is the dominant alpha emitter in most of the samples. Additional contributions to the gross alpha activity are indicated for some of the samples, particularly those with lower activity levels. Little gross alpha activity is contributed by Radium-228. Because of the greater availability of data on gross alpha activity, and because most of that activity can be attributed to Radium-226, only gross alpha activity was mapped in this study, and it was used to approximate Radium-226 activity.

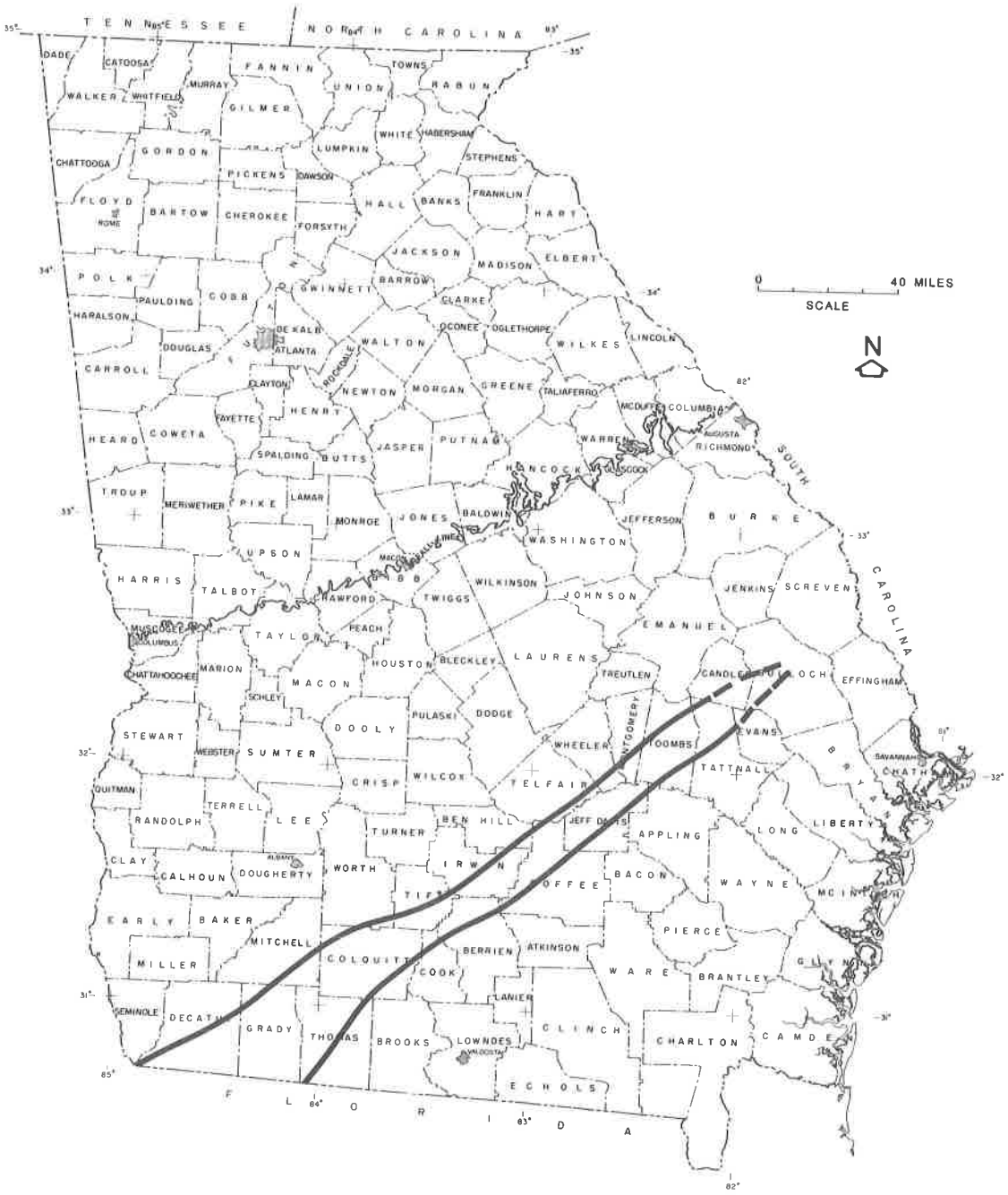

Figure 1 - Geographic extent of the Gulf Trough/Apalachicola Embayment.

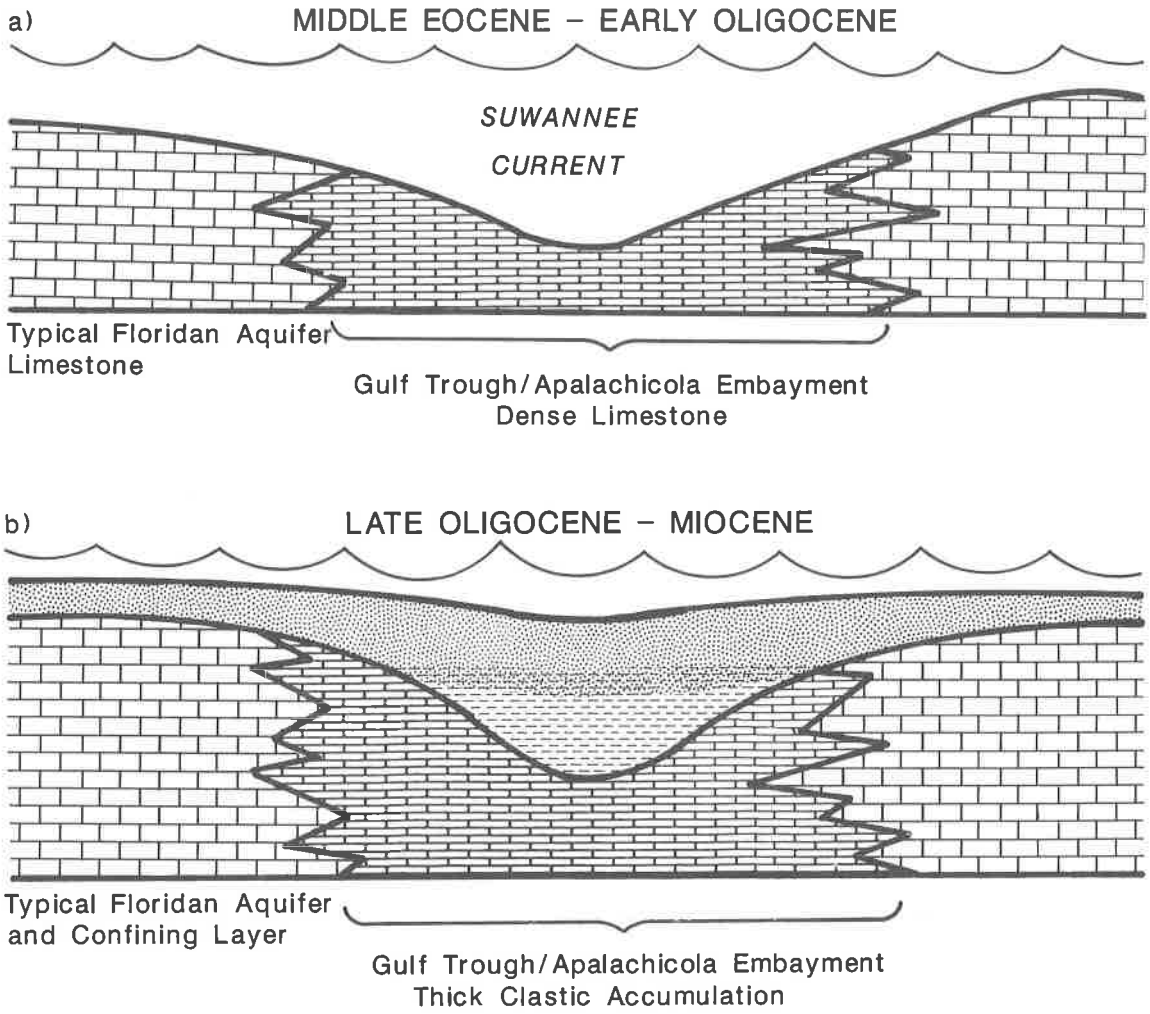

Figure 2 - Development of the Gulf Trough/Apalachicola Embayment. 2a. is a schematic cross section of the Gulf Trough/Apalachicola Embayment during the Middle Eocene through the Early Oligocene. 2b is a schematic cross section of the Gulf Trough/Apalachicola Embayment during the Late Oligocene and Miocene.

The two geographic areas that show the highest gross alpha activity are the Tift-Berrien Counties area and the Wheeler-Montgomery Counties area. The occurrence of radioactivity in these areas follows two separate patterns.

Radioactivity in the Wheeler-Montgomery Counties Area

High gross alpha levels in ground water can be associated with high gamma-ray activity resulting from the unstable decay of other radionuclides in the uranium decay series. Therefore, gamma-ray logs of water wells can help identify depth intervals within the wells which will produce water with high gross alpha levels.

Two distinct depth zones of elevated radiation can be identified on gamma-ray logs in the Wheeler-Montgomery Counties area. The upper zone occurs above the Floridan aquifer in the Miocene section. The lower zone of high gamma radiation occurs at the top of the Floridan aquifer system (fig. 5). Several public supply wells in the area produced water which exceeded drinking water standards for radiation. The cities of Alley, Alamo, Mount Vernon, and Tarrytown drilled new

Figure 3 - Sites where gross alpha activities in public water supply systems exceed the background level of 4 picocuries per liter (Kellam and Gorday, in press).

wells to replace those that yielded water with high radiation levels. The new wells were cased to greater depths in an attempt to exclude the radioactive zones. Most of these wells subsequently produced water which met standards, with one exception. The replacement well at Alamo was constructed prior to geophysical logging, and was cased to four feet above the base of the gamma-ray anomaly. Water from the well met drinking water standards for five years before the radiation again exceeded standards. In 1987, a third well was drilled and logged, and casing was installed to a depth below the gamma-ray anomaly. This well now produces water free from significant amounts of gross alpha activity.

Radioactivity in the Tift-Berrien Counties Area

High radiation levels in ground water from the Tift and Berrien Counties area are restricted to wells that are in or near the Gulf Trough; however not all of the wells within the trough produce radioactive

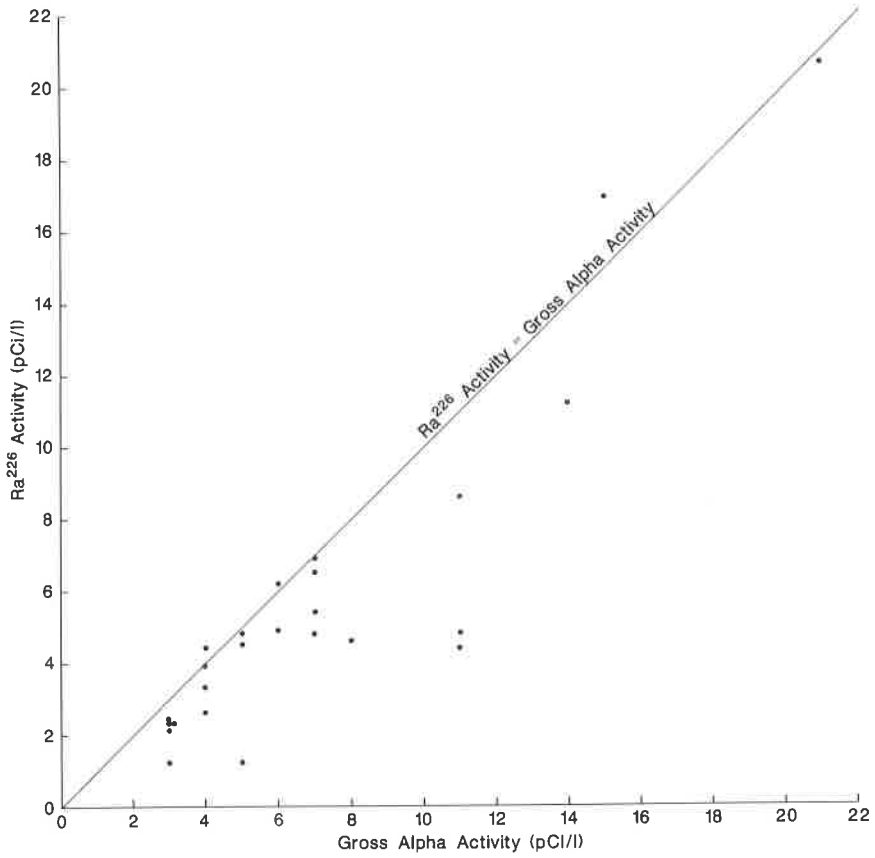

Figure 4 - Comparison of gross alpha activity with Radium-226 activity. Points that fall along the line of equal Radium-226 and gross alpha activities indicate samples for which Radium-226 is the dominant alpha emitter.

water. Highest levels (20 pCi/l) are found in the vicinity of Tifton, in Tift County, and Alapaha, in Berrien County.

The city of Tifton, on the north flank of the Gulf Trough, has removed municipal well 5 from production due to high radioactivity levels. The gamma log of this well shows large gamma anomalies at depths of 350 feet (cased), 495 feet, and 525 feet. The city replaced this well with municipal well 7, located 3400 feet to the northwest, farther from the trough. The gamma log of well 7 shows moderate gamma-ray activity at 190 feet (cased) and at 290 feet. The gross alpha activity of the water from this well is at or below background levels. Gross alpha activity of water from nearby municipal well number 4 has declined from 72 pCi/l to 41 pCi/l since well 5 was taken off line.

The city of Alapaha, which lies in the Gulf Trough, has two production wells, both of which produce water with higher than normal amounts of radioactivity. Gamma-ray logs of these wells show high gamma-ray activity between depths of 380 and 400 feet. A test well (GGS 3555) located south of the city (fig. 6) was drilled, logged, and sampled in an attempt to develop a new well to supply water to the city of Alapaha. An inflatable packer was used to isolate and sample discrete depth intervals. The packer was set at depths of 360, 375, and 381 feet. Tests of water samples collected from beneath the packer for each of these depths indicated gross alpha activities of 122, 122, and 102 pCi/l respectively. This well was not grouted because it was designed as a test hole. The well sat idle for several months prior to sampling, possibly allowing water from overlying strata to enter the aquifer through the open borehole. A gamma-ray log showed no discrete zones of high radiation within either the aquifer or the overlying strata.

A nearby domestic well, located 800 feet to the east of GGS 3555, produces water which meets drinking water standards, but this well is significantly shallower than the city of Alapaha test

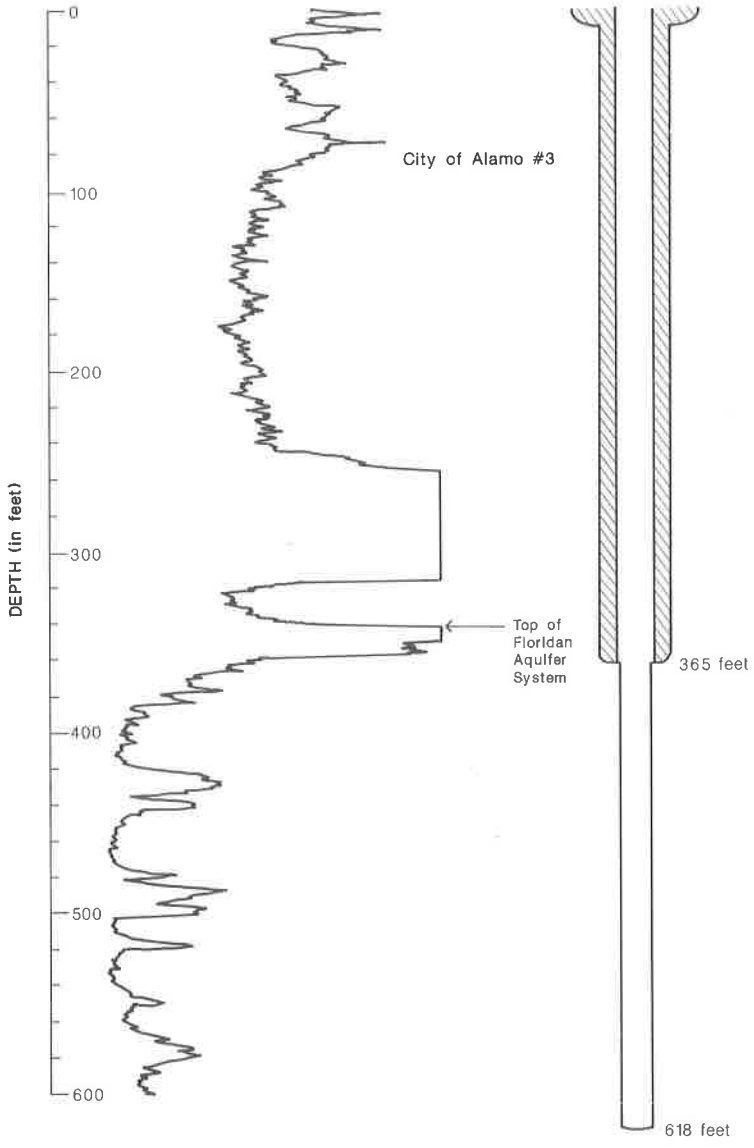

Figure 5 - Natural gamma log, City of Alamo well number 3. Gamma radiation increases to the right.

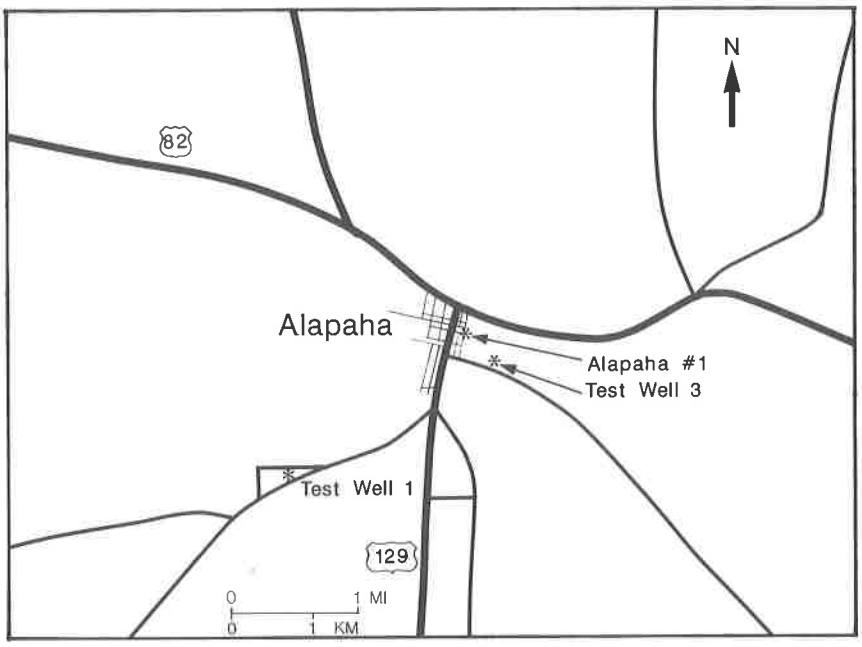

Figure 6 - Well locations, City of Alapaha

well. Although at the same land elevation, the domestic well is cased to 272 feet, whereas the test well is cased to 358 feet. Assuming that both wells are cased to the top of the aquifer, this means that there is a significant amount of relief on the top of the aquifer. Logs of the city of Tifton municipal wells also indicate that the top of the aquifer is irregular, and wells number 4 and 5, which produce water with higher than normal gross alpha activity, are located in areas where the top of the aquifer is low. Drillers in the Berrien County area also report that high radioactivity seems to be associated with low areas on the top of the aquifer.

SOURCE AND CONTROLS OF RADIOACTIVITY IN GROUND WATER IN THE STUDY AREA

Sources of Uranium

Uranium-bearing minerals are the ultimate source of the Radium-226 in ground water in the study area. Elevated radioactivity levels are geographically widespread, indicating that the source of the parent isotopes is also widespread. The Miocene and younger sediments in the Coastal Plain contain clastic sediments derived from the crystalline rocks of the Piedmont, which may include radioactive minerals such as monazite. Portions of the Miocene sediments are rich in phosphate minerals, which incorporate uranium in their crystal structure. Under proper conditions the uranium contained in these minerals can be leached and can enter the ground water.

Solubility of Uranium

Uranium is soluble under oxidizing conditions, such as those found in waters in recharge areas. Typically, ground water in recharge areas has relatively high levels of uranium, which has a low activity level (Korosy, 1984). As ground water enters reducing conditions, the uranium is deposited on the aquifer matrix, lowering concentrations of uranium in ground water. The uranium then decays, producing daughter products with high activity levels, such as Radium-226, which enter the ground water (Gilkeson and others, 1983).

Reducing conditions in an aquifer can be produced where ground-water flow is sluggish, or where reducing agents such as pyrite or organic matter are present in the aquifer. The Gulf Trough and Apalachicola Embayment provide these conditions. The thick sediments overlying the Floridan aquifer system in the Gulf Trough and parts of the Apalachicola Embayment retard the inflow of oxygen-rich water. In addition, the limestones that comprise the Floridan system in the trough and embayment are less permeable and contain more pyrite than their counterparts outside the feature. Finally, the top of the Oligocene section was exposed and eroded. The paleo-karst developed on this surface trapped fine-grained sediments, rich in organic debris.

Precipitation of Uranium

High radioactivity levels follow the trend of the Gulf Trough and Apalachicola Embayment, appearing most often in water from the lower Miocene section and the upper portion of the Floridan aquifer system. It is probable that reducing conditions produced in the Lower Miocene sediments and the Oligocene limestones of the Floridan system caused the precipitation of uranium on the aquifer matrix and overlying sediments. The Floridan aquifer system in the Wheeler-Montgomery-Toombs Counties area, though outside the Gulf Trough, is thickly confined and its upper surface karstic and irregular. Therefore it would also provide the reducing conditions necessary for the precipitation of uranium. Radioactive decay of the uranium would then contribute Radium-226 to the ground water.

Gilkeson and others (1984) and Michel and others (1982) demonstrate the importance of analyzing data on all isotopes in the decay series in order to develop a comprehensive model of the distribution of radioactivity in ground water. Thus, further delineation of the controls on the occurrence of Radium-226 will require more data on the distribution of the parent and daughter isotopes. However, the available information is useful in understanding the mechanism by which Radium-226 enters the ground water, and in identifying areas where high levels of natural radioactivity are likely to be encountered.

CONCLUSIONS AND RECOMMENDATIONS

High levels of natural radioactivity in ground water from the Floridan aquifer system are associated with the Gulf Trough and Apalachicola Embayment. The highest levels are found in the Wheeler-Montgomery Counties area, and in the Tift-Berrien Counties area.

The ultimate source of radioactivity in the ground water in this area is Uranium-238, probably derived from sources in or near the study area. The crystalline rocks of the Piedmont province to the north contain such uranium-bearing minerals as monazite, which were weathered and transported into the Coastal Plain. Also, the phosphate minerals of the Miocene sediments overlying the aquifer incorporate uranium in their crystal structure, and hence are another potential source. Uranium is soluble under oxidizing conditions and precipitates under reducing conditions. Oxidizing conditions in the recharge areas of the aquifer dissolves uranium from these sources and transports it until reducing conditions are encountered. A reducing environment provided by the limestones of the trough-embayment causes the precipitation of uranium-bearing minerals on the aquifer matrix. Reducing conditions in and above the aquifer are produced by a complex interaction of thick overburden, which causes sluggish ground-water flow, and an irregular upper aquifer surface, which traps organic matter. Once the uranium is deposited on the aquifer matrix, radioactive decay produces Radium-226, which enters the ground water.

Municipalities in the Gulf Trough-Apalachicola Embayment area can reduce the risk of producing radioactive water by siting their wells as far from the center of the trough-embayment as possible and by running gamma-ray logs on newly drilled wells to identify any radioactive zones. By installing casing through these intervals, the production of radioactive water can often be prevented.

REFERENCES

Gilkeson, R.H., Cartwright, K. Cowart, J.B., and Holtzman, R.B., 1983, Hydrogeologic and geochemical studies of selected natural radioisotopes and barium in ground water in Illinois: Champaign-Urbana, University of Illinois, Water Resources Center Research Report No. 180.

Gilkeson, R.H., Perry, Jr., E.C., Cowart, J.B., and Holtzman, R.B., 1984, Isotopic studies of the natural sources of radium in groundwater in Illinois: Champaign-Urbana, University of Illinois, Water Resources Center Report No. 187.

Huddlestun, P.F., Hetrick, J.H., Kellam, M.F., and McFadden, S.S., in press, Geology of the Gulf Trough-Apalachicola Embayment area, Georgia: Atlanta, Georgia Geologic Survey.

Kellam, M.F., and Gorday, L.L., in press, Hydrogeology of the Gulf Trough-Apalachicola Embayment area, Georgia: Georgia Geologic Survey, Bulletin 94.

Korosy, M.G., 1984, Ground-water flow patterns as delineated by uranium isotope distributions in the Ochlockonee River area, southwest Georgia and northwest Florida: Unpublished M. S. thesis, Tallahassee, Florida State University, Geology Department.

Michel, J., Cole, K.H., and Moore, W.S., 1982, Uraniferous Gorceixite in the South Carolina Coastal Plain (U.S.A.): Chemical Geology, vol. 35, p. 227-245.

GEOLOGIC CONTROLS ON RADON OCCURRENCE IN GEORGIA

L. T. Gregg
Atlanta Testing & Engineering, Inc.
Duluth, GA 30136
Gene Coker
United States Environmental Protection Agency
345 Courtland Street, N.E.
Atlanta, GA 30365

ABSTRACT

Conventional wisdom holds that high radon concentrations occur mostly in areas of thin and/or sandy soils underlain by granitic bedrock, that other soil conditions and bedrock lithologies are somehow exempted from or less prone to high radon concentrations, and that high radon levels in ground water represent an isolated phenomenon. Through a combination of geologic models and field measurements, each of the four geologic provinces of Georgia can be characterized for radon concentration. The results to date indicate that no area or geologic province should be exempted per se and that a careful study of site/area geology along with field measurement will yield dividends in understanding the occurrence of radon in soil and ground water.

The combinations of bedrock lithology and soil characteristics most likely to exhibit higher radon concentrations in Georgia, and throughout the Southeast, are a) granites, granodiorites, granite gneisses, pegmatites, mylonites, carbonaceous shales, phosphates, and monazite/heavy mineral placers, coupled with b) high to medium permeability soils such as gravels, sands, and uniformly-graded silts and sandy silts. Saprolite and surficial (alluvial) deposits may act as either a conduit or an impediment to radon migration, as may hydrogeologic characteristics and rock structures such as faults and joints/fractures.

Ground water levels as high as 840,000 picocuries per liter have been measured in private wells, but a representative average across the southern Piedmont is yet to be determined. A major ground water testing pilot program is underway by the EPA to measure radon, uranium, radium, lead-210, polonium, thorium, gross alpha, and gross beta concentrations for selected bedrock aquifer types.

INTRODUCTION

There are four radioisotopes to be considered in this paper: uranium, thorium, radium, and radon. The principal uranium isotope is U^{238}, which decays to Ra^{226}. Radium^{226} decays to Rn^{222}, which decays to polonium, bismuth and finally lead. The principal thorium isotope is Th^{230}, which decays to Ra^{228}. Radium^{228} decays to Rn^{220}, which decays to polonium, bismuth and finally lead. Because of its half-life of 3.8 days, Rn^{222} is of much more concern and interest than Rn^{220} (56 seconds half-life).

Radon is gaseous (the only gaseous radioisotope in the U and Th decay series) and therefore is highly mobile. It is an alpha and gamma emitter so its presence can be measured (usually with an alpha-particle measuring device). Radon is moderately soluble in water and its solubility decreases with increasing temperature. Radon does not combine chemically with other elements. These

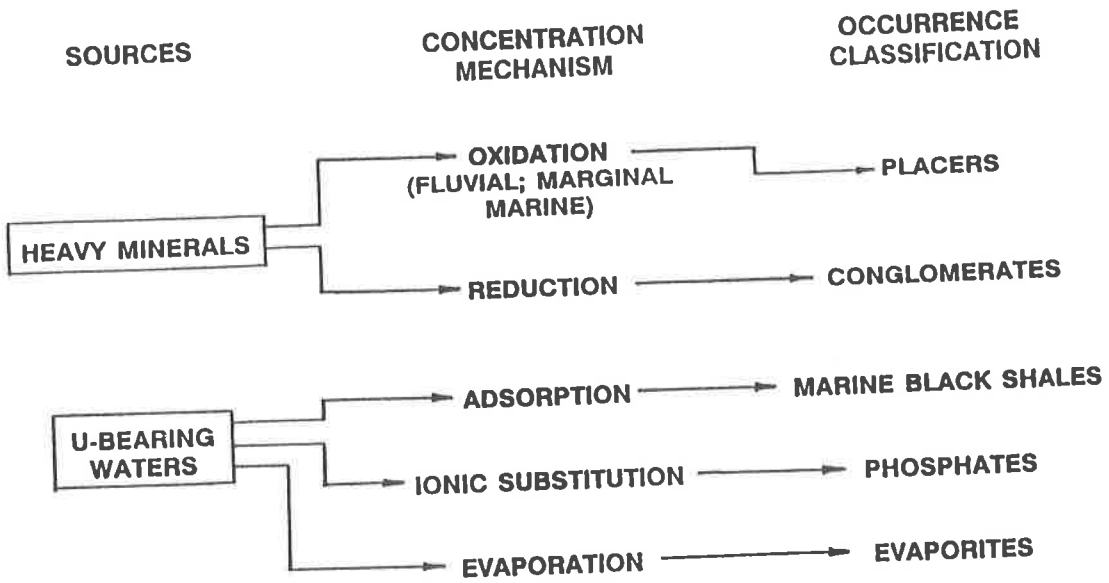

Figure 1 - Syngenetic uranium in sedimentary environments.

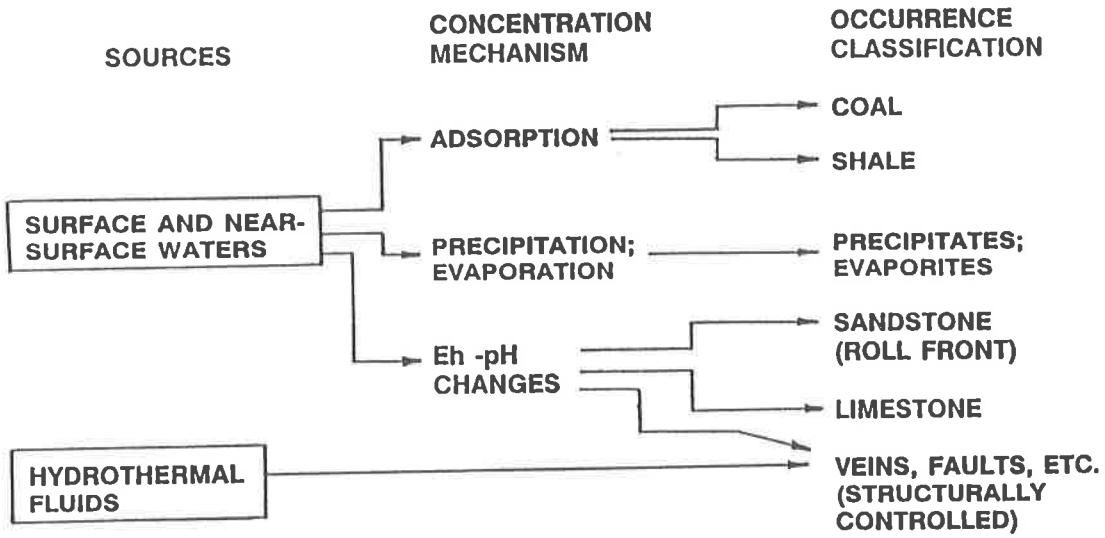

Figure 2 - Epigenetic uranium in sedimentary environments.

properties form the framework for our understanding of radon generation, occurrence and migration in rocks, soils, and ground water.

In considering the geologic setting of Georgia and the Southern Appalachians, the major structural and lithologic trends run from northeast to southwest, both above the Fall Line and below. The principal rock types in the Cumberland Plateau and the Valley and Ridge provinces are limestones, shales, and sandstones: igneous and metamorphic rocks such as granites, gneisses, and schists in the Blue Ridge and Piedmont provinces; and limestones, sandstones, phosphates, and unconsolidated sediments in the Coastal Plain.

URANIUM GEOCHEMISTRY

Uranium abundance (Durrance, 1986) typically ranges from 2 to 5 parts per million (ppm) in granites to as high as 9 ppm in nepheline syenites, from 0.5 to 2 ppm in the andesites and mafic rocks and much less in the ultramafic rocks to as high as 34 ppm in the Marcellus Shale (an analog of the Chattanooga Shale), and 120 to 140 ppm in the phosphates and phosphorites. Thorium shows similar ranges, as high as 50 ppm in granites.

Why is uranium so widely distributed? Uranium is polyvalent, with the three principal ions being +4, +5, and +6. It has a large ionic radius of 0.8 to 0.97 angstroms; it is highly active chemically; the hexavalent compounds are soluble and the tetravalent compounds are basically insoluble; and tetravalent uranium is isomorphic with Ca, Th, Zr, W, and Mo. This suite of properties results in a complex geochemistry.

During magmatic differentiation, uranium does not seem to form separate mineral precipitates. There is isomorphic substitution in some rock-forming minerals, but most importantly uranium tends to concentrate in late stage crystallization in silicic rocks and minerals such as granites and felsic volcanics, and through hydrothermal action in pegmatite dikes and veins. This is primarily due to its ionic radius and affinity for late-forming members in the reaction series such as quartz, potassium feldspar and muscovite. In igneous rocks, we feel the petrofabric of the rock is all important to uranium concentration. The petrofabric provides microstructural control of uranium deposition such as coatings around mineral grains, in microfractures and crystal cleavages (which provide a type of porosity for the uranium-bearing waters), and in inclusions. In felsic volcanics, both silicic and alkalic, uranium is highly dispersed so it is readily leachable. There is some concentration of uranium observed in ashes and tuffs and in cross-cutting dikes and veins.

In sedimentary rocks, uranium concentration is dependent upon the geochemical cycle: such mechanisms as oxidation-reduction, absorption, adsorption, precipitation, solution, formation of organic complexes, the relative mobility of the hexavalent and tetravalent ions, and the weathering of the uranium source and the transport of the weathered uranium. Figure 1 shows the processes controlling deposition of syngenetic uranium in the sedimentary environment. Through various concentration mechanisms -- oxidation, reduction, absorption, ionic substitution, and evaporation -- uranium concentrates in different sedimentary rocks. Figure 2 shows the processes controlling epigenetic uranium deposition. Concentration mechanisms here are primarily absorption, precipitation, evaporation, and changes in redox potential and pH. The structural control in veins and faults is influenced by both Eh-pH changes and hydrothermal fluids.

Figure 3 shows an idealized sequence in metamorphic rocks, where recrystallization results in a grain size increase, which results in porosity reduction, liquid-gas expulsion, and uranium loss into and concentration in fractures, shear zones, and lower pressure zones.

To summarize, the principal factors in uranium mobility and concentration are the uranium content of the source, the amount and rate of circulating water, climatic factors, pH and Eh, the presence or absence of complexing agents, and the presence or absence of sorptive materials.

RADIONUCLIDE MOBILITY

Uranium is much more mobile than its daughter product radium (Durrance, 1986). Uranium is quite mobile in an oxidizing environment and very immobile in a reducing environment, whereas radium is

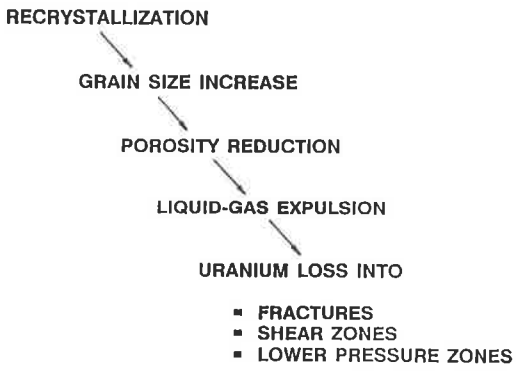

Figure 3 - Uranium in metamorphic rocks.

more mobile in a reducing environment and relatively immobile in an oxidizing environment. Radium tends to behave chemically somewhat similar to the alkaline earths such as calcium; oxidizing waters are much less likely to remove radium, and radium is most mobile in chloride-rich reducing waters.

Since radon is a gas, the oxidation-reduction environment is immaterial. Radon has two principal components to its movement: diffusion, which is generally thought to be a minor component, probably an average of about 1 meter from the source (which is a radium atom), and convection, which is the major component. Radon can move many meters through convection, but it has to be carried in some type of "geo-gas" that can be either a mixture of helium, nitrogen, methane, carbon dioxide and so forth, or ground water, or both.

Once radon is liberated (or "emanates") from its radium parent source, it will tend to migrate vertically toward the surface. High permeability soils will allow radon to much more readily permeate up toward the surface than will low permeability soils, such as soils high in the clay minerals with resultant high porosity and low permeability. Figure 4 shows a cross-section from surface soils down through massive saprolite, structured saprolite, partially weathered rock and fresh bedrock. We feel that the percentage of removal of uranium, thorium and radium by circulating meteoric waters is highest in the upper soil zones and lower in the saprolite and bedrock zones, so that the percentage concentration of uranium, thorium, and radium is low in the upper soil zones and high in the structured saprolite and bedrock zones. In those latter two zones, iron and manganese tend to concentrate and act as uranium scavengers. Also, there is relict structure in the saprolite and original structure in the bedrock such as joints, fractures, faults, and so forth. These are possible or probable zones of concentration of uranium, thorium, radium, and thus sources for radon. The relict and original structures also provide conduits for radon movement toward the surface.

NURE STREAM SEDIMENT DATA

Under the NURE Program, uranium and thorium were measured in stream sediments. The mean in Georgia stream sediments for uranium was about 11.5 ppm and for thorium about 56.5 ppm (Koch, 1988). The average upper continental crustal abundances are 2.5 ppm and 10 ppm for uranium and thorium respectively. Thus, the ratio of the mean to the crustal abundance in Georgia is about 4.5 for uranium and 5.5 for thorium. One can conclude that Georgia is a relatively hot province for uranium and thorium when compared to crustal abundances.

Figure 5 shows the NURE stream sediment data for uranium. The outlined zones include the two highest concentrations of uranium, ranging from 6.1 ppm to 426 ppm. Note the trends from northeast to southwest. Figure 6 shows the highest ten percent of those uranium stream sediment measurements. Again, there is a trend from northeast to southwest. The NURE thorium data in stream sediments is almost a perfect overlay of the uranium data, which is not too surprising if one considers the location of the so-called monazite belt as it traverses the Carolinas and Georgia.

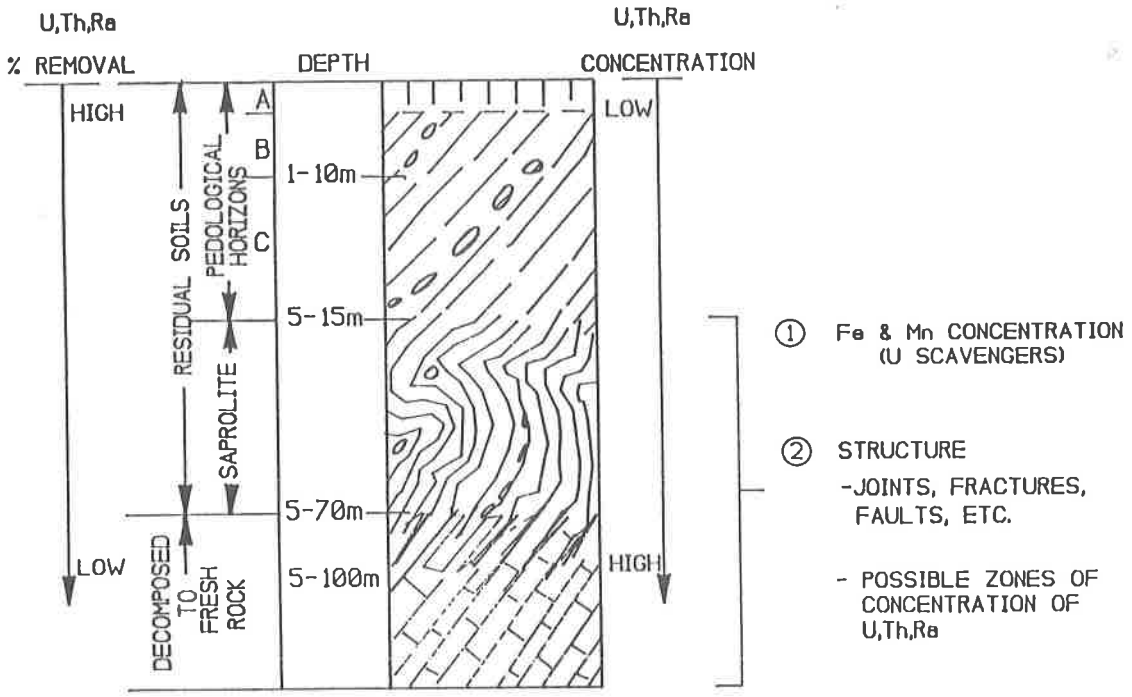

Figure 4 - Idealized Piedmont subsurface model

GEOLOGIC CONTROLS IN THE PIEDMONT PROVINCE

We have categorized the geologic factors controlling radon occurrence in the Piedmont province as bedrock, saprolite, soil, ground water, and surface processes. Obviously these factors must interact with one another, but the degrees and types of interaction are not well known, except in a few instances. In examining bedrock, we must consider the lithology, the mobility of radium in either an oxidizing or reducing environment, the amount and continuity of near-surface jointing and fracturing, the proximity of major faults and shear zones, the depth of the water table, and the proximity of pegmatite dikes and veins. In saprolite, the lithology of the parent rock, the amount and degree of jointing and fracturing and interconnection, the degree of water saturation, permeability and porosity, thickness, zonation (whether the saprolite is structured or massive), and the distribution and extent of nanopores (pores less than one micron in width), influence radon migration. For surface and near surface soil the principal influences are thickness, zonation (A, B, and C zones), moisture content (8 to 15 percent has been suggested as optimum for radon emanation), permeability and porosity of the soil, and finally the temperature gradient from the surface, which determines the water vapor pressure of the soil. The major ground water influences are the recharge area, the flow directions and flow rates, seasonal fluctuations and the presence of water supply wells (both of which cause a pumping effect), and the infiltration of surface precipitation. Finally, there are meteorologic and topographic effects on radon migration that can be enumerated but are not well understood. Meteorologic controls on soil-gas transport that have been identified and studied are temperature, humidity, precipitation, barometric pressure, presence or absence of snow cover, and wind speed and direction. Topographic effects or controls are primarily seen as varying thickness of soil cover on ridge tops and hillsides versus that in valleys.

EPA GROUND WATER SAMPLING PROGRAM

This program started in 1988 in Georgia and Tennessee (Coker and Olive, 1989). In Georgia, 9 sampling cells were delineated, where a sampling cell is defined as one or two counties with more

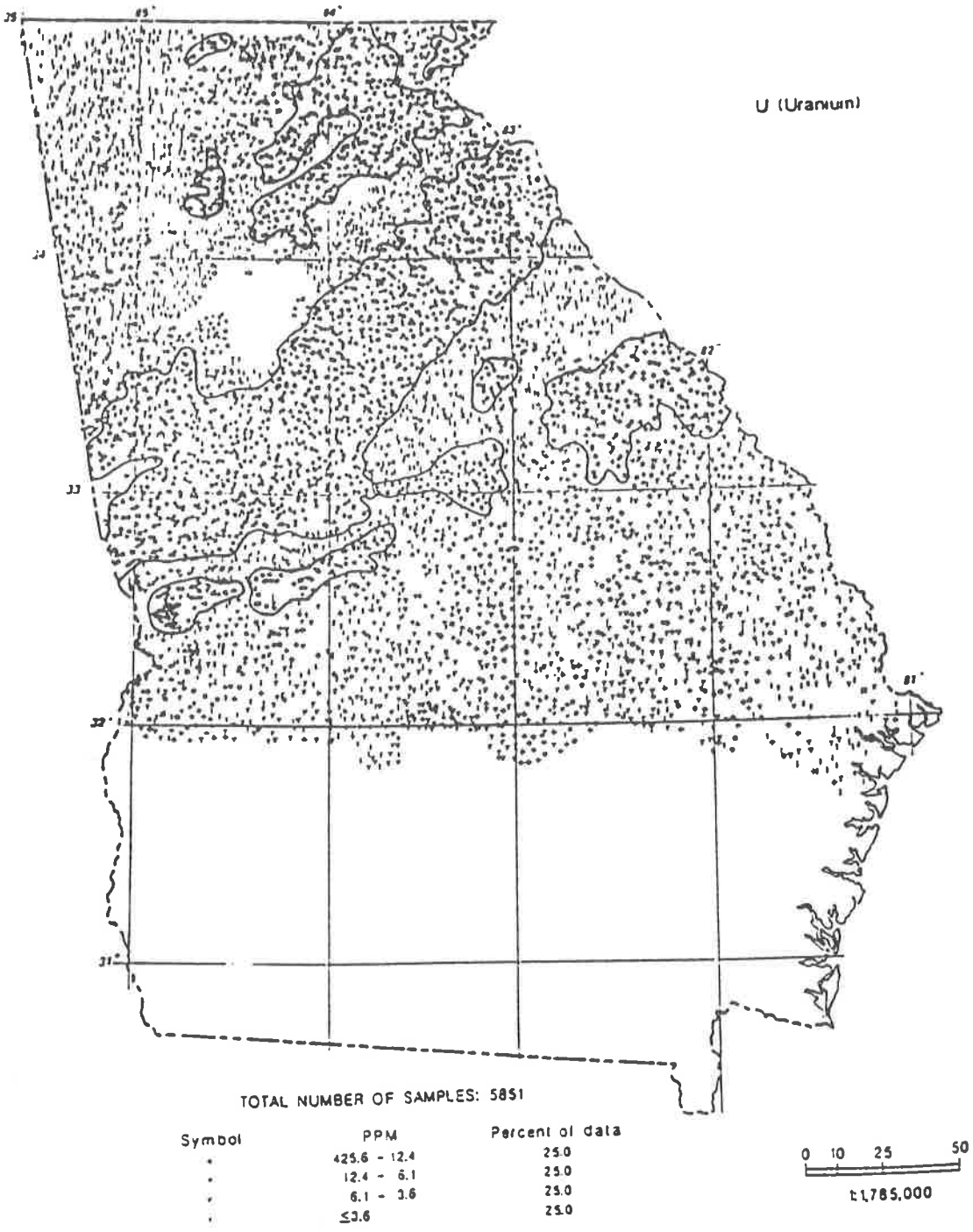

Figure 5 - NURE stream sediment data.

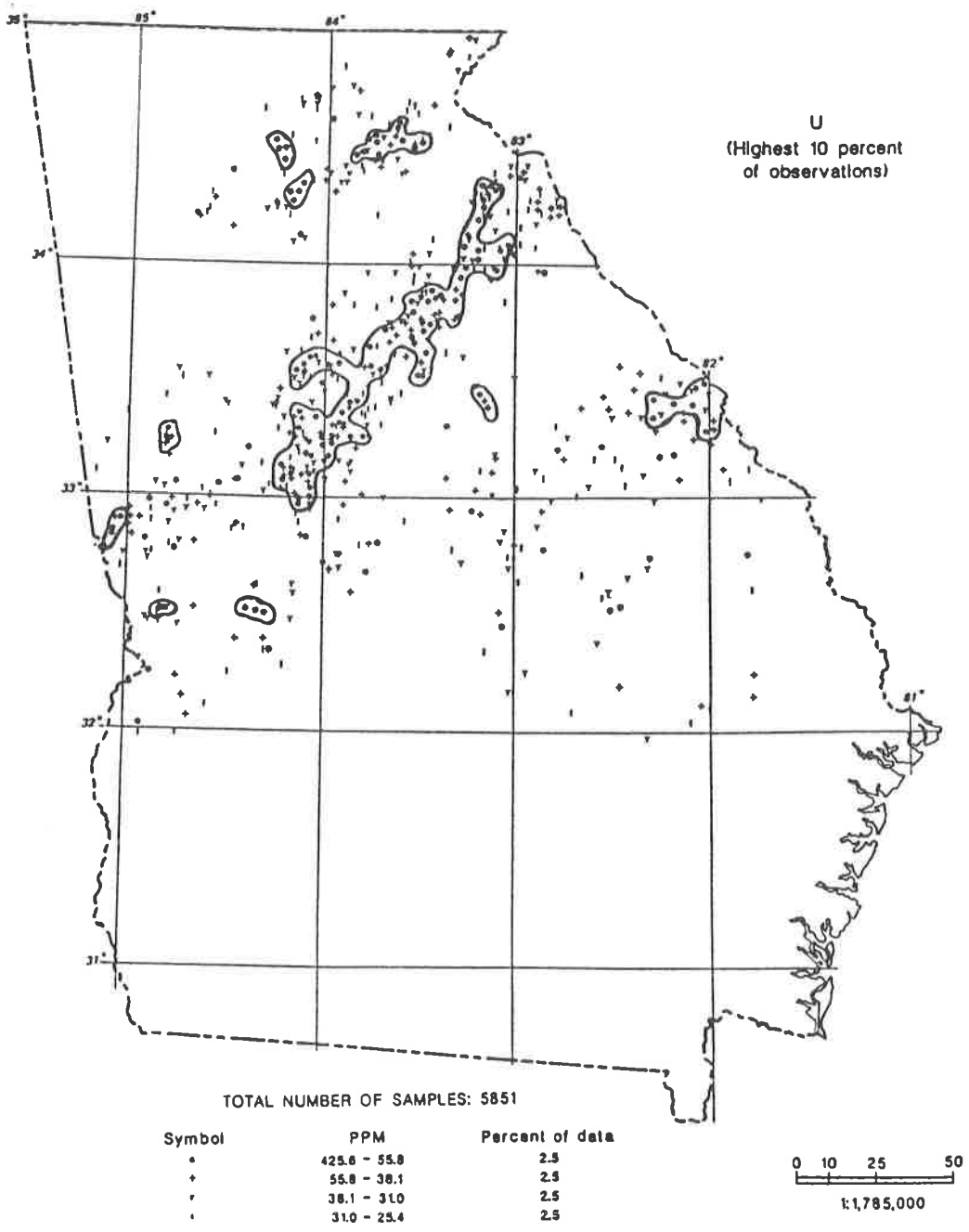

Figure 6 - NURE stream sediment data.

or less homogeneous geology. In each sampling cell, 10 sample sites were located, where a sampling site is defined as a set of paired wells about 500 to 1,000 feet apart. The sampling protocol requires measuring temperature, specific conductance, dissolved oxygen and pH every five minutes. When these parameters stabilize, a water sample is taken and analyzed at an EPA lab for the principal radionuclides and for dissolved inorganic constituents such as cation suites.

Some preliminary results from the EPA ground water sampling program in Georgia show a range of radon in ground water in a Piedmont granite gneiss from 3,160 to 268,500 picocurles per liter (pCi/l) with an average of nearly 82,000 pCi/l. In the Blue Ridge, as expected, the minimums, maximums and average are much lower, as is the case in the Valley and Ridge and the Coastal Plain.

SUMMARY

We feel that the most suspect terranes for radon occurrence in Georgia and throughout the Southeast are granite, granodiorite, granitic gneiss, pegmatites, mylonites, carbonaceous shales, phosphates and phosphorites, and monazite/heavy mineral placers, which are overlain by high to medium permeability soils and which have conduits for radon migration from the source to the surface, such as joints, fractures, faults, bedding planes and foliation planes.

Much more research remains to be done. The EPA ground water sampling program currently underway will be an important contributor to understanding radon occurrence in ground water in the Southeast.

REFERENCES

Coker, Gene, and Olive, Robert, 1989, Radionuclide concentrations from waters of selected aquifers in Georgia: U.S. Environmental Protection Agency, Region IV.

Durrance, E.M., 1986, Radioactivity in geology - principles and applications: John Wiley & Sons, New York.

Koch, G.S. Jr., 1988, A geochemical atlas of Georgia: Georgia Geologic Survey, Geologic Atlas 3.

AEOLIAN TRANSPORT IN A SMALL DUNE FIELD ON ST. CATHERINES ISLAND, GEORGIA

JoAnne M. Shadroui
Department of Geology and Geography
Georgia Southern College
Statesboro, GA 30460

ABSTRACT

St. Catherines Island is a 16 kilometer long and 3.2 kilometer wide, undeveloped mesotidal barrier island on the Georgia coast. Examination of aerial photographs taken between 1945 and 1988 shows that McQueens Inlet, a tidal creek transecting the Holocene portion of the island, has redirected its main channel from a southeastward to eastward orientation. In conjunction with other geomorphic changes caused by this migration, a small active dune field about 0.5 kilometers x 0.35 kilometers has developed during this interim on washover sands 1 kilometer south of the inlet. These mostly unvegetated dunes range from 1 to 4 meters high and have migrated laterally across the adjacent Holocene marsh. Five transects were surveyed into position across the dune field in December 1987. These stations were monitored every three weeks for fifteen months to determine vertical changes in ground elevation resulting from aeolian deposition and erosion. Overall, this study shows that significant erosion took place during Winter 1987/88 and Spring 1988 and consistent accretion took place during Summer and Fall 1988 and Winter 1988/89. Areas of consistent erosion or accretion are present along each transect. The dune field is vertically eroding on the north side and vertically accreting on the south side. Profiles of the transects illustrate that the sand tends to shift from the top to the sides of the dunes. Continuous wind data, available from an offshore buoy, shows a consistent northeast-southwest dominant pattern. Photomosaics of each transect, made during each data collection event, show changes between stakes and along the foredune ridge, which eroded landward about 2.0 meters during this study.

INTRODUCTION

Sand dunes have always been of great interest to both scientists and the general public, not only because dunes provide a cushion of protection for man's coastal developments, but also because they afford us an opportunity to witness the dramatic interaction between opposing physical forces operating within a dynamic environment. Preservation, protection and management of this important natural resource is needed to maintain the ecologic health and aesthetic value of the coast.

Although many aspects of the Georgia barrier system have been previously examined, much work still needs to be done to understand the evolution and natural history of these fascinating and mostly undeveloped barrier islands. The major objective of this study was to monitor and document both vertical and lateral changes within a small, mostly unvegetated dune field by utilizing several data collection techniques and to determine whether or not this dune field is enlarging or diminishing in size.

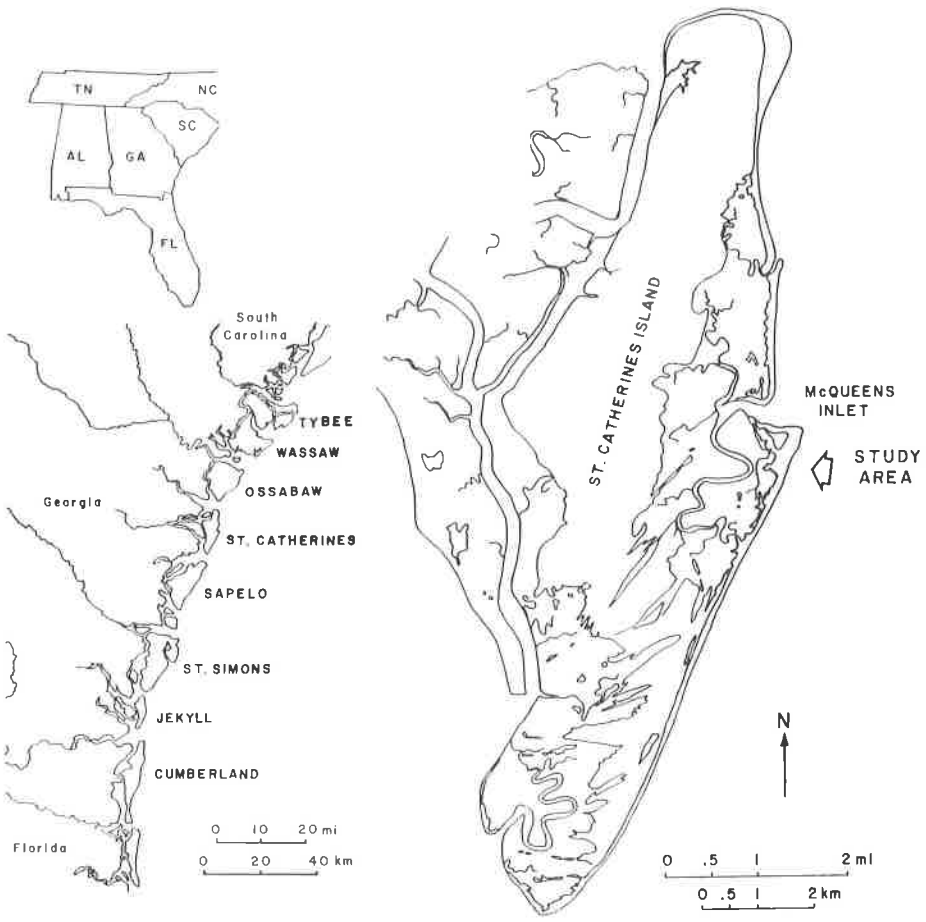

Figure 1 - Regional location map showing position of St. Catherines Island on the Georgia Coast. A close up of St. Catherines Island shows the study area south of McQueens Inlet.

STUDY AREA

Dunes on the Holocene Georgia coast are typically 0.5 meters to 2 meters high but can be up to 6 meters high in some places (Howard and Frey, 1980). In a study of washover fans on the Georgia coast, Deery and Howard (1977) stated that dunes sometimes form on inactive washover fans, during the passive phase of washover fan development. Such dunes grow upward and outward as foredunes and coalesce to form dune ridges (Oertel and Larsen, 1976). Washovers on St. Catherines Island, near McQueens Inlet, were present as early as the 1930's and active at least until 1964 (Deery and Howard, 1977).

St. Catherines Island is a 16 kilometer long, 3.2 kilometer wide, undeveloped mesotidal barrier island on the Georgia coast (fig. 1). Tidal range and wave height average 2.5 meters and 0.25 meters, respectively (Howard and Frey, 1980). Dominant onshore winds are from the northeast. The island is separated from the mainland by an expanse of tidal marsh about 6 to 10 kilometers wide and is bounded by two tidal inlets, St. Catherines Sound to the north and Sapelo Sound to the south. The island has a Pleistocene core and Holocene marsh, dunes and beach accreted to the seaward and southern side of the island. According to Griffin and Henry (1984), most of the shoreline of St. Catherines Island has been in retreat since 1858, and the overall coastline is eroding as sea level rises, at a rate of about 2 millimeters per year (Hicks and others, 1983).

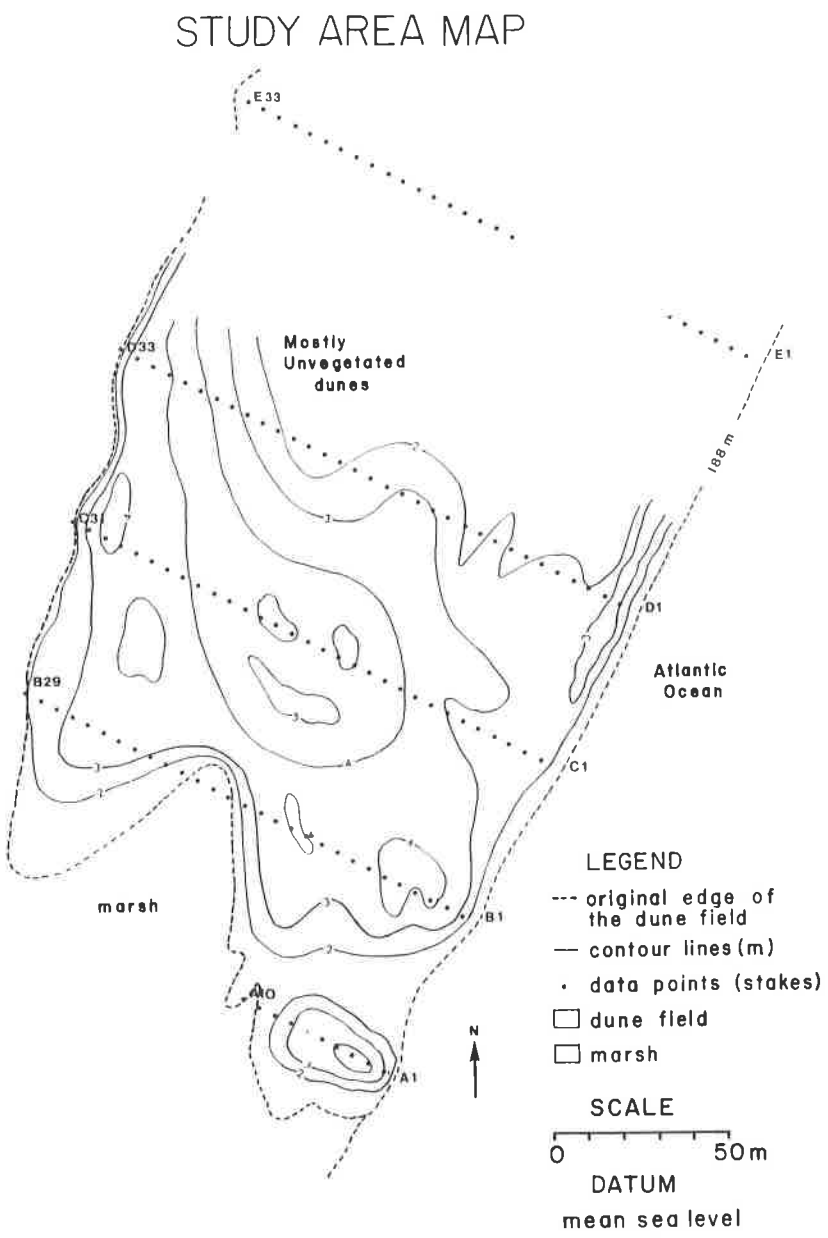

Figure 2 - A detailed map of the study area. Note that Transect E is located 188 meters north of the rest of the dune field.

The dune field examined in this study is located about 1 kilometer south of McQueens Inlet, the centrally-located tidal creek that transects the Holocene beach and marsh, adjacent to an area locally referred to as the "high dunes". This dune field was selected for several reasons: 1) the area is far from any man-made structures that might interfere with sand dune development and migration; 2) the area is isolated from most human visitors who might disturb the dunes or stakes; 3) the elevation of the field is sufficient to prevent overwash except during the most severe weather conditions, thus only aeolian transport would be recorded during the study; and 4) although it is isolated, research facilities are available on the island, provided by the St. Catherines Research Center funded through the Edward John Noble Foundation at the American Museum of Natural History.

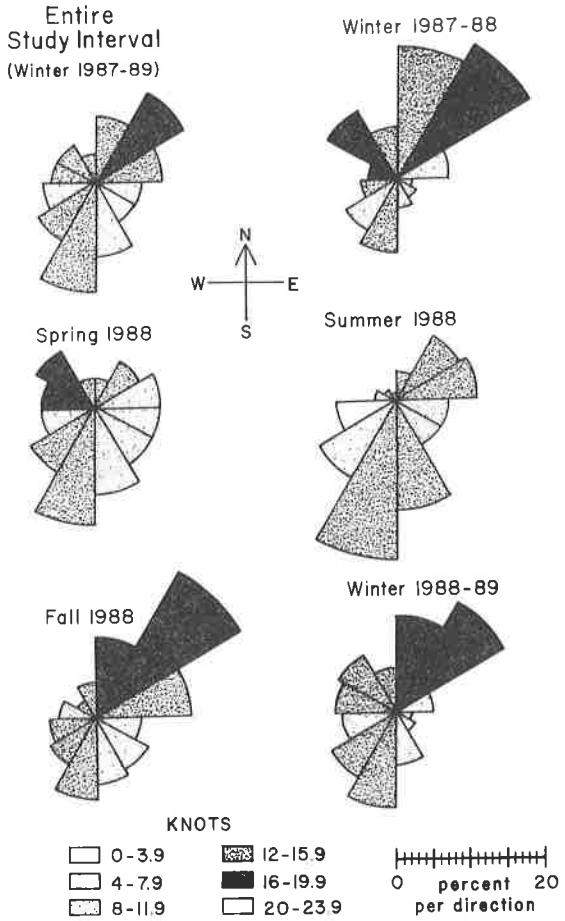

Figure 3 - Wind data processed for this study shows a dominant northeast-southwest trend. For each rose diagram, the length of the segment indicates the percent per direction, whereas the patterned areas represent average velocity for the time interval stated.

PREVIOUS STUDIES

Several studies illustrate the cyclic behavior of wind blown sand along the coast. In a study of aeolian transport rates on barrier islands, Rosen (1977) showed that on Tabusintac barrier, New Brunswick, the greatest rates of aeolian sand transport on the island occurred across overwash areas. Overall, maximum cross island sediment transfer volumes were offshore due to prevailing offshore winds. A long term study of seasonal and biennial fluctuations in subaerial beach sediment along Warilla Beach, New South Wales documented that the locus of onshore-offshore sediment exchange can shift along the shoreline (Eliot and Clarke, 1982). In a study of aeolian transport on Westhampton Beach, New York (Nordstrom and others, 1986), it was demonstrated that large volumes of aeolian sand move alongshore on the beach but the greatest volume of sand was transported offshore due to prevailing offshore winds. Oertel and Larsen (1976) examined the relationship between the development of dunes and floral zones on several islands on the Georgia Coast and concluded that the dunes are stabilized by the vegetation, which may affect the overall morphology of the dunes. Deery and Howard (1977) showed that washover fans are common on the Georgia coast and that dunes sometimes form on the central portion of the washover fan.

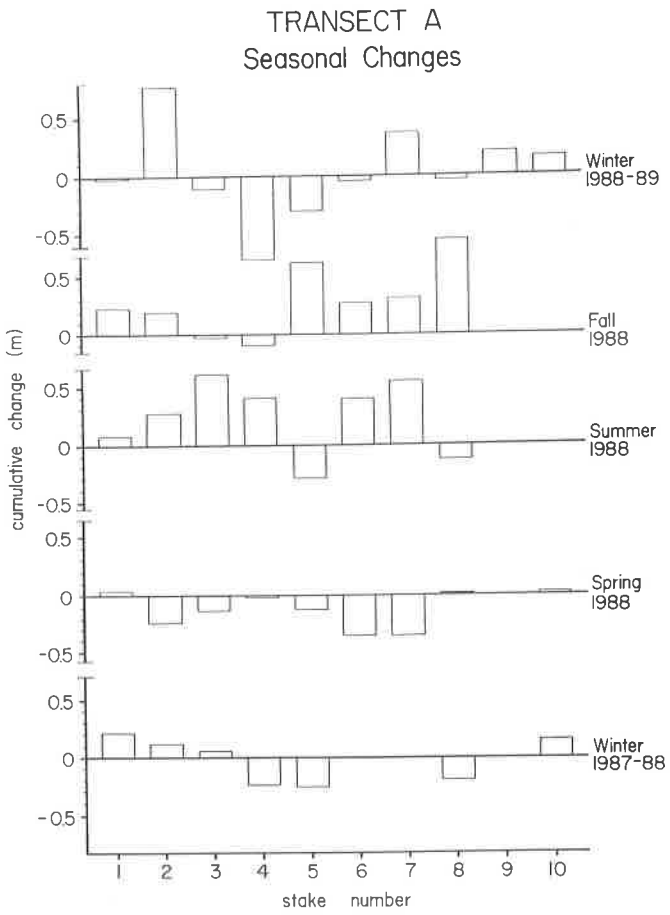

Figure 4 - Seasonal stake data for Transect A. The length of the bars above or below zero represent the amount of net accumulation or net erosion for each stake during the time interval stated.

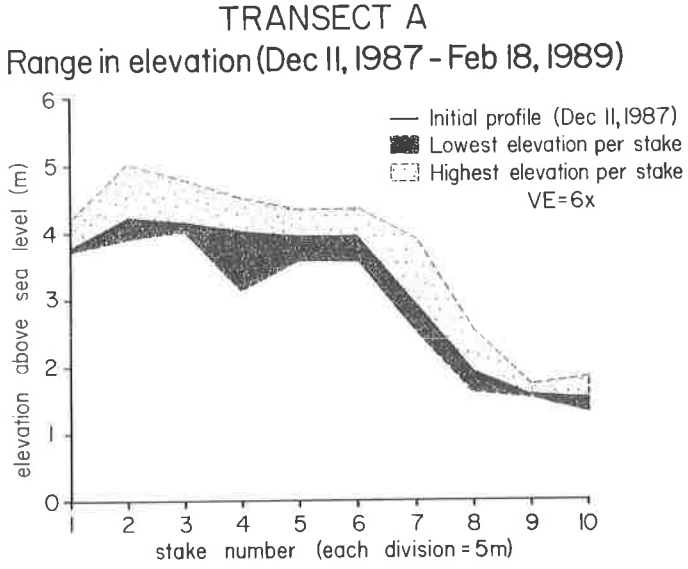

Figure 5 - Using the initial profile as a baseline, the ground elevation along Transect A was plotted to show the maximum and minimum elevation for the ground at each stake. The patterned areas represent the maximum or minimum elevation at each stake.

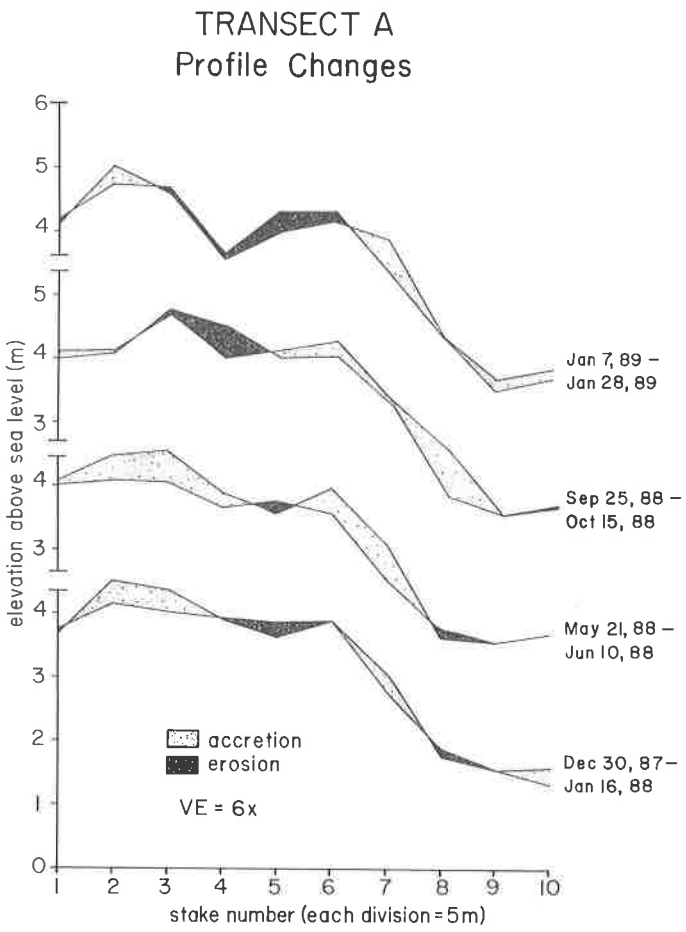

Figure 6 - The change in ground elevation at each stake along Transect A from one data collection event to the next is shown for selected dates. Note that the patterned areas represent the amount of accumulation or erosion, respectively, at each stake.

METHODS

To document changes as a result of aeolian transport within the study area, five transects, spaced 50 meters apart with wooden stakes spaced 5 meters apart, were surveyed into position across the dune field in December, 1987 (fig. 2). The elevation of the top of each stake and the ground elevation at each stake was determined during this initial survey by using a nearby spot elevation. These stations were monitored every three weeks for fifteen months to determine vertical changes in ground elevation resulting from aeolian deposition and erosion. Changes in ground elevation were recognized by measuring the height of the stakes. When a stake eroded out and fell over, it was put back in place and the new ground elevation was determined by surveying with a level and Brunton compass from an adjacent, in-place stake. The elevations were subsequently used to construct profiles of each transect. A follow-up survey, performed one year after the initial survey, demonstrated that the tops of stakes that had not fallen during the course of the year were still at their original elevation. Lateral changes in the size of the dune field were documented by measuring the initial horizontal dimensions of the dune field and then remeasuring this dimension at the end of the study. A series of photomosaics of each of the transects was taken during each data collection event to document both the vertical and lateral changes along the transects.

Continuous wind data was obtained and processed for the time interval of this study (fig. 3) from an unmanned buoy located about 70 miles northeast of St. Catherines Island. Despite the

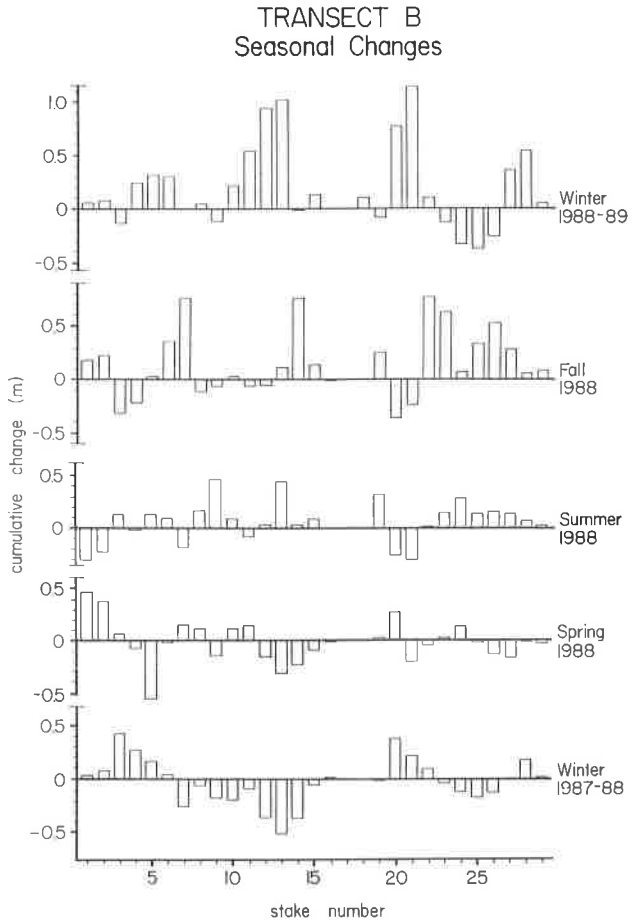

Figure 7 - Seasonal stake data for Transect B. The lengths of the bars above or below zero represent the amount of net accumulation or net erosion for each stake during the time interval stated.

relatively great distance between the buoy and study area, these data are useful as a general indication of the wind regimes during the study interval. Averaging the wind data to accommodate the three week sampling interval of stake data decreases the significance of short term, high velocity storm events. Nonetheless, the buoy data do provide a general indication of the wind conditions that caused the observed changes within the study area. This study attempts to identify overall trends and does not attempt to document, describe or explain cycles of deposition or erosion caused by daily sea breezes such as were discussed in Hunter and Richmond (1988).

There were no washover events in the dune field during the course of this study. However, one portion of the study area did get wet periodically due to accumulated rain and high tide seepage.

RESULTS

Summary of changes along Transect A

During the study interval, Transect A had an overall net accumulation of sand. Cumulatively, the dune field along Transect A lost sand during Winter 1987/88 and Spring 1988, and accumulated sand during Summer and Fall 1988 and Winter 1988/89 (fig. 4). Vertical erosion prevailed at stakes A4 and A5 and vertical accretion was fairly consistent at the east and west ends of Transect A. Each of the ten stakes along Transect A had accretion and erosion at some time during the study. Using the original profile as a baseline, the maximum total range in elevation during the study occurred at stake A4,

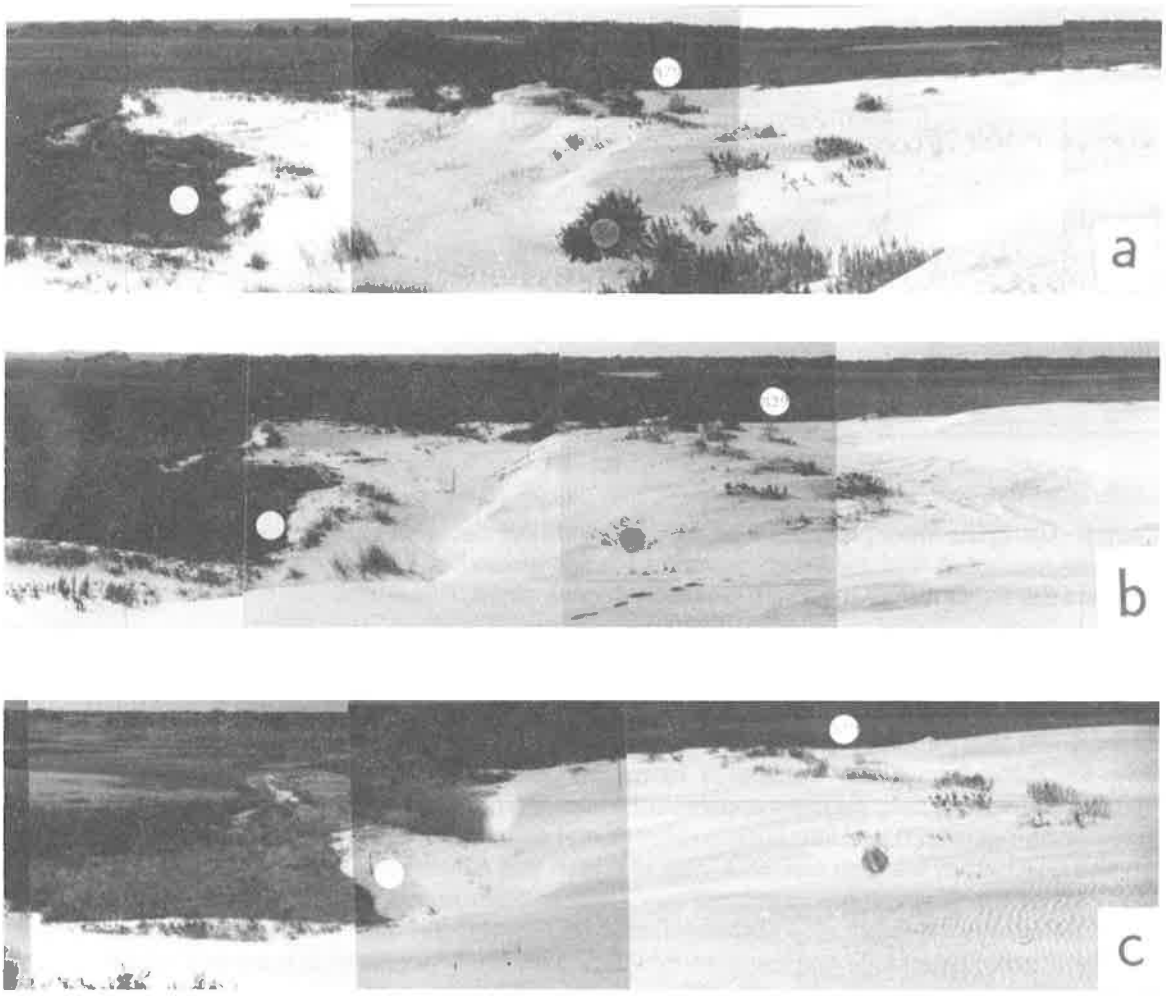

Figure 8 - This series of photomosaics shows the sand waves which migrated southward between Transect B and C during the study. Dots provide points of reference along the transect and the wooden stakes are about 0.5 to 0.75 meters in height. Photographs were taken facing west. a. October 15, 1988; b. December 20, 1988; c. March 11, 1989.

located near the crest of the foredune ridge, which ranged from a low of 3.147 meters (February 18, 1989) to a high of 4.502 meters (September 25, 1988) (fig. 5). The maximum vertical accretion for any single stake during a sample period was at A8, 0.717 meters (September 25-October 15, 1988), located on the landward edge of the dune field and maximum vertical erosion was at A2, 0.495 meters (June 29-August 13, 1988), located near the crest of the foredune ridge. Changes recorded during selected events can be examined by looking at the event to event diagrams (fig. 6). This diagram shows that dunes along Transect A did not change shape very much during the study. Sand tended to accumulate at the crests or on the slipfaces of the dunes but typically eroded from the low lying dune slacks.

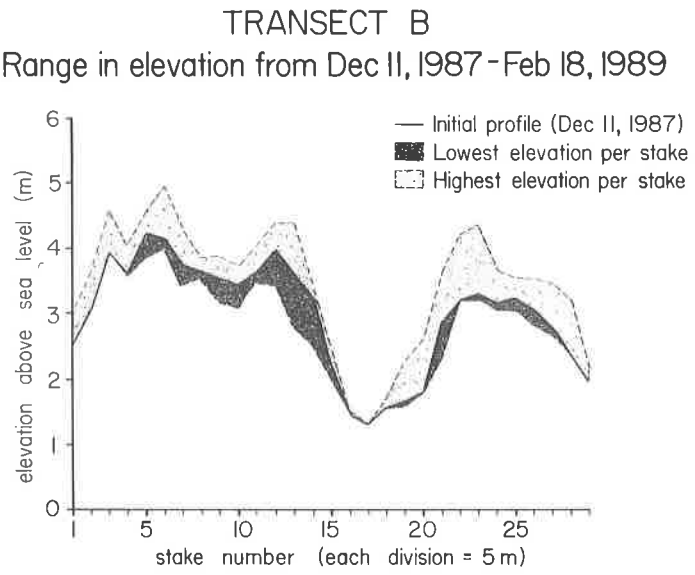

Figure 9 - Using the initial profile as a baseline, the ground elevation along Transect B was plotted to show the maximum and minimum elevation for the ground at each stake. The patterned areas represent the maximum or minimum elevation at each stake.

Summary of changes along Transect B

For the entire study interval, Transect B had a significant overall net accumulation of sand. Cumulatively, the dune field along Transect B lost sand during Winter 1987/88 and Spring 1988 and accumulated sand during Summer and Fall 1988 and Winter 1988/89 (fig. 7). Each of the twenty-nine stakes along Transect B had accretion and erosion at some time during the study interval, except for B16 and B17, which were located in a lobe of marsh that extended into the dune field. During the latter part of the study, large sheets of sand, about 0.25 meters to 0.50 meters high, migrated southward across the study area between Transects B and C (fig. 8). Using the original profile as a baseline, the maximum total range in elevation during the study occurred at stake B13, which ranged from as low as 2.786 meters (April 30, 1988) to as high as 4.395 meters (February 18, 1989) (fig. 9). This stake is centrally located along the landward facing edge of this part of the dune field. The maximum vertical accretion for any single stake during a three week period was at B21, 0.779 meters (January 7-28, 1989) and the maximum vertical erosion was at B24, 0.382 meters (January 7-28, 1989), both located on the high area on the western side of Transect B. Selected events can be examined on the event to event diagram (fig. 10). This diagram shows that sand tends to accumulate at the crests and on the slipfaces of the dunes, but tends to erode from the low lying dune slacks. Note that, although sand shifts from event to event, the overall shape of the profile remains the same. The western part of this transect had a significant amount of accretion.

Summary of changes along Transect C

During the study interval, Transect C had a significant overall loss of sand. This transect extends across the highest elevations in this part of the study area (fig. 2) and underwent continual erosion during the study. Cumulatively, the dune field along Transect C lost sand during all seasons of the study except during Spring 1988, when there was a net accumulation of sand (fig. 11). Changes at stakes along Transect C showed distinct trends during the study interval. There was consistent erosion at the eastern stakes during the entire study period, whereas the centrally positioned stakes alternately underwent significant amounts of accretion and erosion. Using the original profile as a

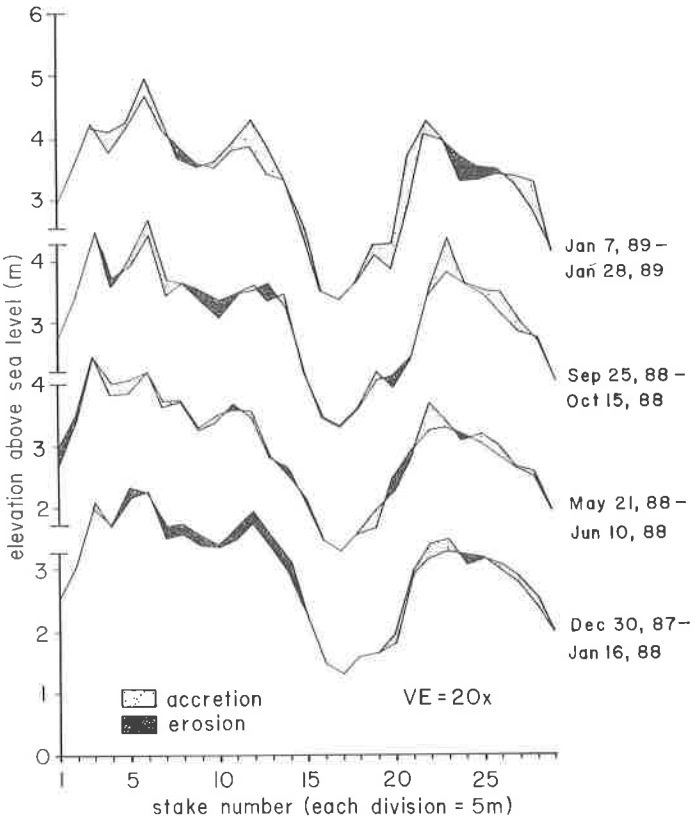

Figure 10 - The change in ground elevation at each stake along Transect B from one data collection event to the next is shown for selected dates. Note that the patterned areas represent the amount of accumulation or erosion, respectively, at each stake.

baseline, the maximum total range in elevation during the study took place at stake C22, located on a landward facing slipface of a large dune in this part of the dune field. The elevation ranged from as low as 3.773 meters (February 18, 1989) to as high as 5.353 meters (September 4, 1988) (fig. 12). The maximum vertical accretion for any single stake during a sample period was at stake C22, 0.669 meters (June 29-August 13, 1988) and the maximum vertical erosion was also at C22, 0.734 meters (September 25-October 15, 1988). Selected profiles can be examined for changes from one event to another (fig. 13). This diagram shows that the overall shape of the profile changed through time. The only area of substantial accretion was at the highest point of this transect whereas the rest of this area underwent consistent erosion.

Summary of changes along Transect D

For the entire study interval, Transect D had an overall net loss of sand. Cumulatively, the dune field along Transect D lost sand during Winter 1987/88, Fall 1988, and Winter 1988/89 and there was accretion during Spring and Summer 1988 (fig. 14). Changes in elevation along Transect D show that the eastern and western stakes had mostly accretion whereas the central stakes had mostly erosion during the study interval. Using the original profile as a baseline, the maximum total range in elevation for Transect D took place at stake D26, located on the seaward-facing slipface of the highest dune on this transect. The elevation ranged from as low as 2.895 meters (December 20,

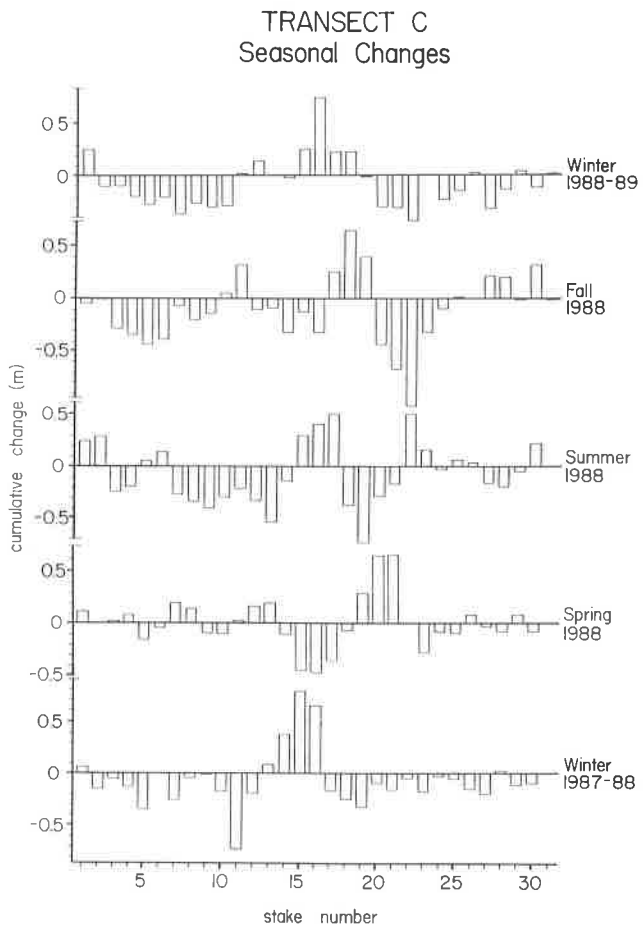

Figure 11 - Seasonal stake data for Transect C. The length of the bars above or below zero represent the amount of net accumulation or net erosion for each stake during the time interval stated.

1988) to as high as 3.671 meters (June 10, 1988) (fig. 15). The maximum vertical accretion for any single stake during a three week period was at D2, 0.565 meters (November 27-December 20, 1988) and maximum erosion was also at D2, 0.569 meters (December 20, 1988-January 7, 1989). D 2 was located at the crest of the foredune ridge. Event to event changes along this transect were relatively small and the overall morphology did not changed significantly.

Summary of changes along Transect E

This transect is located in the area locally referred to as the "high dunes." There were very minor changes in elevation in this stabilized, vegetated part of the study area. Changes occurred on the scale of a few millimeters and this transect showed a small overall net accumulation. Examination of the aerial photographs shows that this transect is located across old dunes, which were part of the old foredune ridge. These dunes were present prior to the creation of the washover upon which the unvegetated dunes of this study are located (fig. 2).

CHANGES IN THE HORIZONTAL DIMENSION

The horizontal dimensions of the dune field were measured at the beginning and at the end of the study. Considering the significant amounts of sand being transported within the area, it was surprising that the dune field did not show much lateral accretion in the landward direction. After one

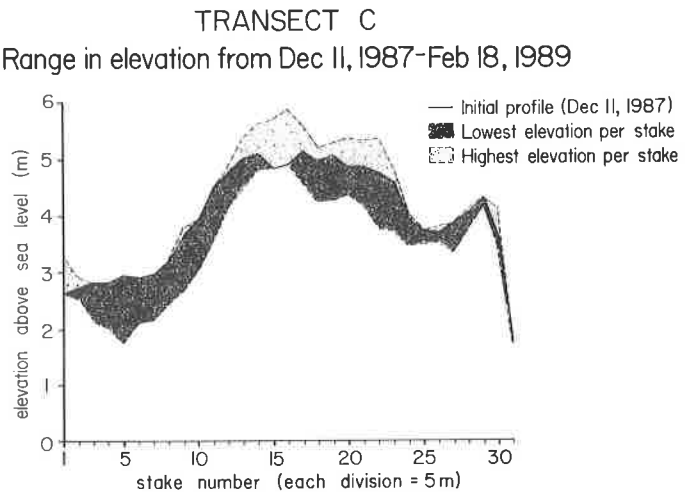

Figure 12 - Using the initial profile as a baseline, the ground elevation along Transect C was plotted to show the maximum and minimum elevation for the ground at each stake. The patterned areas represent the maximum or minimum elevation at each stake.

northeastern storm, a lobe of sand extended southward from the western end of Transect A, enlarging the dune field in this direction. The lobe measured 6 meters wide, 13 meters long and was about 0.25 meters high. The stake data indicate that sand does move to the back side of the dune field but because it is an area of alternating erosion and deposition in response to shifting winds, net lateral landward accretion is offset by offshore erosion. Vertical growth of barriers results from aeolian transport and horizontal growth is caused by washover; however, due to the dominant northeast winds, there is a slow, landward migration of the dune field and accretion is occurring both vertically and laterally.

The position of the shoreline moved landward so that there was a total of about 2 meters of the dune ridge lost to erosion, as measured from the front of each transect to the base of the beach ridge. During one particularly strong storm, as much as 4.0 meters of the dune ridge was lost to erosion and the beach elevation decreased about 0.75 meters. During subsequent data collection events, most of the lost sand was replaced, in part, by sand transported seaward across the dune crest by offshore winds.

CHANGES AT MCQUEENS INLET

Aerial photographs taken between 1945 and 1988 (including 1945, 1951, 1953, 1971, 1975, 1976, 1979, 1981, 1983, 1985, 1988) indicate that this dune field (fig. 2) developed sometime during this time period on the washover sands located 1 kilometer south of McQueens Inlet (fig. 16). The inlet transects the Holocene barrier and has redirected its main channel during this 43-year period from a southeastward to eastward orientation. In conjunction with other geomorphologic changes caused by this migration, the growth of this dune field is the result of localized shoreline accretion associated with washover evolution, channel migration and shoaling at McQueens Inlet. These mostly unvegetated dunes have migrated laterally across the adjacent Holocene marsh. Sand is transported to the dune field across the dune ridge and through low areas between dune crests. The rate of sand movement is so great in this area that the geomorphic and floral zones of Oertel and Larsen (1976) are not readily distinctive at this particular locality.

Adjacent to the mostly unvegetated portion of the study area is the area of mostly vegetated dunes, locally referred to as the "high dunes," where Transect E is located. These high dunes were located along the southernmost boundary of the channel when it was oriented southeastward. This

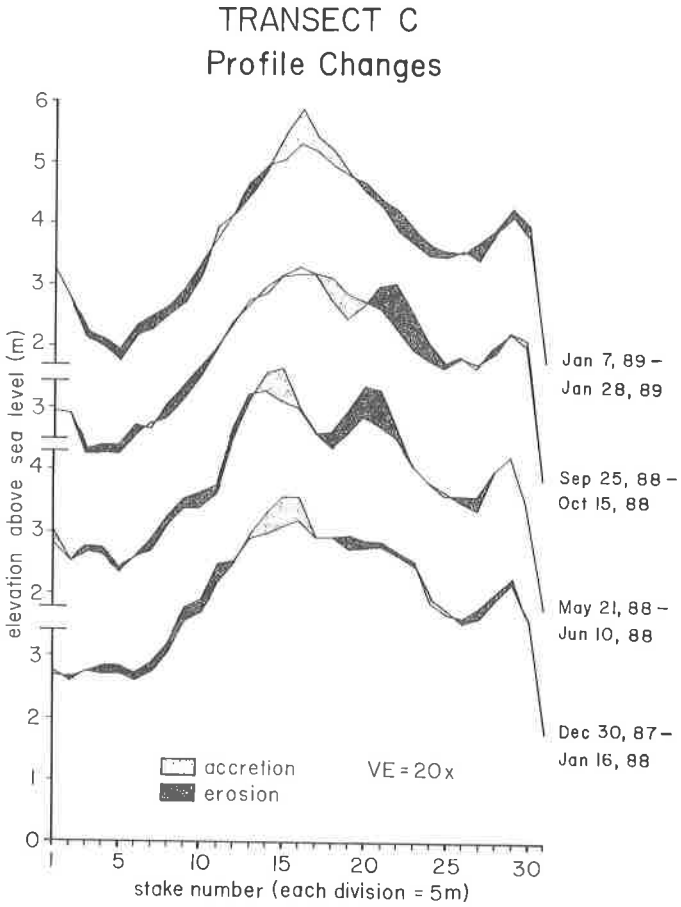

Figure 13 - The change in ground elevation at each stake along Transect C from one data collection event to the next is shown for selected dates. Note that the patterned areas represent the amount of accumulation or erosion, respectively, at each stake.

area decreased significantly in elevation during the 1970's. During the past ten years, these dunes have begun a slow return to previous elevations (Mr. Royce Hayes, Superintendent of St. Catherines Island, personal communication, 1989).

Examination of aerial photographs shows that the area around McQueens Inlet has undergone significant erosion and accretion during the past 43 years. The major changes that have occurred involve the isolation of the old dune ridges as a result of shoreline accretion along the southern side of the inlet and reorientation of the inlet from a southeastward trend to an eastward trend. At times the inlet has flowed through two channels, one southeastward and one northeastward, separated at the channel mouth by a large area of shoals (fig. 16). Since 1981, the inlet has drained through one eastward-oriented channel. During the 1960's and 1970's, the southern portion of the old dune ridge was overwashed and the dune field of this study did not "stabilize" until the early 1980's. A distinctive hook-shaped spit began forming just north and seaward of the old dune ridge during the early 1980's and has closed off the low area between the spit and the old dune ridge, where the channel was once located. The northernmost part of the spit is frequently overwashed, destroying small dunes and foredunes, whereas the southern portion of the spit, welded to part of the old dune ridge, has become an elevated area of active dune growth and migration.

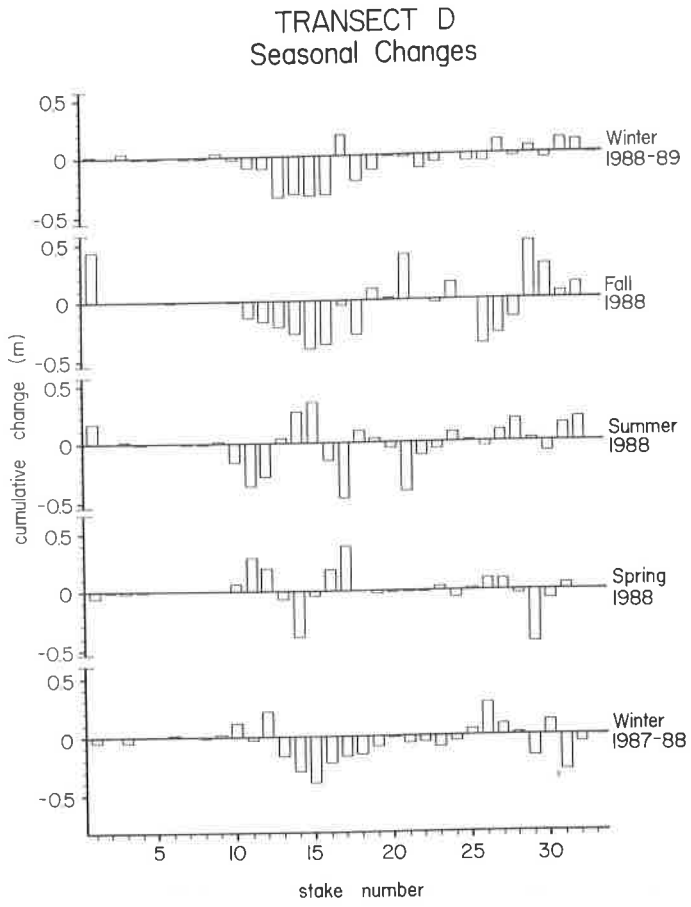

Figure 14 - Seasonal stake data for Transect D. The length of the bars above or below zero represent the amount of net accumulation or net erosion for each stake during the time interval stated.

CONCLUSIONS

The major objective of this study was to observe and measure vertical and lateral changes in coastal sand dunes for an extended period of time. These data can be used to evaluate the amount of erosion and accretion in this dune field and to determine whether or not the dune field is enlarging or diminishing.

1. Utilizing the cumulative results of this study, the dune field shows a net accumulation during the past fifteen months. Specifically, the northern side (at Transects C and D) has vertically eroded, whereas the southern side (at Transects A and B) has vertically accreted. Particularly significant accretion is visible along the western half of Transect B. The ground surface has accreted as much as 0.75 meters at some data points. Significant erosion took place at the eastern and western portions of Transect C.
2. Generally, Transect A had both accretion and erosion at the data points throughout the study interval. Transect B had mostly accretion and minor amounts of erosion during the study period, except in the low lying mid-section. Much of the accretion occurred along the central and western part. Transect C had mostly erosion during the study and alternately erosion and accretion in the central section. Transect D had mostly erosion along the central portion throughout the study interval and minor amounts of accretion along the eastern half.
3. The horizontal dimensions have changed in some parts of the dune field. Measurements along the southern side of Transect A and Transect B show that the dune field has migrated

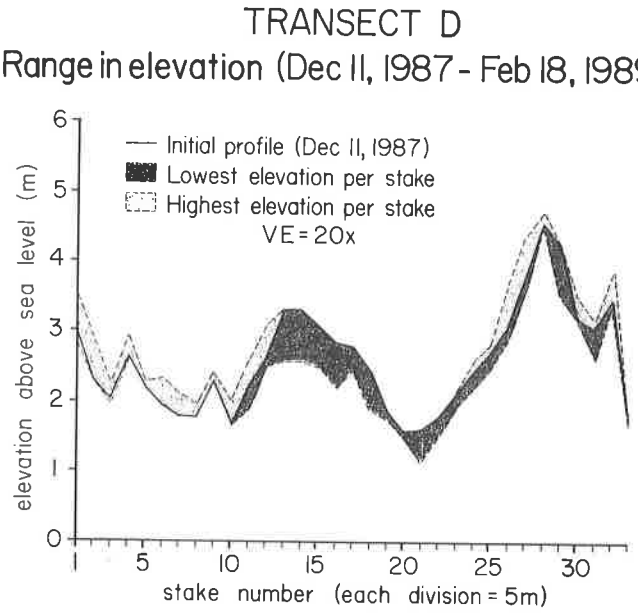

Figure 15 - Using the initial profile as a baseline, the ground elevation along Transect D was plotted to show the maximum and minimum elevation for the ground at each stake. The patterned areas represent the maximum or minimum elevation at each stake.

southward across the adjacent marsh. For example, at data point A10, a lobe of sand extending from the dune field has reactivated after a year of essentially nondeposition. The dune field at that location has accreted 6 meters to the west and 13 meters to the south across the adjacent marsh. Overall, the dune field has accreted westward by only a minor amount.

4. Photomosaics of the transects demonstrate the physiographic changes that occurred during the study. Of particular interest was the documentation of sand waves that migrated in the southward direction between Transects B and C. These sheets of sand account for some of the vertical and horizontal accretion observed along the southern side of Transect B. The photomosaics show that vegetation is frequently buried by sand but, in many cases, such burial is temporary.
5. Sequences of profiles were constructed for each of the transects for each data collection event. These were examined with the intention of recognizing patterns of erosion and deposition from one data collection event to the next. Overall, sand shifts from the front or back of a dune and accumulates along the crest or, more commonly, on the slipface adjacent to the crest. However, due to the three-dimensional nature of the sand dunes, directional changes are hard to interpret from the profiles. More detailed analysis is needed to make direct comparisons between the profiles and wind data.
6. Transect E, located north of the other transects, is in an area of relatively high, mostly old vegetated dunes. Changes along this transect are on the scale of a few millimeters to a few centimeters and there was a minor amount of accretion along this transect during the study.
7. Major storms and spring tides periodically eroded the toe of the dune ridge but the steepened, seaward face of the dune ridge was quickly healed by sand deposition. Nonetheless, the shoreline has consistently migrated, in the landward direction and the present shoreline (April 2, 1989) is about 2.0 meters landward of its January 16, 1988 position.
8. For the data stations, vertical accretion from one monitoring event to the next event ranges between zero and 0.5 meters; whereas, maximum total accretion at a single stake from initiation of the study to date is 0.75 meters. Likewise, vertical erosion from one monitoring

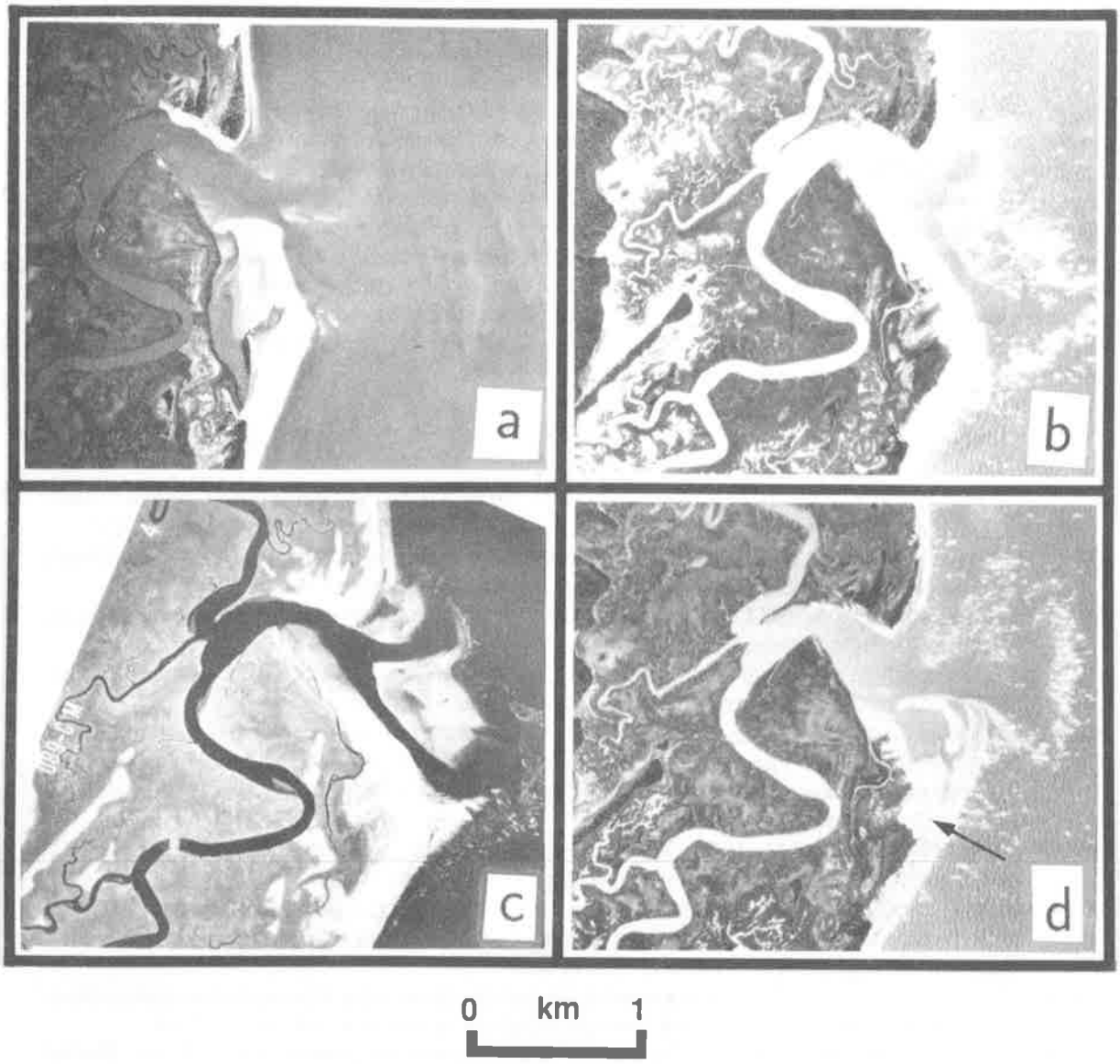

Figure 16 - Aerial photographs of the area around McQueens Inlet. Note the reorientation of the inlet. The arrow shows position of the study area. a. 1953; b. 1975; c. 1976; d. 1981.

event to the next event for the stations ranges between zero and 0.6 meters, while maximum total erosion at a single stake from initiation of the study to date is only 0.5 meters.

9. The reorientation of McQueens Inlet has played a major role in the relocation of nearshore, sandy shoals and has caused major changes in the ebb tidal delta morphology. These changes seem to have indirectly aided in the creation of the active dune field that has formed on washover sands just south of the inlet. The recently formed shoals provide an abundant northeastern source of sand to the nearby dune field. Dominant northeast winds and longshore drift move some of the sand away from the shoals, down the beach and eventually the sand is blown into the dune field. Additional aerial photographs and further study are needed to document more specific changes.

ACKNOWLEDGEMENTS

This project was funded by two research grants from the St. Catherines Island Research Program of the American Museum of Natural History, supported by the Edward John Noble Foundation and by a grant from the Faculty Research Committee at Georgia Southern College.

I would like to thank the personnel at St. Catherines Island for their cooperation and consistent field support during this study. I would also like to thank the colleagues who helped implement the study, especially Dr. Gale Bishop, Dr. Dan Good and Dr. Richard Petkewich. Thank you to the many students and friends who helped with the data collection, to Bob Hacker who helped design and prepare materials used in this project and to Grace Holder for assistance in preparing some of the diagrams used herein. Finally, thanks to the Georgia Southern Department of Geology and Geography for their administrative and technical support.

REFERENCES CITED

Deery, J.R. and Howard, J.D., 1977, Origin and character of washover fans on the Georgia Coast, U.S.A.: Gulf Coast Association of Geological Societies Transactions, vol. 27, p. 259-271.

Eliot, I.G. and Clarke, D.J., 1982, Seasonal and biennial fluctuation in subaerial beach sediment volume on Warilla Beach, New South Wales: Marine Geology, vol. 48, p. 89-103.

Griffin, M.M and Henry, V.J., 1984, Historical changes in the mean highwater shoreline of Georgia: Georgia Geologic Survey, Bulletin 98.

Hicks, S.D., Debaugh Jr., H.A., and Hickman Jr., L.E., 1983, Sea level variations for the United States, 1855-1980: National Oceanic and Atmospheric Administration.

Howard, J.D. and Frey, R.W., 1980, Holocene depositional environments of the Georgia coast and continental shelf: in Howard, J.D., DePratter, C.B., and Frey, R.W. eds, Excursions in Southeastern Geology: the Archaeology-Geology of the Georgia Coast, Georgia Geological Survey, Guidebook 20, p. 66-134.

Hunter, R.E. and Richmond, B.M., 1988, Daily cycles in coastal dunes: in Hesp P. and Fryberger, S.G. eds, Eolian Sediments, Sedimentary Geology, vol. 55, p.43-67.

Nordstrom, K.F., McCluskey, J.M., and Rosen, P.S., 1987, Aeolian processes and dune characteristics of a developed shoreline: Westhampton Beach, New York: in Nickling, W.G. ed., Aeolian Geomorphology, Boston: Allen and Unwin, p. 131-147.

Oertel, G.F. and Larsen, M., 1976, Developmental sequences in Georgia coastal dunes and distribution of dune plants: Bulletin of the Georgia Academy of Science, vol. 34, p. 35-48.

Rosen, P.S., 1979, Aeolian dynamics of a barrier island system: in Leatherman, S.P. ed., Barrier Islands, New York: Academic Press, p. 81-98.

CLASS V INJECTION WELL INVENTORY OF GEORGIA

Cassandra Shetler, Wayne Fuller, and Jerry Lineback
Georgia Geologic Survey
Atlanta, GA 30334

ABSTRACT

Ground water protection activities in Georgia include the identification, ground-water quality sampling and plugging of Class V agricultural drainage wells. Most of these Class V wells are located in southwestern Georgia and were constructed prior to passage of laws requiring permits for such wells.

An inventory of drainage wells undertaken since 1985 resulted in the identification of 58 suspected wells. After extensive field investigation by the Georgia Geologic Survey, 37 drainage wells were verified. Of these, 22 have been plugged and 1 converted for water supply. Timely enforcement action is being undertaken to plug the remaining drainage wells.

Water quality samples were taken from selected drainage wells prior to plugging. Some wells have been repeatedly sampled to determine if the wells are serving as avenues for contaminants, especially agricultural chemicals, to gain access to drinking water supplies. Sampling has been performed at various stages of the growing season and following rainfall. Twenty-one sampling events have been evaluated to date. No agricultural chemical pollutants were detected in any of these samples.

INTRODUCTION

The Georgia Geologic Survey Branch of the Environmental Protection Division (EPD) has administered primary enforcement of the Georgia Underground Injection Control (UIC) Program since 1984. There are no Class I, II, III or IV injection wells in Georgia. UIC activities include the permitting, field verification, ground water quality sampling, and plugging of Class V injection wells, as well as educating the public about injection wells.

Class V injection wells are defined by Federal Regulations 40CFR, Par 146, and the Georgia Rules of Underground Injection Control. This class of injection wells includes, but is not limited to, heat pump wells, cooling water return flow wells, recharge wells, dry wells into which wastes are injected, improved sinkholes, and drainage wells.

Initially, EPD contracted with the Georgia Tech Research Institute to assess and inventory Class V injection wells in Georgia. This assessment and inventory was completed in 1986. A follow-up inventory was undertaken by the Georgia Geologic Survey as part of the Federal Fiscal Year 1987 UIC Program. The result was an assessment of permitted, verified, and reported Class V injection wells (Franzen, 1987). Investigations were undertaken in 1988 to verify the existence of Class V injection wells that had been reported in the 1987 inventory, but had not yet been verified by field inspection.

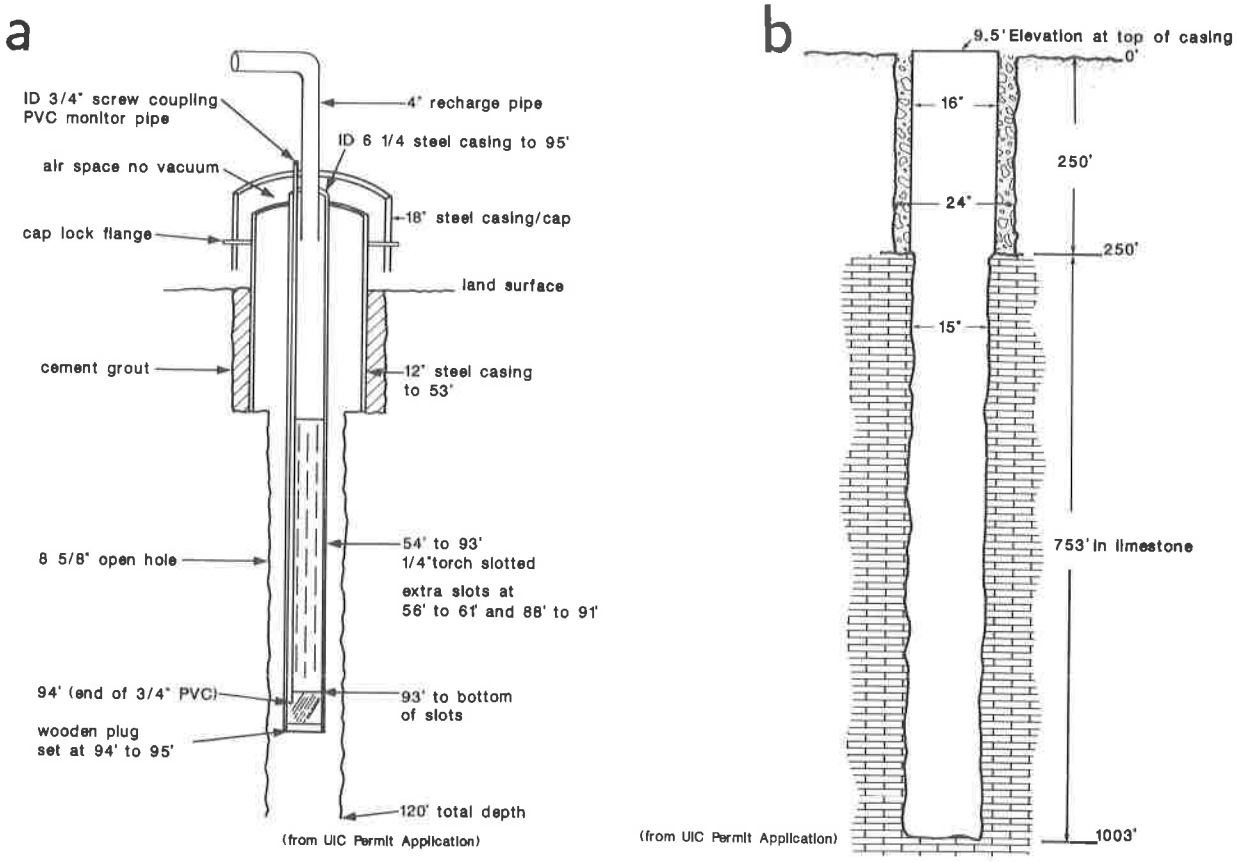

Figure 1 - Types of injection wells: a. injection wells in Gordon County, Georgia, and b. injection wells in Chatham County, Georgia.

UIC PROGRAM PROCEDURES

Unpermitted Wells

UIC correspondence, published inventories, and 7.5 minute topographic maps were utilized to tentatively locate 35 unverified injection wells prior to going into the field to carry out the 1988 updating of the Class V inventory. The tax assessor's office in the appropriate county was visited to obtain land ownership information if a well owner was not identified. The well owner was approached to gain permission and to assist in locating any drainage wells that were reported on the well owner's property. If the landowner or operator did not know where the well was located, topographic maps were used to define a 5 acre circular tract centered on the reported well location. A maximum of 8 hours was allotted for the field inspection of each well. Any well that could not be located within this time frame was removed from the list of wells.

Once an agricultural drainage well was verified to exist by EPD, the owner of the well was asked to sign a release allowing the Georgia Geologic Survey to collect certain data from the well. In return, the State would plug the well at its expense, eliminating the well's potential to contaminate aquifers. If the owner was uncooperative, consent orders could be issued by EPD, if necessary, to plug the wells.

Verified injection wells were sampled, logged and plugged under the direction of the UIC Program when possible. The wells were sampled by means of a 3 liter PVC bailer. A total of 5.41 liters of water was taken from each well to fill the 11 sanitized sample bottles required for analysis. Sterile gloves were worn during the process and all undedicated equipment was thoroughly rinsed

with distilled water between sampling events. The bottles were placed on ice and delivered to the analytical laboratory within 3 days of the sampling event. The water samples were analyzed for organics, nutrients, metals and corrosivity.

Borehole logs were obtained prior to plugging drainage wells if weather permitted and the borehole was accessible. A complete survey included gamma ray, spontaneous potential, single point resistivity, caliper, temperature and fluid resistance logs. Spontaneous potential and resistivity logs were reviewed to determine the depth of casing and the volume of cement needed for plugging a well.

Injection wells were plugged by pumping or hand-pouring cement grout down the well until the casing was full. The plug was verified at a later date to ensure that it had cured properly.

The field inspections, sample results, logging information, plugging information, and recommendations for further action were documented and placed in the files of the Georgia Geologic Survey. The results of the field work were sent to Region IV of the EPA.

Permitted Wells

Three UIC permits have been issued in Georgia covering five injection wells used by two industries. Strict UIC permit guidelines for injection wells include regular testing of the water quality of the injectant and mechanical integrity of the injection wells. Injection wells in Georgia are allowed by permit only on a case by case basis. EPD reserves the right to revoke such permits and require plugging of injection wells as deemed necessary to protect drinking water sources.

Three of the permitted injection wells are located in Gordon County in northwest Georgia and are operated by a mining company. Some ground water pumped from a quarry is reinjected into the aquifer to maintain local water levels. All three wells are constructed in a similar manner (fig. 1a), the deepest of the three is 120 feet deep and all bottom in the Conasauga Formation (Cressler, 1974, Arora, 1984).

Two permitted injection wells are located in coastal Georgia, in Chatham County and are operated by an electric power company. The two wells have similar construction (fig. 1b). Ground water is used for non-contact cooling and returned to the Florida aquifer so that the potentiometric surface of the aquifer is not lowered by the withdrawal and the ground water is available to other users downgradient.

RESULTS OF THE UPDATED CLASS V INVENTORY

An updated inventory and assessment of Class V injection wells was prepared in FY 1989. The inventory of drainage wells resulted in the identification of 58 suspected wells and 8 permitted wells since 1985:

a) 23 wells were no longer active injection wells, 10 were plugged by EPD, 12 were plugged by the owner, 1 was converted for supply by the owner;
b) 14 remain to be plugged under the direction of the UIC Program;
c) 21 investigated wells turned out not to be injection wells;
d) 3 previously permitted wells have been plugged; and
e) 3 permits allow 5 wells.

There are concentrations of unpermitted drainage wells in two main areas of the State. Most of the drainage wells are in southwest Georgia and were drilled for the purpose of agricultural drainage and mosquito control. The remainder are located in the coastal region of the State.

The Coastal Region

Many old supply wells, mostly drilled over 100 years ago, are present in the marshlands, canals, and islands of coastal Georgia. Many of these wells supplied agricultural labor and crops with fresh water prior to the Civil War. Rice and other crop farming declined in the area after that war

Table 1. Change in metal concentrations in drainage wells over time, FY 1989.

Inventory #	Date Sampled	Fe (ug/l)	Mn (ug/l)	Al (ug/l)
Mitchell County:				
#26	9/27/88	28000	6400	22000
	9/23/87	18500	8910	4370
	7/20/87	14700	6190	5070
#27	9/27/88	1200	330	130
	9/23/87	810	175	<200
	7/20/87	650	405	<150
#45	9/27/88	28000	1900	420
	9/23/87	6890	1910	<200
	7/20/87	930	75	1100
#18	9/30/88	4700	7300	940
	9/21/87	160	370	<200
	7/21/87	325	525	500
Miller County:				
#23	9/28/88	-	2000	-
	9/22/87	26300	1080	11700
	2/24/87	3380	200	2300
Dougherty County:				
#14	12/8/87	7390	250	295
	9/21/87	3410	30	<200

due to the lack of labor forces and much of the farmland fell into disuse. Locks, dikes, and natural shorelines deteriorated over time resulting in tidal waters encroaching over once dry ground and submerging some abandoned supply wells, especially during high tide. These wells are not capped and allow direct access of salty tidal waters into the fresh water aquifers. The natural deterioration of the shorelines and unused locks and dikes is an ongoing process and will result in more of these wells coming into a position to accept tidal drainage in the future. Efforts will be made to identify and plug these wells to protect coastal fresh water aquifers.

Agricultural Southwest Georgia

The majority of unpermitted Class V wells serve as agricultural drainage wells in southwest Georgia. They were constructed prior to passage of laws requiring permits for injection wells, usually over 20 years ago. Many are approximately 100 feet deep, are four to six inches in diameter, are cased with iron or steel casing and are always in a low lying area. Often they are surrounded by an iron mesh housing to help keep the well from clogging. Some are not cased, and others may have the casing cut at the ground surface. One is a sinkhole improved by the construction of drainage ditches.

The regional topography of southwest Georgia is generally flat and karstic. Because there is little regional slope, local depressions tend to accumulate water. Drainage wells were constructed in the depressions to facilitate drainage and improve field conditions. Water accumulation has many adverse effects on farmland yield. Crops can not grow on land that is underwater or too wet and walking irrigation systems become bogged down in muddy soil. Also, irrigation system leakage adds to accumulation problems. Expensive ditch, tile, and underground pipe systems are required to transport accumulated water to suitable above ground outlets.

The drainage wells were installed as a cheaper method of drainage before the possible adverse environmental impact was realized; that is, agricultural drainage wells can provide a direct pathway for agricultural chemicals to enter underground drinking water supplies. Many agricultural

chemicals are toxic. Even a small spill of an undiluted chemical into a drainage well could cause widespread contamination of drinking water supplies.

Water samples from agricultural drainage wells in southwest Georgia have been collected and analyzed as part of Georgia's UIC Program. Twenty-one sampling events have been evaluated to date. Some wells were sampled several times, at different stages of growing seasons and after heavy rains. Levels of iron and manganese, exceeding the Secondary Maximum Contaminant Levels established by the Rules for Safe Drinking Water, are present in some samples. Aluminum, although not regulated by the Rules for Safe Drinking Water, has been recorded at levels that would affect the aesthetic quality and taste of the water. Although these metals are naturally occurring constituents in surface and ground waters of Georgia (Moody and others, 1986, United States Geological Survey, 1981), the recorded levels found in drainage wells far exceed expected ambient conditions. For instance, water samples from nearby sinkhole ponds show elevated levels of these metals, but of a lesser order than that recorded for drainage wells (Fuller, in preparation).

Drainage wells located relatively close to one another showed wide ranges of these metals and levels of the metals (especially iron) tend to increase with time (table 1). An explanation for this phenomenon is that these constituents are derived from the deterioration of the casing of the wells. All drainage wells that were analyzed had casing of iron or steel. It is possible that the constituents of the casing leached into the water.

Fertilizers, pesticides and herbicides have not been detected in any of the 21 water samples collected from Georgia agricultural drainage wells.

CONCLUSIONS

Georgia is blessed with some of the cleanest underground drinking water supplies in the nation due to the low incidence of pollution. However, agricultural drainage wells can provide a direct pathway for agricultural chemicals to enter underground drinking water supplies. Improperly abandoned supply wells accepting tidal drainage also endanger underground freshwater supplies. Field investigations of reported wells are important to verify their existence and these investigations often result in additional wells being reported.

Drainage wells are located primarily in coastal and southwestern Georgia and are constructed to reach the major aquifer systems in these regions. To date 68% of the verified drainage wells have been plugged or converted to supply wells because of the efforts of the Georgia UIC Program.

The analysis of water samples collected from drainage wells indicates that detectable levels of agricultural chemicals are not presently entering Georgia's ground water via this type of Class V well. Nevertheless, EPD requires the plugging of agricultural drainage wells to help safeguard Georgia's underground drinking water supply from possible sources of future pollution, and to preserve the purity of Georgia's underground drinking water for future generations.

REFERENCES

Arora, Ram, ed., 1984, Hydrogeologic evaluation for underground injection control in north Georgia: Georgia Geologic Survey Hydrologic Atlas 12.

Cressler, C. W., 1974, Geology and ground-water resources of Gordon, Whitfield, and Murray Counties, Georgia: Georgia Geologic Survey Information Circular 47.

Franzen, P. B., 1987, An assessment of Class V injection wells in Georgia: Georgia Geologic Survey Open File Report 87-2.

Fuller, W., in preparation, Water quality in Georgia sinkhole ponds: Georgia Geologic Survey Information Circular.

Moody, D. W., 1986, National water summary 1986 - hydrologic events and ground-water quality: United States Geological Survey Water-Supply Paper 2325.

Water Resources Data Georgia, Water Year 1981: United States Geological Survey Water-Data Report GA-81-1.

For convenience in selecting our reports from your bookshelves, they are color-keyed across the spine by subject as follows:

Red	Valley and Ridge mapping and structural geology
Dk. Purple	Piedmont and Blue Ridge mapping and structural geology
Maroon	Coastal Plain mapping and stratigraphy
Lt. Green	Paleontology
Lt. Blue	Coastal Zone studies
Dk. Green	Geochemical and geophysical studies
Dk. Blue	Hydrology
Olive	Economic geology
Yellow	Environmental studies Engineering studies
Dk. Orange	Bibliographies and lists of publications
Brown	Petroleum and natural gas
Black	Field trip guidebooks
Dk. Brown	Collections of papers

Colors have been selected at random, and will be augmented as new subjects are published.